Modelling and Design of Double Skin Façades

Aalborg University
Indoor Environmental Engineering

Master's Thesis

Authors:
Anna Joanna Marszał
Sara Jessica Thomas

Supervisors:
Per Heiselberg
Olena Kalyanova

19.06.2008

Modelling and Design of Double Sin Façades

Master's Thesis

Authors:

Anna Joanna Marszał

Sara Jessica Thomas

Supervisors:

Per Heiselberg

Olena Kalyanova

Aalborg University

Indoor Environmental Engineering

June 19th 2008

Abstract

This project focuses on the energy performance of a Double Skin Façade operating accordingly to the concept of preheating fresh air incoming into the building in cooperation with a mechanical ventilation system. The first part of this report deals with three sets of results from measurements performed in a full scale model during: November 2006, the turn of April and May 2008 and May 2008. In the last case a shading device was added in the Double Skin Façade air cavity. The experimental set-up has been validated through tracer gas experiments determining the airflow. Different weather conditions have been analyzed, with special focus on solar radiation and the effect of solar shading. This provided important insight on how such building constructions can have a beneficial or negative influence on a building's power load. Conclusions have been drawn considering application of solar shading in Double Skin Façades and their operation strategies.

Later on the gathered data formed the basis for conducting three sets of theoretical energy calculations, according to a simple method developed by the Bestfaçade Project Group, as well as three dynamic computer simulations in BSim. The aim of these tools is to provide a preliminary assessment of the impact of a Double Skin Façade on a building's energy consumption, which might be used in the conceptual phase of a project. The obtained results have been compared with the measurements and both theoretical methods have been evaluated. Unfortunately, in most cases results from the theoretical tools gave values very different from reality. Finally, conclusions have been drawn including suggestions for improvement of Double Skin Façade and solar shading modelling methods.

Abstract in Polish

Streszczenie

Niniejszy projekt zajmuje się Podwójną Fasadą Budynku działającą w trybie wstępnego podgrzewu świeżego powietrza podawanego do pomieszczenia we współpracy z systemem wentylacji mechanicznej i jej wpływu na energochłonność budynku. Pierwsza część pracy dotyczy trzech zestawów danych zgromadzonych podczas pomiarów w pełnowymiarowym modelu podwójnej fasady w listopadzie 2006, na przełomie kwietnia i maja 2008 oraz w maju 2008. W ostatnim przypadku w środku Podwójnej Fasady został zamontowane rolety. Stanowisko pomiarowe zostało sprawdzone pod względem rzeczywistego przepływu powietrza poprzez badania za pomocą gazu znacznikowego. Różne warunki pogodowe zostały zbadane, szczególnie pod względem natężenia promieniowania słonecznego oraz wpływu zacienienia. To pozwoliło lepiej zrozumieć w jaki sposób konstrukcja Podwójnej Fasady może mieć pozytywny lub negatywny wpływ na zapotrzebowanie energetyczne budynku. Wyciągnięto wnioski dotyczące zastosowania rolet w Podwójnych Fasadach Budynków oraz strategii ich użytkowania.

W dalszej części pracy, zgromadzone dane posłużyły do przeprowadzenia trzech zestawów teoretycznych obliczeń zużycia energii, w oparciu o uproszczoną metodę opracowaną przez Bestfaçade Project Group, oraz trzech dynamicznych symulacji komputerowych w programie BSim. Narzędzia te mają na celu wstępną ocenę wpływu Podwójnej Fasady na energochłonność Budynku, którą można się posłużyć w początkowych fazach projektu. Uzyskane wyniki porównano z pomiarami i obie teoretyczne metody zostały poddane ocenie. Niestety w większości przypadków rezultaty uzyskane za pomocą w/w narzędzi znacznie różniły się od rzeczywistości. Wyciągnięto wnioski, w których zawarto min. sugestie poprawek do metod modelowania Podwójnych Fasad Budynków i ich zacienienia.

Preface

This report is the documentation of the work done by Anna Joanna Marszał and Sara Jessica Thomas in the final semester of the Master of Science Programme in Indoor Environmental Engineering. The topic of the project is Modelling and Design of Double Skin Façades.

The project documentation consists of the printed report and a CD, which can be found at the back. Apart from measurement results, a simple calculation method and BSim – a dynamic computer simulation tool have been used. All the gathered data, results as well as figures placed in the report can be found on the attached CD in relevant folders. References to literature are placed at the end of the report and the appendix.

The authors of this project would like to express their gratitude for the supervisors – Per Heiselberg and Olena Kalyanova, for sharing their knowledge, many useful suggestions, guidance and patience. We would also like to thank: research assistant Rasmus Lund Jensen, engineer assistant Torben Christensen, study secretary Bente Jul Kjærgaard and our fellow students, especially Michał Pomianowski and Alexandre Fleury.
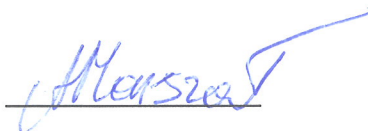
Anna Joanna Marszał   Sara Jessica Thomas

Table of contents

Table of Figures

Table of Tables

Table of Equations

1. Introduction

Double skin façade (DSF) is a general term used for external building walls consisting of two layers, separated by an air gap. Façades with only one transparent layer and the other one made e.g. of concrete, can be found in buildings from the late 1990s and their construction serves primarily esthetical purposes. The more interesting case are double skin façades whose both layers are made of glass. Such solutions appear first at the beginning of the XX century, and at that time their main function was to maximize the amount of daylight entering the building. [1]

Figure 1.1 *Example of double skin façade construction. [2]*

At present, this is also one of the most useful aspects of DSF, especially in deep office buildings where daylight is needed. DSF is also much favoured by architects because it gives a building a light and modern look. The indoor visual performance is improved as well as the occupants' comfort. Engineers also see the virtues of such constructions. This is why such concepts must be developed as part of an integrated design process, where the esthetical preferences meet with construction and operation requirements. Increasing daylight can significantly lower the energy costs as well as heat gains from artificial lighting and the air gap could be seen as a layer of acoustic and thermal insulation. Air cavities in double skin façades with openable windows can be used for natural ventilation, where the solar heat gains increase the stack effect. Finally, they could also be used for purposes of night time cooling. [2] In this sense glass double skin façades can be seen as an important passive technology, which when properly applied

can result in significant energy savings. This is especially important when considering the new EU regulations about the energy frame for office buildings.

1.1. Operation concepts

Nowadays, DSF with openable windows are gaining popularity not only because they allow occupants to adjust the environment to their individual needs but also may prove to be useful when applying natural ventilation. This leads to the concept of *Active façade*, with openings at the bottom and top of both the exterior and interior glass layer. Many types of active façades can be distinguished, some of which have been shown in Figure 1.2 [3]. All of them fulfil different functions.
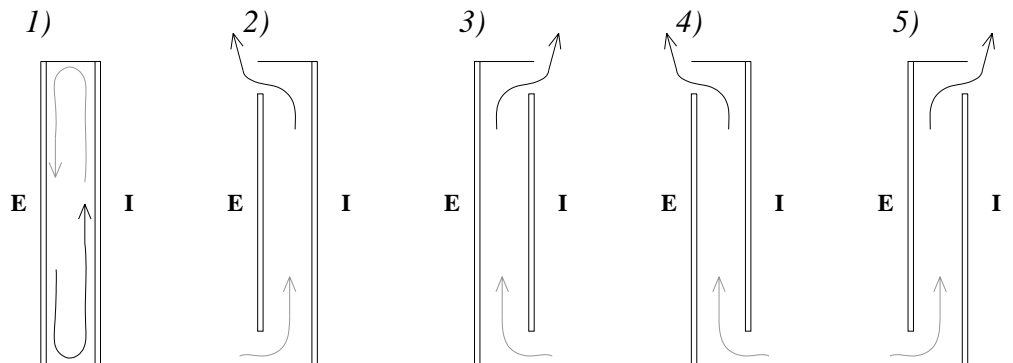
Figure 1.2 *Types of Double skin façades. E - exterior environment, I - interior. 1) not ventilated air gap; 2) outdoor air curtain; 3) indoor air curtain; 4) air exhaust; 5) air supply.*

1) Not ventilating the air gap was the first concept of DSF, and it may be used as an additional insulation layer.

2) An outdoor air curtain is primarily used for cooling the façade during the cooling season by means of natural driving forces (thermal buoyancy and wind generated pressure). The airflow inside the DSF construction can be reinforced by the stack effect increased by accumulating the energy of solar radiation inside the air gap, similarly to a green house.

3) The indoor air curtain also depends on the stack effect and is most often applied for preheating the indoor air during the heating season. This solution may operate through recirculating the air directly in the room or being incorporated in the building's HVAC system. Neither of the air curtains deals with exchanging air between the exterior and interior environments.

4) Air exhaust through an active façade is another solution using thermal buoyancy increased by solar radiation. It is especially useful in naturally ventilated buildings during the cooling season, when the difference between indoor and outdoor air density is close to 0 or even negative.

5) Finally, one of the most popular solutions applied during the heating season is air supply through an active façade. The natural forces of wind and thermal

buoyancy allow increasing the airflow and at the same time preheating the fresh air. Sometimes the air is supplied directly into the room, but more often it is taken into the HVAC system.

A construction fulfilling several of the above functions through opening the windows adequately to the season and indoor conditions is called a *Multifunctional façade*. This project deals with the case of air supply through an active façade with and without shading.

1.2. Objectives

All of the above concepts of applying a multifunctional façade can lead to significant energy savings, which are especially important in the context of energy consumption in buildings. However, a badly operating or designed DSF may give the opposite result of overheating in the cooling season and huge heat losses in the heating season. There have also been reports of moisture condensation inside the air cavity. DSFs covering a larger area of the building's façade without any internal division into sections may also cause acoustic flanking problems, because it is very easy for sound to travel inside the air gap. Also special fire security hazards must be considered. [2] How to define a well designed double skin façade?

Unfortunately, double skins are still a new concept. There are not many buildings in Europe with such building constructions, which may serve as examples or study cases. Also the building simulation software is not always capable of calculating the energy performance of DSF correctly. Problems mainly occur when taking into consideration solar irradiation. Therefore, it is necessary to validate any theoretical calculations by comparing them with an existing model, where all necessary values are known.

This report focuses on the concept of air supply through an active façade cooperating with a mechanical ventilation system. It is important to remember that it is a theoretical case study. The aim of it is to assess the importance of different parameters and their influence on the performance of the DSF, and to optimize the indoor climate. Therefore, in reality the active façade should be operated with different strategies, regarding the operation concepts as well as the shading device, depending on the season of the year, outdoor conditions and desired indoor environment parameters. The indoor climate, thermal conditions and energy consumption of this case have been investigated in a real size model, for two measurement series without and one series with shading devices inside the DSF. The results of laboratory measurements have later been compared with results of BSim simulations and a simple calculation method, proposed by the Bestfaçade Project Group [4]. Finally, conclusions have been drawn considering the performance of the double skin façade as well as validation of simulation software and the calculation method.

2. Description of the test facilities 'the Cube'

The following chapter is mainly based on the two technical reports [5] and [6], where more detailed information about 'the Cube' can be found.

'The Cube' is the outdoor test facilities located at the main campus of Aalborg University. It is surrounded by few company buildings and farms (Figure 2.1). This environment assures that the DSF is not shaded by any objects.

Figure 2.1 *The surroundings of 'the Cube'. A) three stories company buildings; B) one story farms C) 'the Cube'*

2.1. Construction and form of 'the Cube'

Figure 2.2 *'The Cube'*

The test facility 'the Cube' consists of the double skin façade (DSF) and three rooms: experiment, instrument and engine (Figure 2.3)
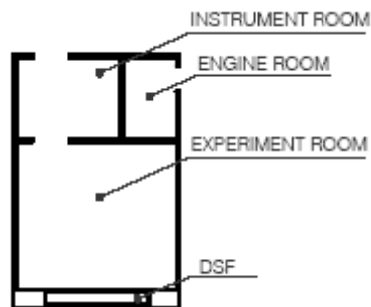
Figure 2.3 *Plan of 'the Cube'*

Double skin façade is facing south. All openings are controlled and can be operated separately. The experiment room is directly connected to the double skin façade. In order to keep the temperature at a constant level in the experiment room an air conditioning system with heating and cooling unit was installed. To avoid creating a temperature gradient in the room the air is constantly recirculated.
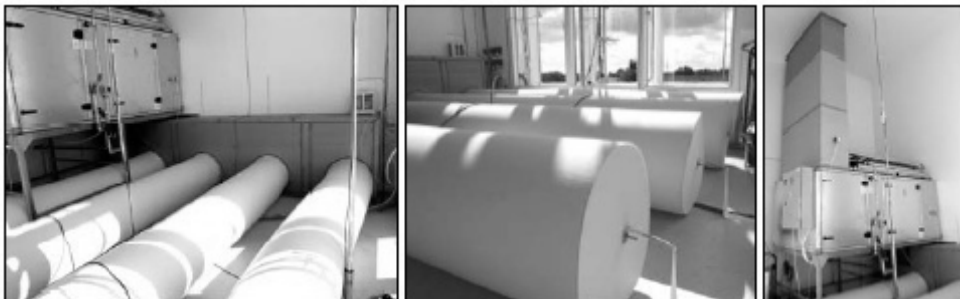
Figure 2.4 *Ke-low impulse ducts (left, centre). Ventilation system in the experiment room (right).*

The air for the recirculation is taken from the top of the room, then it flows through the preconditioning units of the ventilation system and is exhausted at the bottom of the room through the fabric ke-low impulse ducts, with air velocity of approximately 0,2 m/s. The maximum power of cooling unit is 10 kW and heating is 2 kW. The ventilation system and ke-low impulse ducts are shown in Figure 2.4. In the engine room is the cooling machine, which produces cold water for the cooling unit. In the instrument room is located measuring equipment (data loggers, computers etc.)

2.2. Geometry of 'the Cube'

The experimental room and double skin façade together make a cube of external dimensions 6x6x6 m. The instrument room and engine room (both 3 m height and 3 m depth) are attached to the northern wall of 'the cube'.

Figure 2.5 *'The Cube' from the North-west view (left), from the North view (right)*

The internal dimensions of the experiment room and DSF are shown in Table 2.1.

Room	Height [m]	Width [m]	Depth [m]	Volume* [m^3]
Experiment room	5,584	5,168	4,959	11,24
DSF	5,450	3,555	0,580	143,11

*Volume of experiment room and DSF is calculated to the glass surfaces of the window NOT to the window frames or walls

Table 2.1 *Internal dimensions of 'the Cube'.*

2.3. Windows geometry in the DSF

All windows at the test facility produced by VELFAC. The outer part of the window frame is made of aluminum and the inner part is wooden. The windows of the outer shell of the DSF construction consists of 8mm thick, clear single glazing. The windows of the inner shell of the DSF construction are low energy double glazing filled with argon (4-16Ar-4). Window partitions of the double skin façade naturally subdivide the DSF into three sections. The double skin façade and windows division is shown in Figure 2.6.
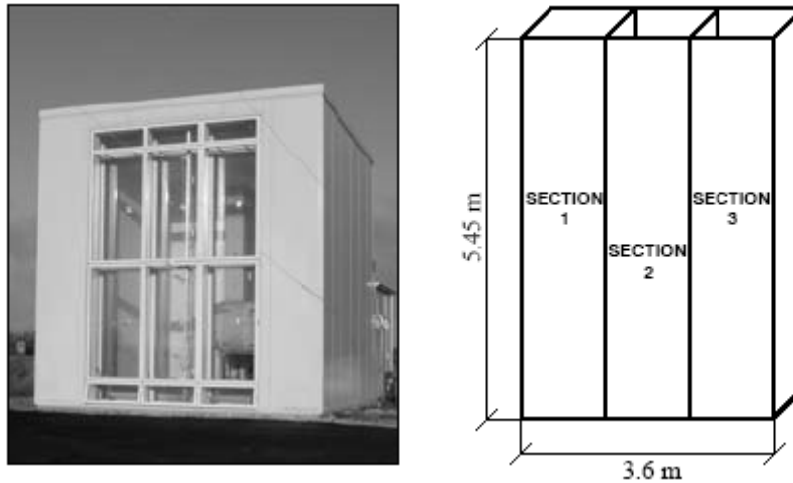
Figure 2.6 *DSF division.*

Each section has the same dimension. The detailed dimensions are shown in Figure 2.7.Frames in external and internal windows are different, they are made of wood and aluminium correspondingly.

* frame of 54mm encloses the glass panes
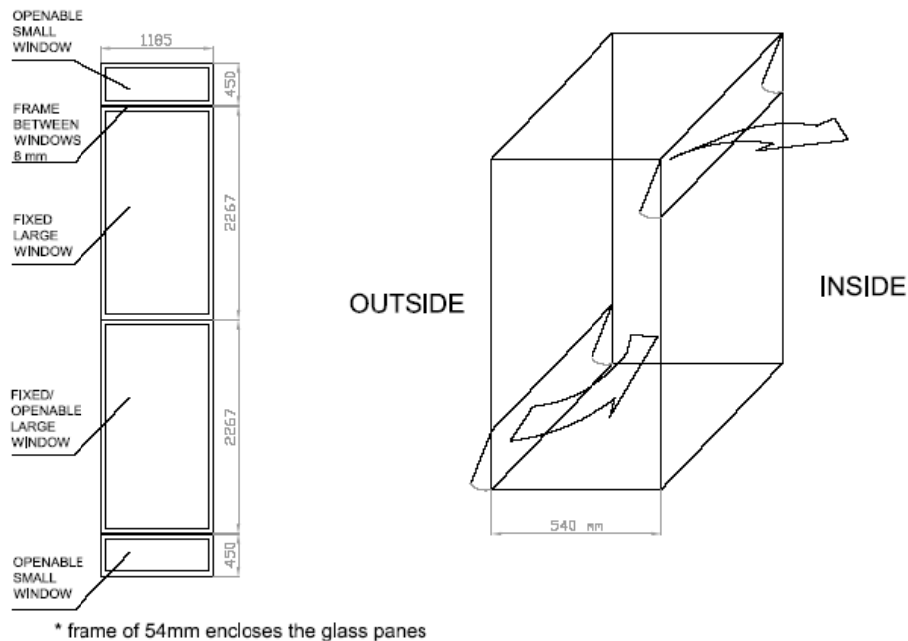
Figure 2.7 *Detailed dimensions of each section, all diameters in mm (left). Air flow direction in DSF (right).*

Apart from the section division of DSF, each window is also divided into: 2 big windows in the middle and 2 small, one on the top and the second on the bottom. The naming code and the definitions of each window are shown in Figure 2.8.
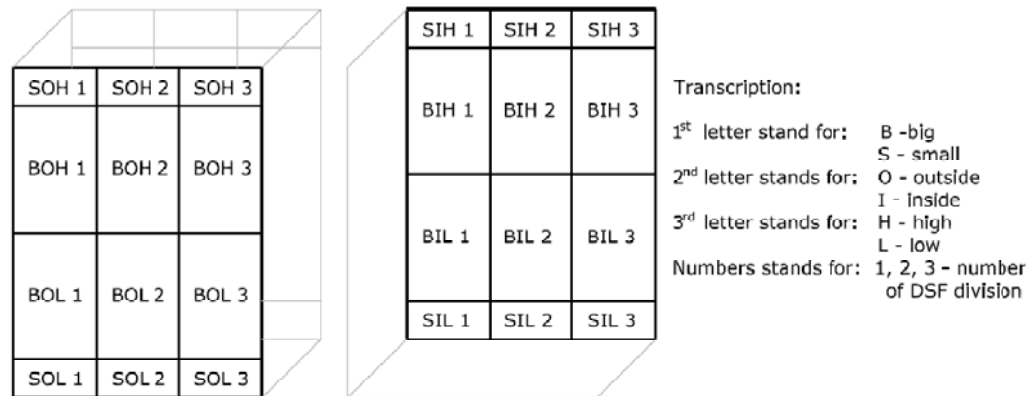
Example:
BIH3 – **B**ig, **I**nside, located **H**igher than the middle plane of the window, in section **3** of DSF
SOL2 – **S**mall, **O**utside, located **L**ower than the middle plane of the window, in section **2** of DSF
Figure 2.8 *Definition of Windows divisions.*

The small widows SOL, SIL, SOH and SIH are operated and can function as openings in DSF. The opening angle is controlled and express in percentage (100% corresponds to the maximum angle of 75,5^o). During the whole experiment the SOL and SIH were open, definition of free opening area, opening angle etc. is shown in Figure 2.9.
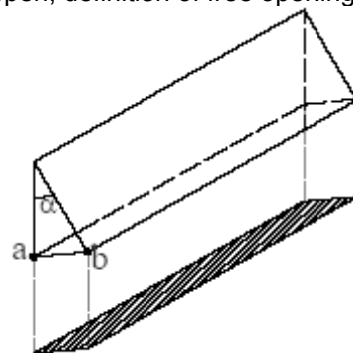
	SIH	SOL
Free opening area of one openable opening, m^2	0.08	0.08
Distance 'ab', m	0.068	0.068
Angle α, deg	8.5	8.5
Opening %	30	30

Figure 2.9 *Free opening area.*

As mentioned in chapter 1.2 this project deals with the case of air supply through the double skin façade. The air enters the DSF at the bottom openings (SOL1, SOL2 and SOL3) in the external windows, flows through the façade and then is exhausted through the top small openings (SIH1, SIH2 and SIH3) in the internal windows to the experiment room (Figure 2.7). The flow motion of air from DSF to the experiment room is mechanically driven by an exhaust fan (see Figure 3.1). The fan was controlled to keep the air change rate constant. The airflow rate was set to 136,5 m3/h that corresponds to around 1/h^{-1} air change rate in the experiment room.

2.4. Ground reflection

To achieve uniform and relatively known reflected solar radiation from the ground, which is an important parameter in the experiments, a large carpet was fixed on the ground in front of southern façade of 'the Cube' – wall with DSF (Figure 2.10).

Figure 2.10 *Illustration of the ground carpet in the front of 'the Cube'.*

2.5. Shading

Shading is a crucial part of the DSF construction, for it may prevent the building from overheating, increase the amount of solar radiation accumulated in the air gap and prevent daylight from blinding the occupants. However, it should be noted that the shading device used, must still allow a certain amount of daylight to enter the building. Otherwise, the primary function of DSF, which is decreasing the amount of artificial lighting, will not be fulfilled. In order for solar radiation to reach the external layer of DSF, shading devices are usually mounted inside the air gap. This solution solves problems of shading high-rise buildings at high wind speeds. The exact position and character of the material used for shading (its absorption and reflection coefficients) are the most important features. [7] The most popularly applied shading devices have a low g-value, which results in reducing solar gains. However, if the DSF is primarily used for preheating of fresh air, it is more important that the shading material has a high absorption. This would allow to retain more heat in the DSF cavity and transfer it to the air.

Figure 2.11 *Samples of proposed shading materials. From left: Nature Provence, Nature Silver, Nature Ivory.*

It has been decided that the shading material used during the second model of measurements DSF_SH should be a universal one, which may be applied in a real office building to various operation concepts of an active façade. Firstly, the type of the shading device was picked. Out of various possibilities, such as roman, venetian or panel blinds, the roller blinds have been chosen. This solution ensures that the surface of the DSF will be evenly shaded, without gaps and cracks. The next step was deciding on the physical properties of the material, such as solar reflectance or transmittance. The final choice was made between three materials, which properties have been specified in the producer's catalogue [8], see Table 2.2.

Material name	Catalogue no	Solar performance [%]			SC	OF
		T *	R	A		
Nature Silver	9448	30	37	33	0,55	1%
Nature Ivory	9449	35	50	15	0,48	1%
Nature Provence	9452	13	16	71	0,64	1%

* The symbols are according to Faber as follows: T – transmittance, R – solar reflectance, A – solar absorptance, SC – shading coefficient, OF – openness factor.
Table 2.2 *Physical properties of shading materials.*

All the above materials are of the same thickness 0,25 mm. 'Nature Provence' seemed to have the best properties, as it had a low solar reflectance and a high absorption – especially important for preheating the fresh air inside the DSF. However, materials of this colour are not typically applied in offices. Therefore, 'Nature Silver' has been chosen, as it is believed to be a compromise between a real life situation, useful physical properties and a good shading performance. All of the above mentioned shading materials have been shown in Figure 2.11. The construction of the shading device inside the cavity and its application in the DSF_SH measurements can be seen in Figure 2.12.

Figure 2.12 *Shading of DSF.*

3. Determining the airflow

This report deals with the operation concept of preheating incoming air in the double skin façade. In reality, such a solution is often part of the building's mechanical ventilation system and so the fresh air is drawn from DSF by a fan. In order to investigate and simulate this case, it was necessary to make sure that the natural driving forces of thermal buoyancy and wind generated pressure would not have a decisive influence on the airflow through the air cavity.

For this reason a mechanical air exhaust installation has been assembled and placed in the experiment room, a detail description of which can be found in the Appendix. The most important elements of it are a fan collaborating with a frequency inverter and a set of dampers. The setup has been adjusted to provide the airflow of 136,5 m^3/h, which corresponds to about one exchange of the experiment room's volume per hour, and a high pressure loss of approximately 600 Pa. This was hoped to reduce the effect of wind and solar radiation on the incoming airflow, so that they could be neglected in further experiments. To measure the volume flow in the installation an orifice connected to a differential manometer was used.

For measuring the airflow in the ventilated gap itself, a tracer gas method was applied. The experiment has been conducted accordingly to the description in the technical report [5], where any further details may be found. The gas used in the experiment had to have physical properties similar to air, in order to mix and flow in the same way. Therefore, carbon dioxide was chosen. Approximately 3,1 l/min of the gas were supplied from a bottle, containing CO_2 at the pressure of 50 bars, to the bottom of the air cavity in the DSF. The concentration of CO_2 in the outside air was measured by URAS and the level at the top of the DSF by BINOS. The measured data was logged every 10 seconds and formed the basis for calculating the airflow through the cavity of the double skin façade, see Equation 3.1 [9].

$$\dot{V}_{airflow} = \frac{\dot{V}_{tracer\ gas} \cdot 0,06}{(Binos - Uras) \cdot 10^{-6}} \left[\frac{m^3}{h} \right]$$

Equation 3.1 *Airflow through the air cavity in DSF, where $V_{tracer\ gas}$ is the flow of CO_2 from the bottle in l/min, BINOS and URAS are the measured concentration levels of CO_2 in ppm.*

A scheme of the experimental setup can be seen in Figure 3.1. All the equipment used has been calibrated, which is documented in the Appendix.
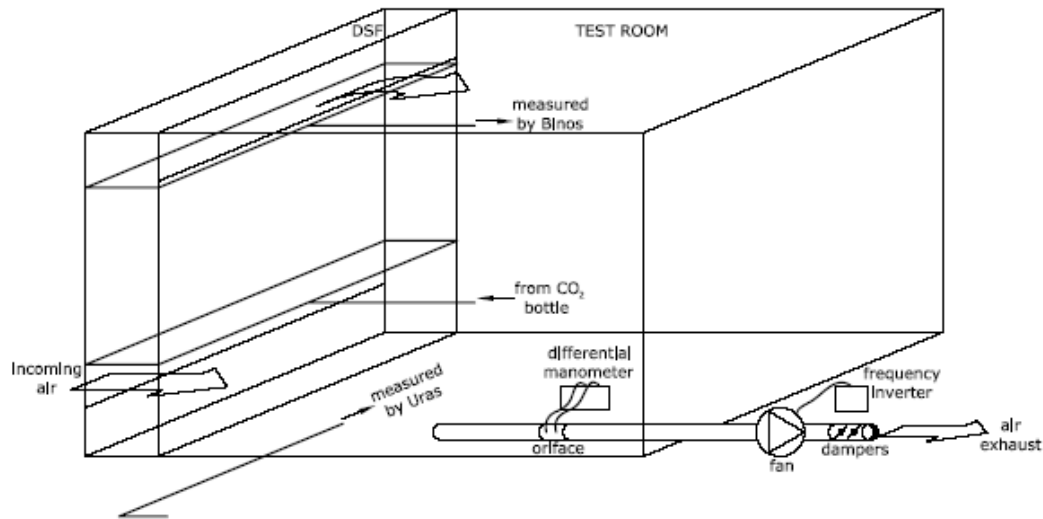
Figure 3.1 *Experimental setup for determining the airflow through the double skin façade.*

3.1. Tracer gas supply at 0,55 m

At first, a set of perforated tubes supplying carbon dioxide was placed in the air cavity at the height of 0,55 m, just above the DSF's lower openable windows. However, the results of the experiment were not satisfactory. The data gathered through about 48 hours resulted in an average airflow of 408 m^3/h, with peaks above 1000 m^3/h, according to the tracer gas measurements. At the same time, the orifice indicated a rather stable flow of about 136,5 m3/h. The data is shown in Figure 3.2. These unexpected results were thought to be caused by the 'wash out' effect. It is possible that strong wind entered through the lower windows of the DSF, whirled inside the air gap and drew some CO_2 outside while leaving at the bottom of the cavity. This situation could significantly affect the tracer gas experiment results, without influencing the actual airflow through the double skin façade. It should be noted that at the time when the measurements began, on March 4th in the afternoon, the wind was very strong with velocities well above 18 km/h. Similar conditions repeated themselves during the next days, on March 5th and 6th wind speed exceeded 20 km/h and strong gust of wind have been noted. The dominant wind direction during the measurements was North, which corresponds to the wind blowing from the DSF, as shown in Figure 3.3. Due to those weather conditions, the air in the ventilated gap was not evenly mixed throughout the double skin façade, not all supplied tracer gas reached the measurement point and the readings were not accurate. It should be noted that the readings from the first 5 minutes

of the experiment show too high airflows, significantly differing from the rest. This is thought to be a result of unstable conditions in the experiment room at the very beginning of the measurements and therefore, they have been discarded. The break in the graphs indicates the short period of time when data was being retrieved from the data loggers after the first 24 hours of measurements and should be ignored.
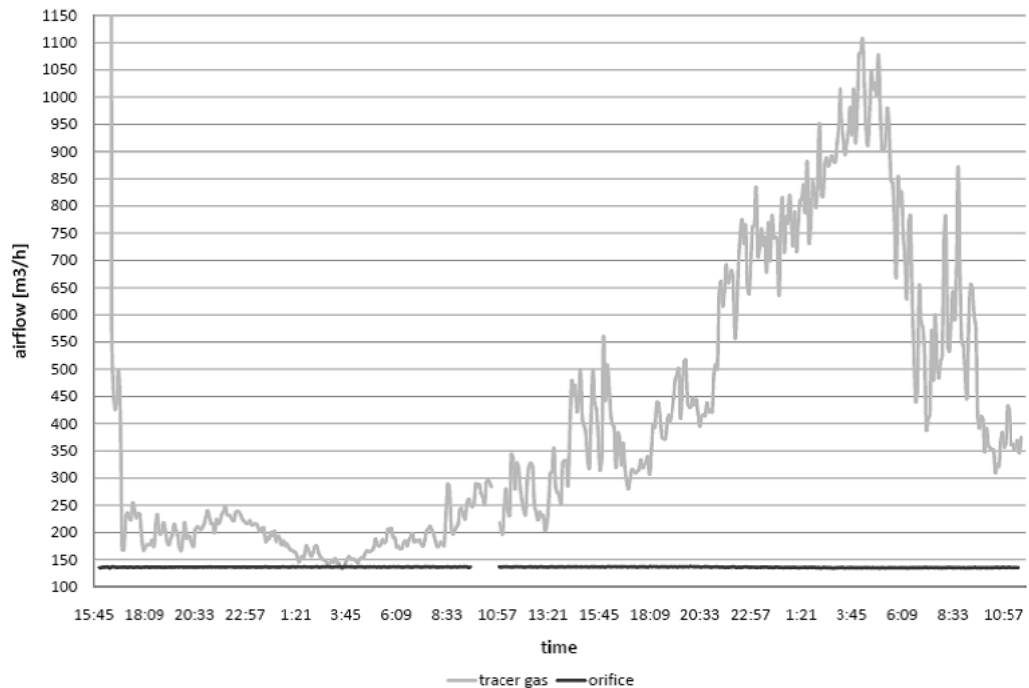
Figure 3.2 *Airflow results obtained from orifice and tracer gas measurements from March 4th to March 6th 2008, for the tracer gas supplied at the height of 0,55 m.*
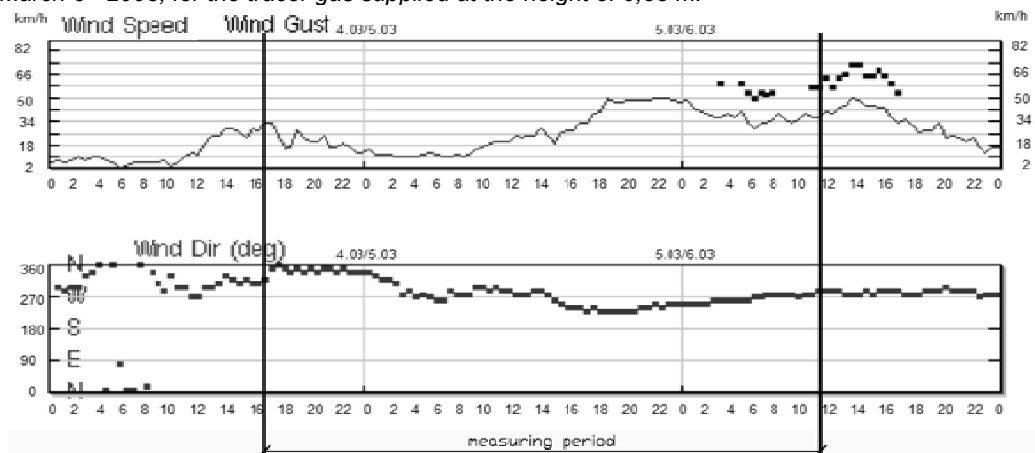
Figure 3.3 *Weather data concerning wind speed and direction from March 4th to March 6th [10].*

Because of the unusual results, the same set of experiments has been repeated during another period of 48 hours. This time, the airflow values obtained from tracer gas measurements were even more surprising, see Figure 3.4. The peaks above 40000 m^3/h and below -10000 m^3/h are thought to be unrealistic and therefore have been ignored. The results should be analyzed in correlation to the weather conditions, depicted in Figure 3.5. Again, the wind speed was quite high at the time corresponding to high airflow values. However, the most significant difference between the two measuring periods is the dominant wind direction. In the period of the most extreme results, the wind was mainly blowing from the South into the DSF. During both of the tracer gas measurement periods described the weather was cloudy and rainy, which excludes a significant influence of solar radiation [10]. This indicates a very strong affect of wind on the tracer gas experiment results, which does not necessarily correspond to the actual airflow through the DSF cavity.

It should be noted that the results of volume airflow obtained from the orifice were stable throughout the measurements and so there was no need of logging them later on.
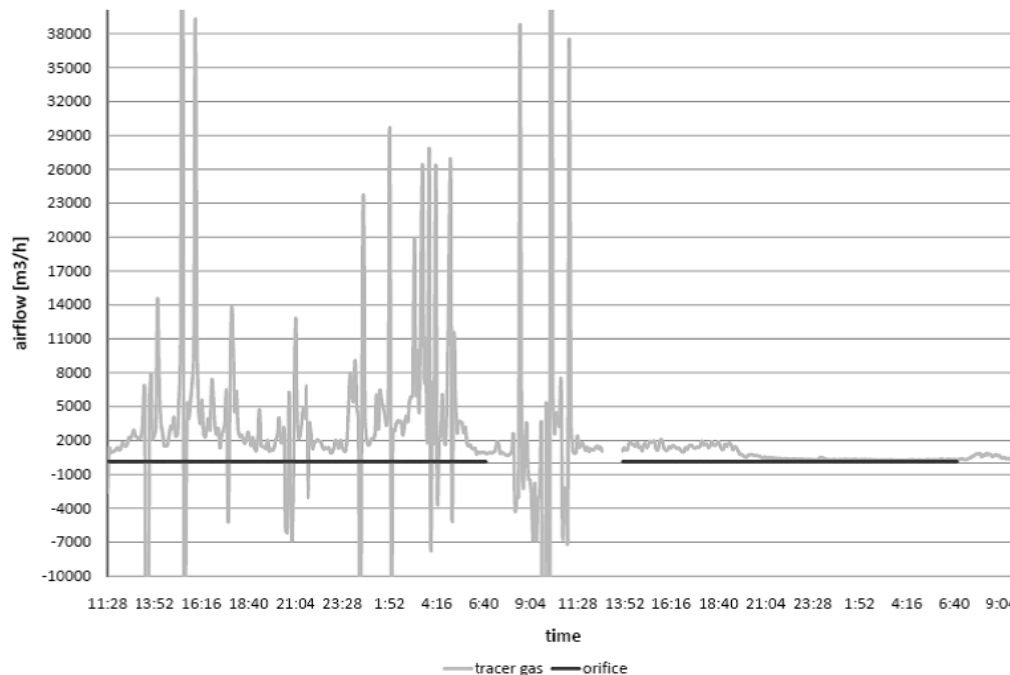
Figure 3.4 *Airflow results obtained from orifice and tracer gas measurements on March 11th and 12th 2008, for the tracer gas supplied at the height of 0,55 m.*
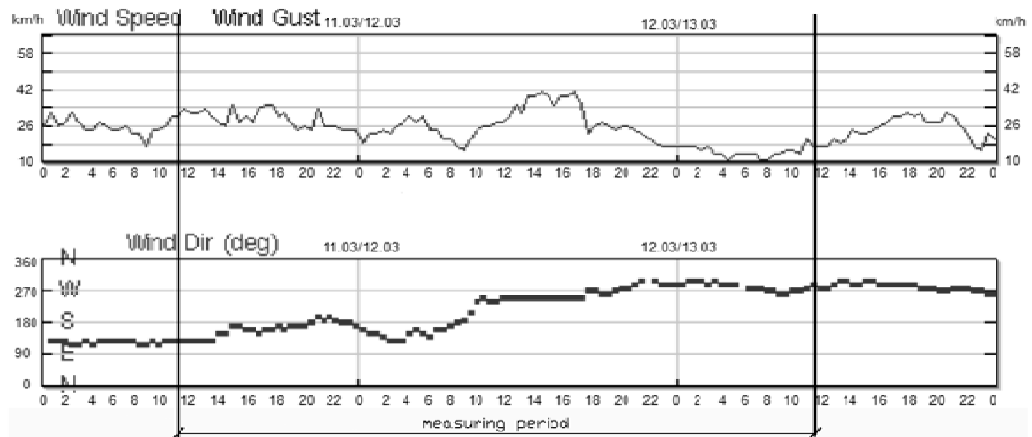
Figure 3.5 *Weather data concerning wind speed and direction from March 11th to March 13th [10].*

3.2. Tracer gas supply at 1,55 m

In order to avoid the 'wash out' effect, another set of measurements was conducted for more than 24 hours with the perforated tubes supplying CO_2 at the height of 1,55 m. Lifting the tracer gas supply gave much better results. The average airflow calculated from these experiments was 183,5 m^3/h, with peaks above 240 m^3/h, as shown in Figure 3.6. It should be noted that at the beginning of this series of experiments a new CO_2 bottle was used and therefore, the reason for the first unusually high results are thought to be unstable conditions in the experiment room. The weather conditions were similar to those from March 4th and 5th – it was cloudy, with wind speeds usually exceeding 20 km/h and the dominant wind direction was North, see Figure 3.7. Still, the results of tracer gas measurements were much closer to the performance of the mechanical exhaust installation, despite strong gusts of wind. This confirms the previous theory concerning the affect of wind speed and direction on the tracer gas measurements but not on the airflow itself.
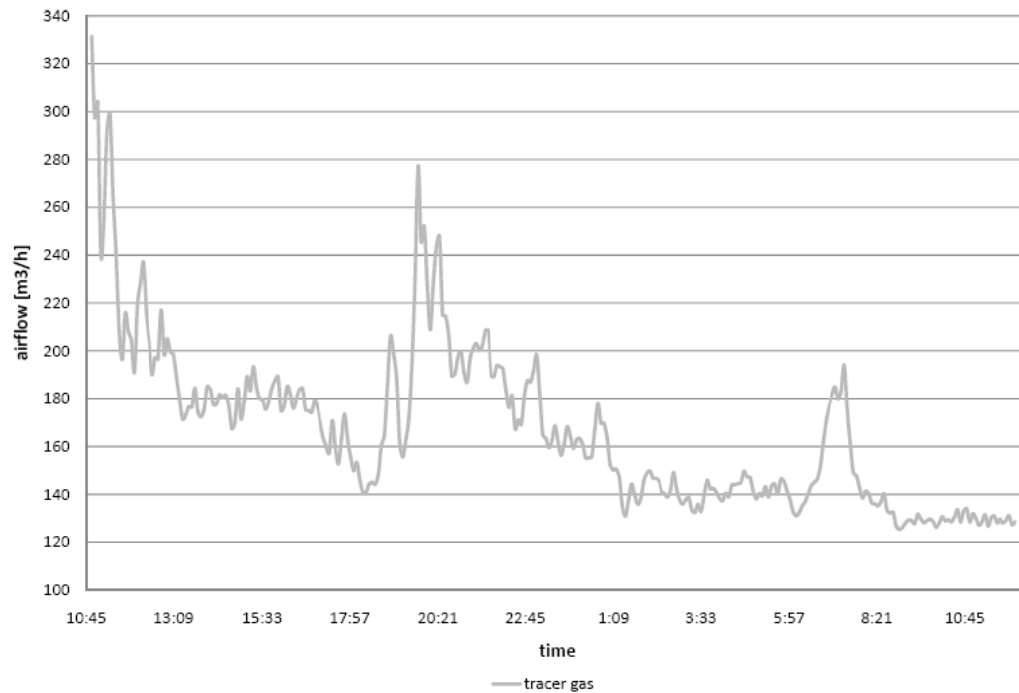
Figure 3.6 *Airflow results obtained from tracer gas measurements on March 17th and 18th 2008, for the tracer gas supplied at the height of 1,55 m.*
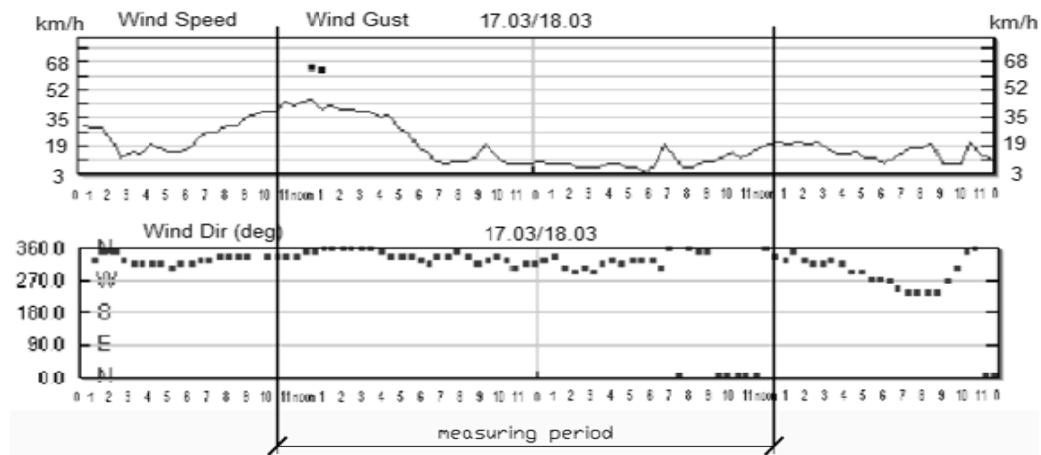
Figure 3.7 *Weather data concerning wind speed and direction on March 17th and 18th [10].*

3.3. Tracer gas supply at 2,0 m

Finally, on March 18th in the afternoon, the tracer gas supply was moved to the height of 2,0 m in order to totally eliminate the 'wash out' effect. As expected, the results gathered for over 36 hours were even more satisfying. The average airflow was 134,2 m^3/h and there were very few peaks above 200 m^3/h, as shown in Figure 3.8. The very high values at the end of the measurements are due to the CO_2 bottle getting empty. It

should be noted that the weather conditions in this case were milder than before – it was cloudy, the average wind speed was 13 km/h and the dominant wind direction was North, see Figure 3.9. However, the results of all tracer gas measurements give reason to believe that this final setup was most independent of the outdoor conditions.
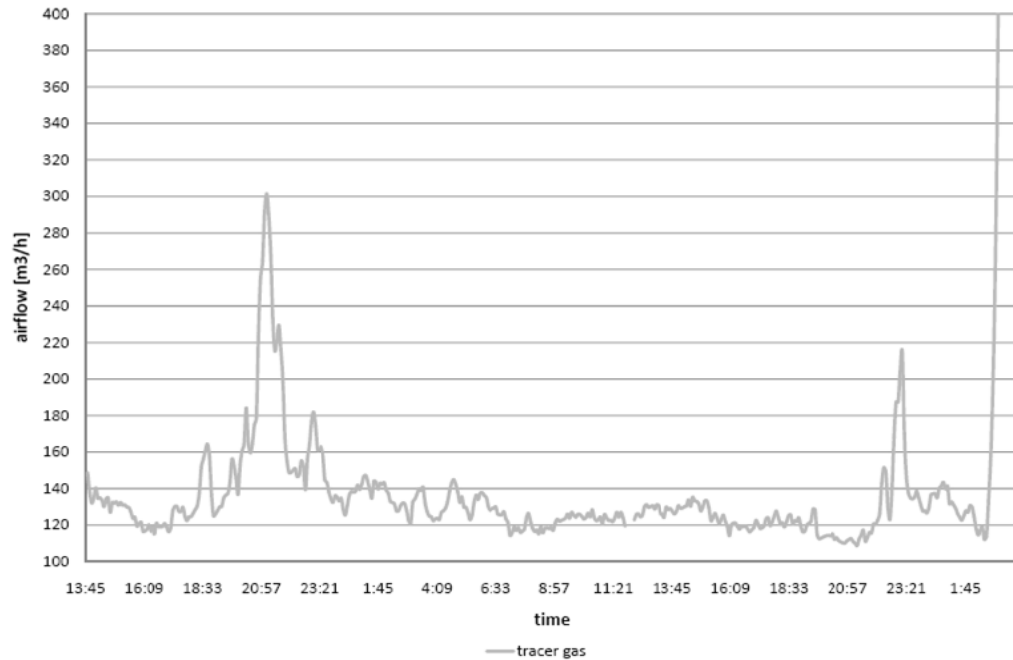
Figure 3.8 *Airflow results obtained from tracer gas measurements from March 18th to March 20th 2008, for the tracer gas supplied at the height of 2,0 m.*
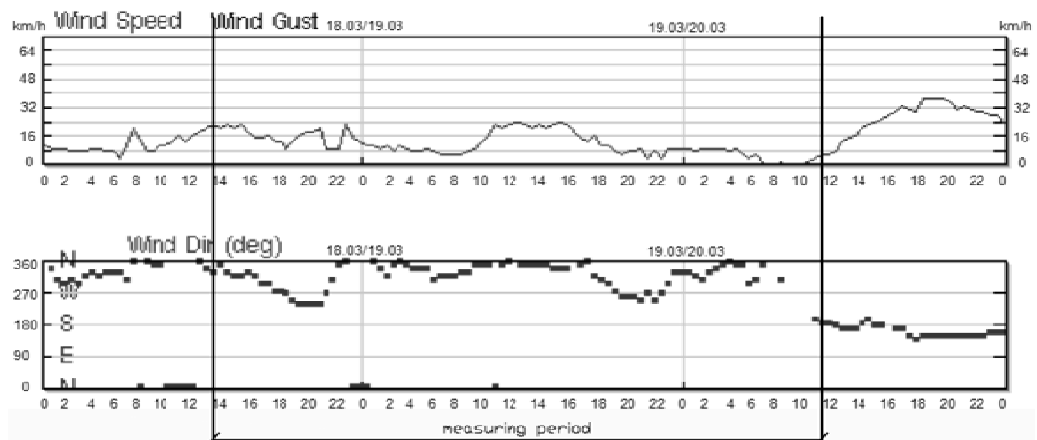
Figure 3.9 *Weather data concerning wind speed and direction from March 18th to March 20th [10].*

All of the analyzed data confirms that the mechanical exhaust system is able to sustain a constant airflow through the DSF cavity, corresponding to one exchange of the

experiment room's volume per hour, and shows the vulnerability of the tracer gas method. Another solution could be modifying the experimental setup and moving the CO_2 supply into the experiment room. The measuring point would also have to be relocated to the beginning of the mechanical exhaust installation. This would protect the perforated tubes releasing the tracer gas from the wind and would provide data on the amount of fresh air entering the room through the DSF. However, the measurements would not be sufficiently sensitive to instantaneous changes in the airflow, due to the air exchange rate of 1 h^{-1}. Therefore, it has been decided that the indications of the orifice are correct and should be relied on in any further experiments in 'the cube'. The most important conclusion it that the exhaust installation is sufficiently independent of the natural driving forces.

The described experiments also provided important insight into air mixing in the ventilated air gap when applying a mechanical exhaust system. At the bottom, where fresh air enters the DSF, the airflow is very turbulent and some of the outdoor air is exhausted without flowing through the entire cavity. However, higher in the double skin façade the fresh air gradually becomes evenly mixed and has an upward direction. Further details about the airflow inside the cavity could be revealed by smoke visualizations.

4. Measurements

In this project the measurements are divided into two types: without and with a shading devices in the cavity of the double skin facade. In the first type, named in this project DSF_1, there are two periods of measurements:

- DSF_1_1 form 09.11.2006 till 30.11.2006.
  This data was collected by Olena Kalyanova, but has been not published in any others papers. The main purpose of using them in this project is to apply the measurements results for more detailed empirical validation of 'Simple Calculation Method' and building simulation software BSim.

- DSF_1_2 from 26.04.2008 till 12.05.2008

In the second model, named DSF_SH, is only one measurement period from 14.05.2008 till 27.05.2008.

Model			DSF_1_1	DSF_1_2	DSF_SH
Measurement period			09.11 - 30.11.2006	26.04 - 12.05.2008	14.05 - 27.05.2008
Shading device			-	-	+
Measured parameters	Air temperature in DSF cavity	tc out	+	+	+
		tc in	-	+	+
	Glass surfaces temperature		+	+	+
	Shading surface temperature		-	-	+
Average outdoor air temperature [˚C]			7,5	13,4	12,2
Average global solar irradiation [W/m^2]			102,6	311,9	343,1

Table 4.1 *Different models specification.*

The energy performance, the air temperature in the DSF cavity, the temperature of the shading device in the cavity and the temperature of the glass surface are the main measurement focus of double skin façade performance.

Both, the interior and exterior environment define the boundary conditions for the DSF, and the detailed knowledge of those was essential for further application of the experimental results and evaluation of the DSF performance. The air temperature in the experiment room of 'the Cube' is kept uniform and constant at apx. 22°C to minimize the influence of the interior environment [5].

4.1.   Experimental set-up

The following chapter is mainly based on the technical report [5], where more detailed information about 'the Cube' can be found.

- **Temperature**

The temperature is measured with the thermocouples type K, silver coated, in order to reduce radiation heat exchange of the sensor [5]. All temperatures are registered with the frequency of every 60 seconds. The air temperature is measured in the engine room - tc 11 (where tc xx – is a sign for a thermocouple with the number xx) and the instrument room - tc 4. The outside air temperature is measured in 2 points - tc 67, tc 77, at the height 2 m above the ground. The ground temperature, underneath the foundation in the experiment room - tc 51, tc 52.

The temperature in the experiment room is measured by thermocouples without silver tubes at six different heights in the middle of the room (see Figure 4.1).
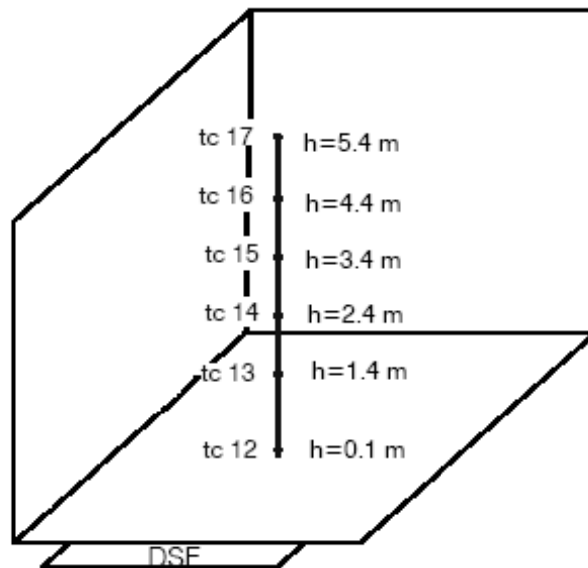
Figure 4.1 *Measuring points of the air temperature in the experiment room.*

The surface temperatures in the experiment room are measured in the middle of every wall, ceiling and floor. The sensors are glued to the surfaces with the paste of high heat transmitting property.

For measurements of the air temperature in the DSF cavity the thermocouples are protected from the influence of direct solar radiation by a silver coated and ventilated tube, the air flow through the tube is ensured by a mini-fan [5]. In both models DSF_1 and DFS_SH the air temperature is measured in 20 points. 12 thermocouples are located closer to the external glass surface of the DSF. In Figure 4.2 the position of those thermocouples is shown.
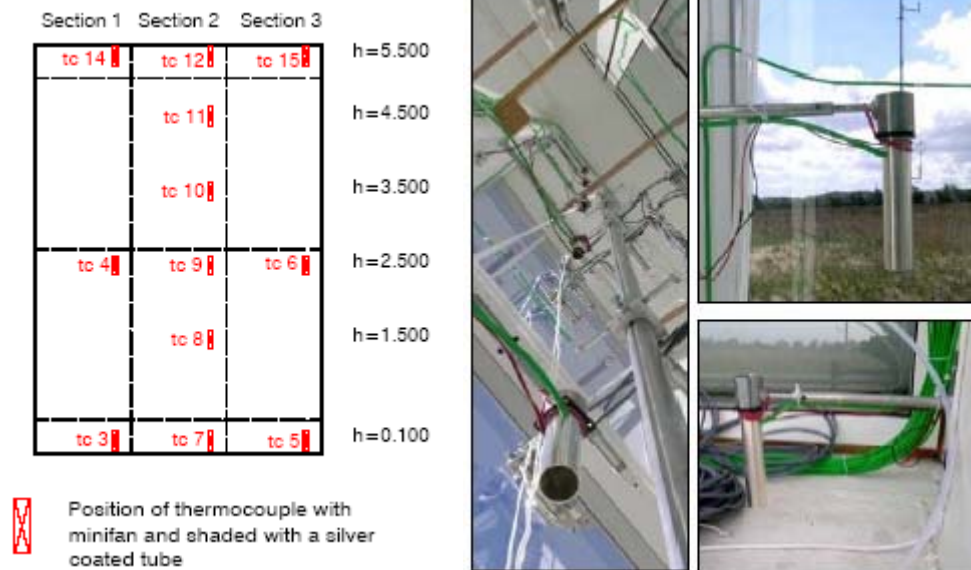
Figure 4.2 *Position of the thermocouples closer to the external glass surface of the DSF (left), view from outside. Photo of the measurement set-up (right).*

The rest of the thermocouples – 8 are located closer to the internal glass surface of the DSF. Those thermocouples are mainly used in the second model DSF_SH to measure the air temperature behind shading devices for more detailed investigation of the DSF performance with shading. In Figure 4.3 the position of those thermocouples is shown.

Position of thermocouple with minifan and shaded with a silver coated tube
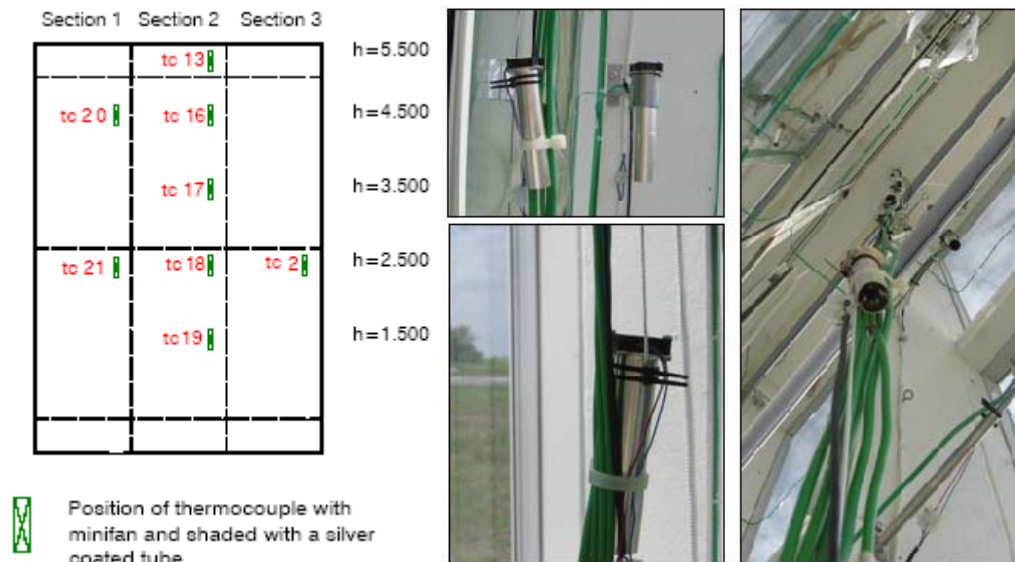
Figure 4.3 *Position of the thermocouples closer to the internal glass surface of the DSF (left), view from outside. Photo of the measurement set-up (right).*

In model DSF_SH beside more points measuring the air temperature in the cavity, there are 8 thermocouples measuring the temperature of shading devices. The thermocouples are sewed to the shading and the sensors are glued with the special conductive paste. Their position is shown in Figure 4.4.
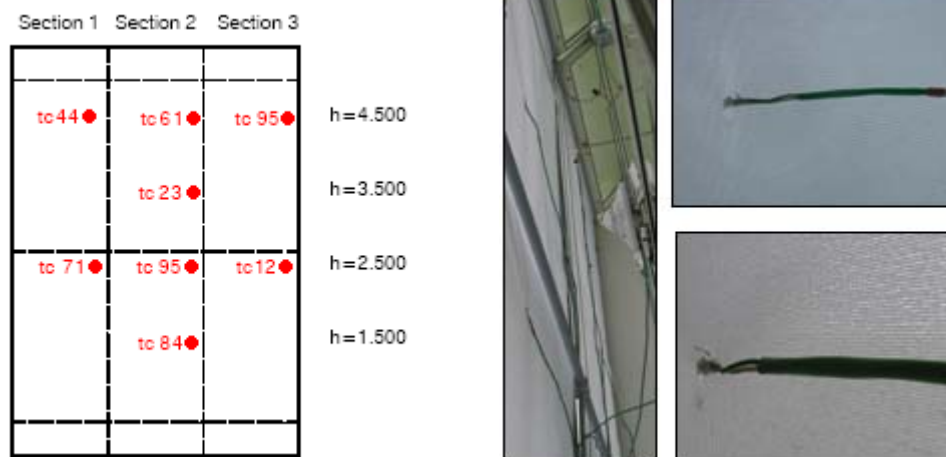
Figure 4.4 *Position of the thermocouples in the shading (left), view from outside. Photo of the measurement set-up (right).*

For measurements of a glazing surface temperature the thermocouple is placed in the centre of the glazing pane of each large window in each section (BOL, BIL, BOH and BIH windows). At the inner skin the temperature is measured at both internal and external surface, at the outer window only at the internal surface. The sensors are

protected from direct solar radiation. Shading of the thermocouples sensors at the inner pain is ensured by a thin aluminium foil fixed around the sensor at the external surface. As a result the foil shaded both the sensors at the external and internal surfaces. The thermocouples at the internal surface of the outer pane are shaded in a similar way by a piece of aluminium sticky tape on the external surface of the outer pain.

In the experiment is assumed that the inlet air temperature to the DSF cavity is the same as the outdoor temperature. The outlet air temperature is measured the same way as the air temperature in the cavity, with thermocouples protected from solar radiation by silver coated and ventilated tubes with mini-fans. The sensors are placed at the middle of top opening in section 1 and 3 (SIH1 and SIH3) see Figure 4.5.

Figure 4.5 *Photo of measurements set-up.*

- **Solar radiance**

For purpose of weather data assembling two pyranometers are placed horizontally on the roof of 'the Cube' (see Figure 4.6). BF3 pyranometer measures global and diffuse solar irradiation on the horizontal surface. The second pyranometer, Wilhelm Lambrecht, measures only global solar irradiation on the horizontal surface in order to control the readings from BF3.
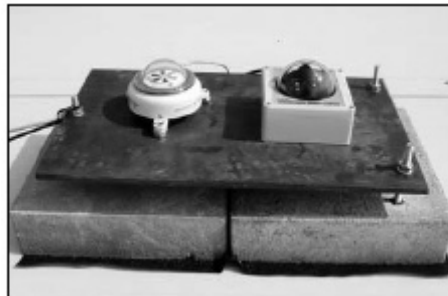
Figure 4.6 *Photo of pyranometers on the roof of 'the Cube', Wilhelm Lambrecht pyranometer at the left and BF3 at the right.*

To measure the total solar radiance received on the external surface of the DSF, total solar radiation transmitted into the DSF and into the experiment room three more pyranometers are used. Wilhelm Lambrecht-pyranometer for measuring the solar radiation received on the DSF external surface, CM11-pyranometer from Kipp&Zonen

for solar radiation transmitted into the DSF and CM21- pyranometer, from Kipp&Zonen for solar radiation transmitted into the experiment room. Pyranometers were installed on the same horizontal distance from each other, in the centre of the DSF surface (see Figure 4.7). However, in order to apply the results assembled by pyranometer CM21 and CM11, this data has to be adjusted to the view factors calculated for the complex geometry in the DSF, as the window frames cover a wide part of the pyranometers' 'view'. All readings from pyranometers are registered with the frequency of every 10 seconds
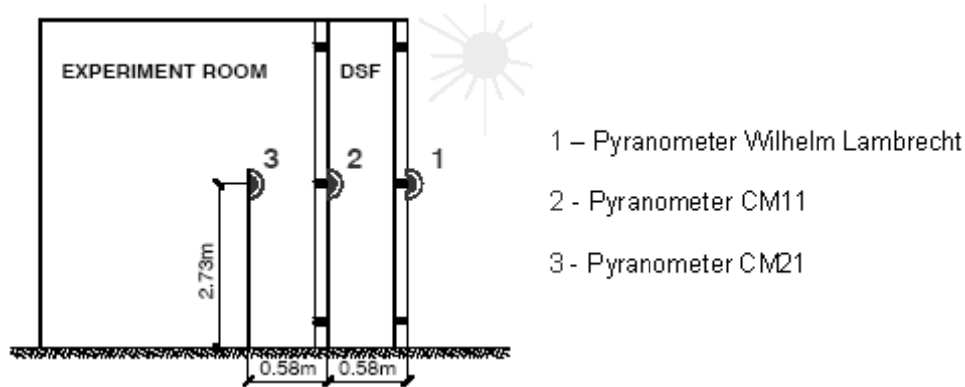
Figure 4.7 *Position of the pyranometers in the experimental set-up.*

- **Climate data from the Danish Meteorological Institute (DMI)**

The measurement procedure described in this project is complex and required a lot of the devices to measure and record the data simultaneously. Thus the pauses in measurement are necessary to offload the data recorded at the high frequencies to release the memory capacity and prolong the long lasting experiments.

Since the complete set of the climate data is required for the empirical validation of the building simulation software – BSim, than the measurement pauses have to be filled in with the reliable data. This has been purchased for a weather station located near by the experimental test facility, from the Danish Meteorological Institute (DMI), which is responsible for planning, establishing and operating DMI's operational observation network and measurement stations at several hundred locations in Denmark. The atmospheric pressure was not measured at 'the cube', but the data from DMI is used instead for.

- **Air conditioning system in the experiment room**

Air conditioning system recirculating the air and maintaining stable conditions in the experiment room is equipped with a fan, cooling and heating unit. In the cooling unit water is used. To avoid condensation on the surface of the cooling unit the minimum water temperature was set to $12^{o}C$, this resulted in a large area of the cooling surface and size of the whole system. The difference between the supply and return water temperature from the cooling unit in the experiment room is measured as voltage in mV, the maximum error of this measurement was $0.1^{o}C$. The mass flow of the water supplied to the cooling unit is measured with a water flow meter MULTICAL from Kamstrup,

which measures in a range from 0 to 1kg/s and can have a total error of ±0.2% of the range. The heating unit is electrical and the electrical power used by the unit is added to the electrical power used by fan. The temperature difference and the water mass flow in the cooling unit as well as the electrical power used by heating unit and fan are registered at a frequency 0.1Hz.

4.2. Results

The aim of the measurements was to assess the energy performance of the double skin façade and gather information about the parameters influencing it. The main focus, apart from the heating and cooling energy consumption of 'the cube', were the air and surface temperatures measured in the DSF as well as the solar irradiation at the location of the test facility. The results shown below have been compared with the simple calculation method and BSim simulation results in later chapters. All of the figures as well as hourly averages of measured values can be found in the relevant Excel file on the attached CD.

When analyzing temperature gradients, whether in the DSF cavity or on a horizontal plane across the DSF, dimensionless temperatures were considered. Dimensionless temperature is defined as shown in Equation 4.1.

$$\frac{t_x - t_e}{t_i - t_e}$$

Equation 4.1 *Dimensionless temperature, where: t_x is the temperature measured in point x, t_e – external air temperature, t_i – temperature in the experiment room.*

Such values give a better understanding of the relative conditions at the time of measurements and the heating or cooling potential of the considered mode. 0 corresponds to temperatures equal to the outdoor temperature and 1 to the internal temperature. Values below 1 show the heating potential of the DSF and above 1 the created cooling load in the experiment room.

4.2.1. DSF_1_1

This chapter presents the analysis of measurement results performed in 'the cube' by Olena Kalyanova from November 9th till 30th 2006. Firstly, the temperature gradient inside the experiment room was analyzed in order to validate the experimental set-up. Two hours were chosen: 23:00 am on November 13th representing the minimum global solar irradiation of 0 W/m^{2} and 12:00 on November 11th corresponding to the maximum solar irradiation of 240,34 W/m^{2}.
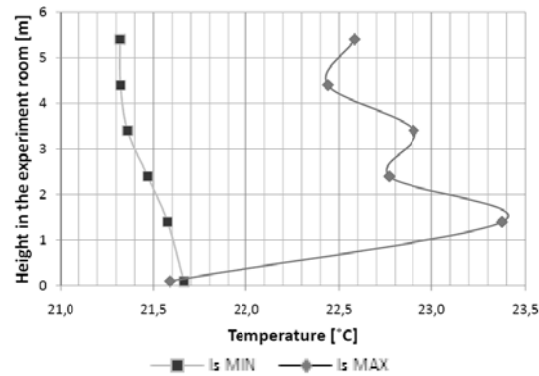
Figure 4.8 *Hourly averages of the vertical temperature gradient in the experiment room for both the minimum and maximum value of global solar irradiation during the DSF_1_1 measurements.*

Clearly, during periods of higher solar gains the air supplied at the floor level has to be colder in order to maintain a stable temperature in the room. However, in either case the air temperature measured at different heights does not differ by more than 1,8 ˚C. It should be noted that the above temperature gradients are based on measurements performed with silver-coated thermocouples, which are not placed in special silver tubes with fans, see chapter 4.1. This results in a higher influence of solar irradiation on measurement results. The temperature in the experiment room has also been measured by one silver-coated tc placed in a silver tube with a fan on the same pole as the other thermocouples at the height of 2,5 m. The readings obtained from it have been compared with the temperatures measured at the height of 2,4 m on the pole, see Table 4.2. The influence of solar irradiation on the measurement results obtained from the tc placed in the silver tube with a fan is very small. Therefore, the temperature gradient formed from values measured by tc without silver tubes is thought to be unreliable and is not considered in further analysis. For practical reasons it has been assumed that there is no temperature gradient inside the experiment room.

	11.11.2006 12:00	14.11.2006 1:00
Global solar irradiation [W/m^2]	240,3	0
tc without ventilated silver tube at 2,4 m	22,77	21,47
tc with ventilated silver tube at 2,5 m	21,85	21,59

Table 4.2 *Comparison of hourly average values of temperature in the experiment room measured by different tc types during the time of maximum and minimum solar irradiation, for mode DSF_1_1.*

Figure 4.9 shows the measured energy consumption. It was mainly caused by the heating need, which during the entire measurement period summed up to 595,55 kW. Values below 0 stand for the cooling demand. The heating load was quite even throughout the period of the experiments, with the average value of 1,21 kW. However, several rapid cooling peaks appeared mainly between 16:00 and 18:00 on sunny days. This resulted in a total energy use for cooling of 39,68 kW and an average cooling load

of 1,1 kW. When considering absolute values, the energy usage both for heating and cooling during the entire experiment period was 635,23 kWh (28,87 kW/day).
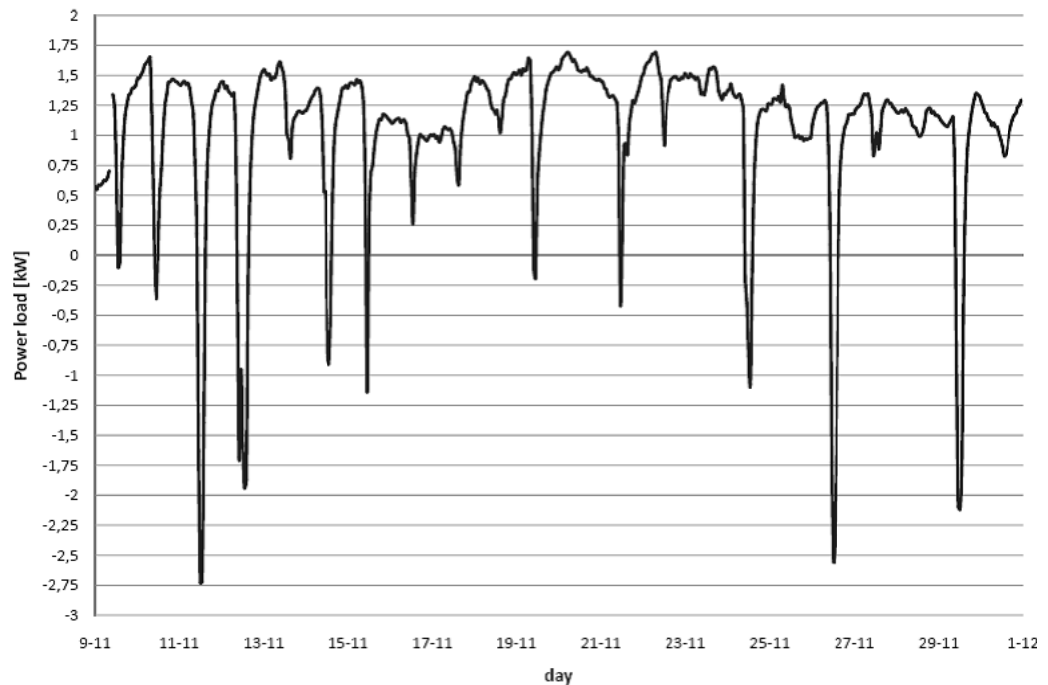
Figure 4.9 *Hourly averages of measured energy consumption, based on results from DSF_1_1.*

An example of a cooling peak has been analyzed more closely for November 11th, when the maximum cooling load of 2,73 kW and the highest value of global solar irradiation measured at the location of the cube of 240,3 W/m^2 appeared, see Figure 4.10. It is clear that the cooling peaks take place just after the time of most intensive solar irradiation, which is the effect of heat accumulation both in 'the cube's' opaque constructions and the indoor air. The cooling peak appears one hour after the highest solar irradiation and two hours after the highest outdoor temperature of 10,2 °C. It seems that at this time of year solar radiation has a bigger influence on the cooling load than the outdoor air temperature. This has also been recognized when looking at the air temperature gradient inside the DSF.
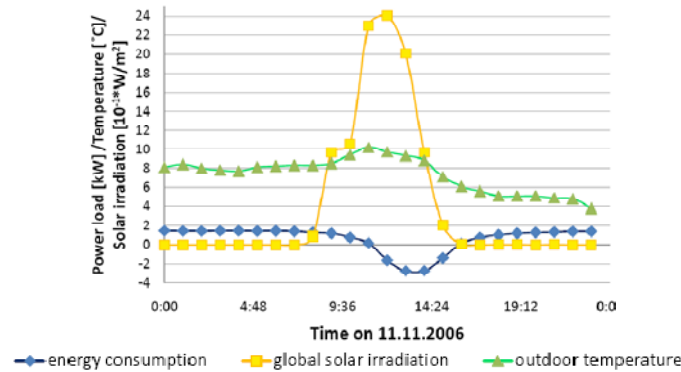
Figure 4.10 *Comparison of hourly averages of power load, global solar irradiation and outdoor temperature, measured on November 11th 2006.*

The average global solar irradiation from the entire measurement period is 33,4 W/m², when taking into consideration only values above 0. This was the basis for defining three ranges of solar irradiation: 0 to ≤ 15 W/m² representing low values, 15 to ≤ 50 W/m² for average values and above 50 W/m² for high solar irradiation. For each of these ranges average temperatures at different heights of the DSF were calculated and formed the dimensionless temperature gradients shown in Figure 4.11. It should be noted that there was an attempt of creating temperature gradients for a bigger number of smaller solar irradiation ranges. However, this approach gave unsatisfactory results, because the ranges were too small to correctly take into consideration the delayed effect of solar irradiation on the air temperature due to heat accumulation.

The unusually high temperature noted at the height of 0,1 m is thought to be a result of error, see Figure 4.11. This thermocouple was placed very close to the concrete floor of the DSF cavity, which accumulated solar energy in the form of heat. The inlet to the silver tube, in which the tc was placed, was just a few mm above the floor. This probably caused the tc to measure the temperature of air heat up by convection from the floor. Therefore, this point has not been considered in further temperature gradients. A corrected temperature gradient in the DSF cavity has also been shown in Figure 4.11 (right).
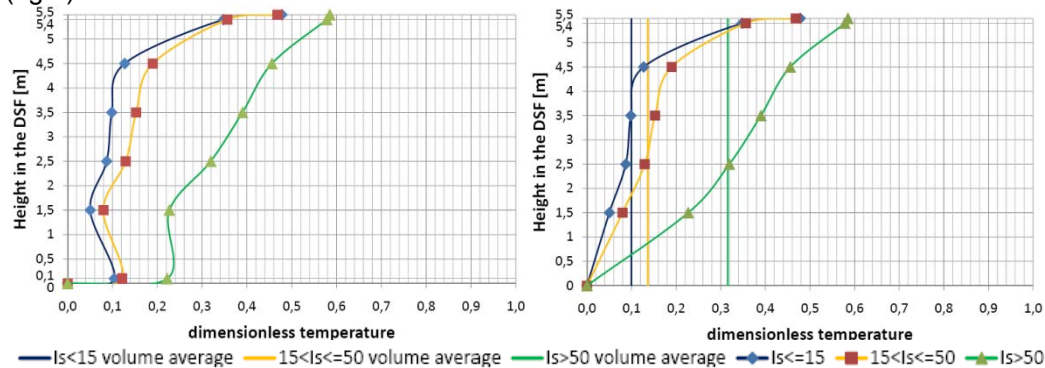
Figure 4.11 *Vertical temperature gradient inside the DSF, based on hourly averages of values measured for DSF_1_1 (left). Vertical temperature gradient inside the DSF excluding the measurement point at 0,1 m, based on hourly averages of values measured for DSF_1_1 (right).*

The vertical lines in Figure 4.11 represent the dimensionless mean volume average temperature in the cavity for each solar irradiation range. These temperatures correspond better to the heat loss through the DSF due to heat transfer from the experiment room. The values are: 8,61 ˚C for low, 10,14 ˚C for average and 12,77 ˚C for high values of solar irradiation. For each range the temperature gradients inside the DSF have a similar shape, but become more tilted with the increase in solar irradiation. The air in the cavity is heat up by 6,9 ˚C for lower solar irradiation and up to 7,7 ˚C for high solar irradiation, which results in a substantial decrees in the energy need for heating. The heating potential of the DSF in this case varies between 48 % and 59 %. The difference in the outdoor air temperature for the low and high solar irradiation is only 1,47 ˚C, but the difference for the outlet temperature is higher – 2,2 ˚C. This confirms the importance of the effect of solar irradiation on the energy consumption.

This conclusion has also been depicted in Figure 4.12, where the power load is shown in function of the global solar irradiation. According to the trend line, even values of solar irradiation as low as 105 W/m^2 cause a cooling load. This stresses the need for shading of double skin façades.
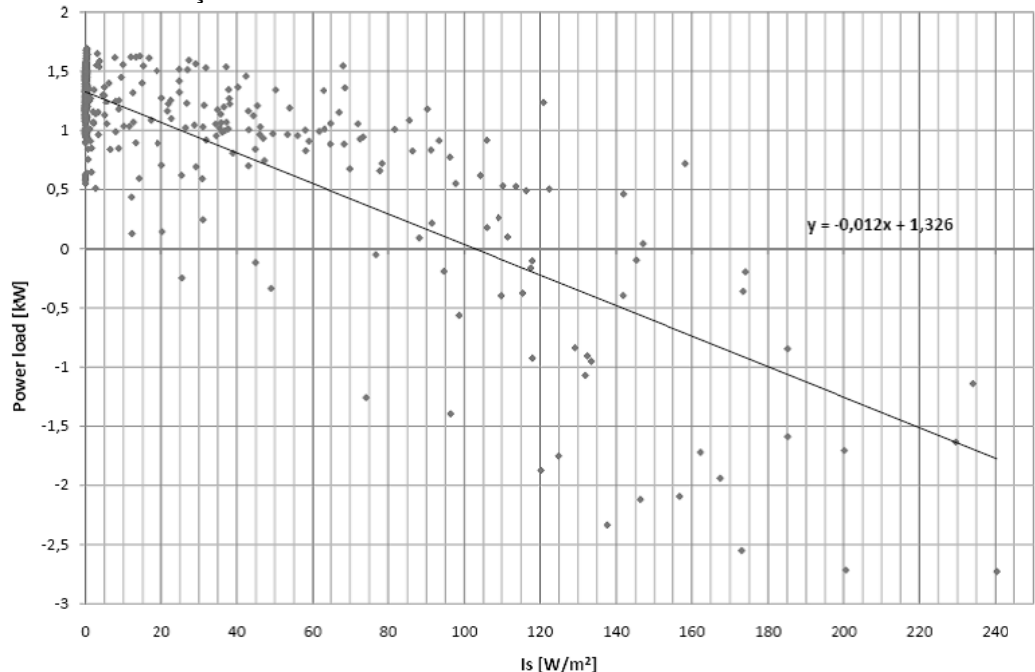
Figure 4.12 *Hourly values of measured power load depending on the global solar irradiation at that time, based on DSF_1_1 measurements.*

Figure 4.13 illustrates the dimensionless temperature gradient on a horizontal plane through the DSF cavity at the height of 2,5 m in the case of the lowest global solar irradiation of 0 W/m^2 and the highest – 240,3 W/m^2. In the first situation there is a hardly noticeable difference in temperature – only 2,3 ˚C on the whole line segment between the outdoor air and the external surface of the inner skin. The rapid increase of temperature values on both sides of the internal DSF window is due to the argon filling, which provides very good thermal insulation. The case of high solar irradiation gives

different results. There is a significant rise of 8,6 ˚C in the air temperature between the outside and the inside of the DSF cavity. This confirms the influence of solar irradiation on the air temperature, similar as the one used in greenhouses. In general it can also be said that the temperatures of the glass surfaces are higher than the air's. The reason for this is that transparent elements absorb part of the solar irradiation in their entire volume and the result is similar to an internal heat source placed in the glass.
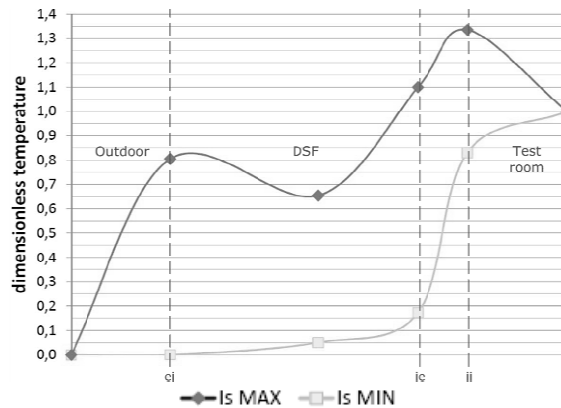
Figure 4.13 *Horizontal temperature gradient through the DSF, based on hourly averages of DSF_1_1 measurements. The dashed lines stand for: ei – external window's internal surface, ie – internal window's external surface, ii – internal window's internal surface*.

4.2.2. DSF_1_2

The analysis of data gathered at the cube from April 24th till May 12th 2008 has been presented below. This time the experiment set-up was very similar to the one of DSF_1_1. There was no shading device and a set of thermocouples placed closer to the internal skin was added. It is interesting to compare the results of mode DSF_1_2 with DSF_1_1, as the measurements took place at different seasons of the year.

The total energy consumption both for heating and cooling of the experiment room measured during the period of 17 days was 414,09 kWh (24,42 kW/day). Unlike in the case of DSF_1_1, the energy usage is mainly due to the cooling load, see Figure 4.14. The total energy need for cooling is 241,94 kW and for heating 172,15 kW. In the latter half of the measurement period, when the weather was warmer and more sunny, the energy consumption falls into a 'rhythm' of high daily cooling peaks corresponding to the time of the highest global solar irradiation. To investigate this phenomenon in more detail the energy consumption, global solar irradiation and outdoor temperature have been compared for two days.
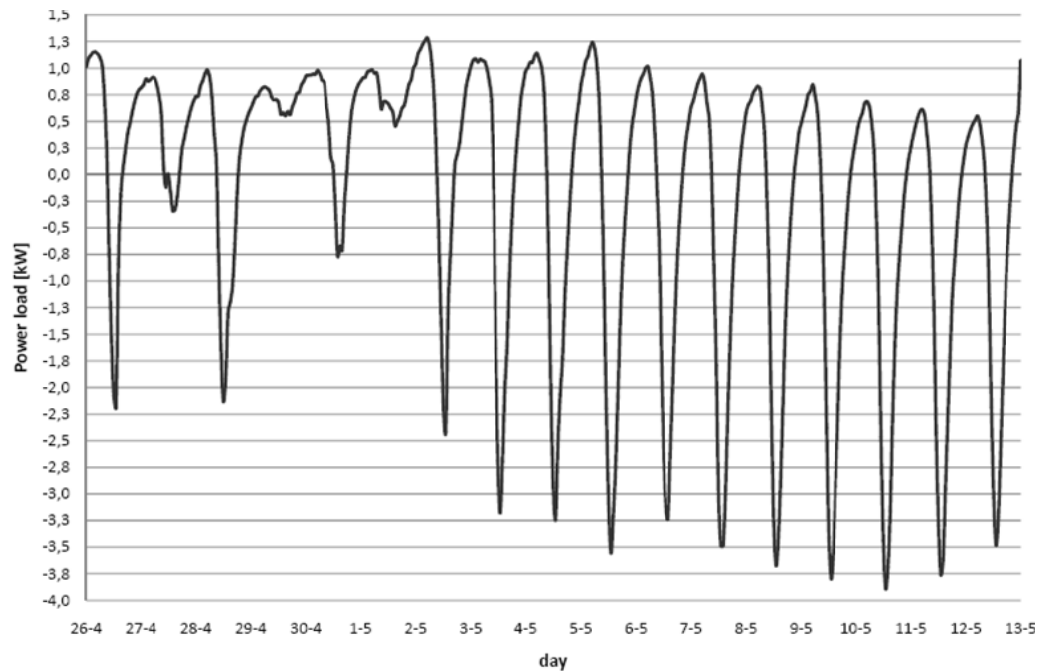
Figure 4.14 *Hourly averages of measured energy consumption, based on DSF_1_2 results.*

Figure 4.15 shows the hourly values during May 3rd, when the cooling demand and global solar irradiation were high, but the external air temperature was not. It also compares the same values for May 11th, but this time not only the energy consumption and the solar irradiation were high but also the outdoor temperatures. The difference in the maximum cooling load and solar irradiation between those two days is only 0,58 kW and 17 W/m^2, respectively. Whereas the difference in the maximum temperatures which have occurred in that time is 11,25 ˚C. In both cases there is no time lag after the occurrence of the maximum value of solar irradiation and the cooling peak. However, the distribution of solar irradiation during the day is more even on May 11th. This must have been an important factor in the slight increase of the energy consumption on that day. The above analysis indicates that solar irradiation has a bigger influence on the energy consumption than the external air temperature. Of course, both of those values are linked to each other. However, this is an important factor when considering solar shading of double skin façades.
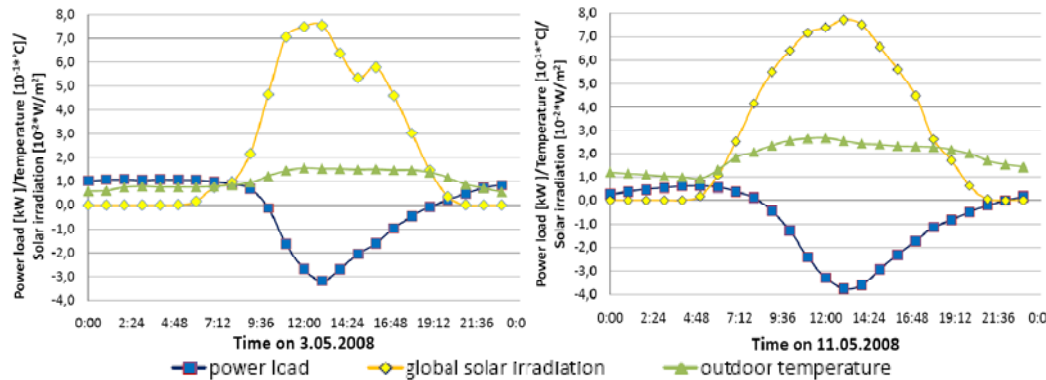
Figure 4.15 *Comparison of hourly averages of the power load, global solar radiation and external air temperature during 3rd May 2008, for DSF_1_2 measurements (left).Comparison of hourly averages of the power load, global solar radiation and external air temperature during 11th May 2008, for DSF_1_2 measurements (right).*

The influence of solar irradiation is also visible when analyzing the temperature gradient inside the DSF. The average global solar irradiation during the measurement period was 312 W/m^2, when considering only values above 0. As in the case of DSF_1_1, three ranges of solar irradiation were defined: 0 to ≤ 200 W/m^2 representing values below average, 200 to ≤ 400 W/m^2 for average values and above 400 W/m^2 for high solar irradiation. The results of dimensionless mean temperature values measured at different heights by both thermocouples placed closer to the internal skin and those near the external window as well as the mean volume average temperature are shown in Figure 4.16. High solar irradiation may warm up the fresh air even by 14,2 °C, which in this case is no longer beneficial for the energy consumption of the cube. In fact only temperature gradients from the first and second range give values which help decrease the power load by preheating the fresh air and give a heating potential of 92% and 115%, respectively. For high values of global solar irradiation (in this case above 400 W/m^2) it is necessary to reduce the cooling load, for example by mounting a shading device in the cavity.
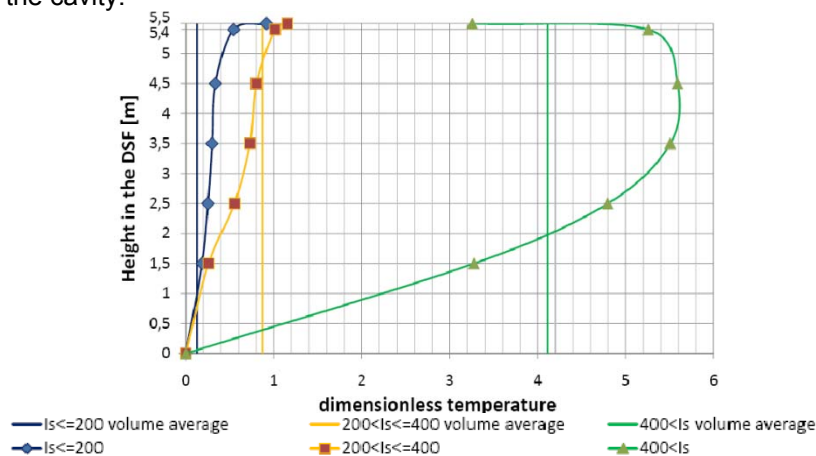
Figure 4.16 *Vertical temperature gradient inside the DSF, based on hourly averages of values measured for DSF_1_2.*

It is interesting to see that in the case of low and average solar irradiation, the outlet temperature (shown as the highest point on the graphs in Figure 4.16) is higher than the one in the DSF. However, for periods of high solar irradiation it is the opposite situation. This indicates that in the first two cases the air inside the experiment room had to be heated to reach the desired temperature. However, when the solar irradiation is too high, the effect of preheating the incoming air has a negative effect on the cube's power load, because the indoor air has to be significantly cooled.

It should be noted that the measurement point for the outlet air temperature was placed in the upper opening of the internal DSF window, on the border between the experiment room and the double skin façade. This means that the indoor air temperature had a significant influence on the measurements, due to the angle at which the ventilated silver tube protecting the thermocouple was placed. This error of the experimental set-up did not occur earlier in the DSF_1_1 model, but repeated itself in the DSF_SH measurements. Therefore, when comparing the temperature gradient in the DSF obtained from the DSF_1_2 and DSF_SH measurements with the simple calculation method or BSim simulation results in later chapters, the outlet point at 5,5 m should not be taken into consideration. The final point of the temperature gradient in those cases, treated as the outlet, is the temperature measured at the height of 5,4 m, where the influence of the temperature inside the experiment room is much smaller, see Figure 4.16.

The correlation between the global solar radiation and the power load at that time has been shown in Figure 4.17. The trend line is tilted at almost the same angle as for model DSF_1_1, but cooling loads appear at lower values of solar irradiation – above 180 W/m^2. This is probably due to higher outdoor temperatures at the time of measurements. The data displayed on the graph gives more reliable results than in the case of DSF_1_1, because this time cooling loads took place nearly as often as heating ones.

Figure 4.17 *Hourly values of measured power load depending on the global solar irradiation at that time, based on DSF_1_2 measurements.*

Finally, the horizontal gradient across the DSF at the height of 2,5 m for the case of the lowest global solar irradiation of 0 W/m^2 (measured on April 27th at 3:00 am) and the highest global solar irradiation – 783,5 W/m^2 (measured on May 12th at 1:00 pm) has been shown in Figure 4.18. As was the case for DSF_1_1, the protection of the argon layer inside the internal window is quite significant. This allows to reduce the heat gains / losses due to heat transfer through the DSF and so stresses the importance of solar irradiation when considering the energy consumption.
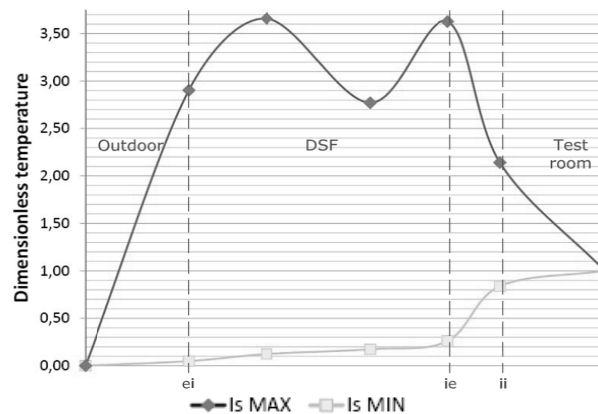
Figure 4.18 *Horizontal temperature gradient through the DSF, based on hourly averages of DSF_1_2 measurements. The dashed lines stand for: ei – external window's internal surface, ie – internal window's external surface, ii – internal window's internal surface.*

Again, the heat accumulation in the glass surfaces facing the inside of the DSF is very noticeable. At the time of high solar irradiation the air temperature measured near the internal skin is lower than the one measure closer to the outside by 5,3 °C. However, the temperatures of the internal surface of the outer window and the external surface of the internal skin are in opposite correlation. It should be noted that glass acts in this case like a heat source, because it accumulates solar energy and releases it to the air. Therefore, it is impossible for the air in the DSF cavity to have a higher temperature than the glass surface. The values shown in Figure 4.18 are thought to be a result of 'back flow', which means that warmer air from higher parts of the DSF flows back down. However, this phenomenon requires more insight and is not discussed further in this report.

4.2.3. DSF_SH

The analysis of data gathered at the cube from 14th till 27th May 2008 has been presented below. The experimental set-up is almost the same as in the DSF_1_2, but in DSF_SH model the shading devices in DSF cavity has been mounted, see Figure 2.12. The outdoor conditions during the measurements were very similar to the ones in second half of DSF_1_2: sunny days with high solar irradiation and outdoor temperature during daytime mostly above 15°C. Therefore, it will be easily to estimate the energy savings caused by the shading devices.

As mentioned in chapter 4.2.1 the thermocouples measuring the air temperature in the experiment room were not placed in the silver tubes with a fan and direct solar radiation influenced the measurements results. However, in DSF_SH model because of shading device, direct solar irradiation is not entering the experiment room. In this situation the temperature gradient inside the experiment room is analyzed. As in model DSF_1_1 two hours, representing boundary conditions, were chosen: 3:00 am 25th of May with minimum global solar radiation of 0 W/m^2 and 1:00 pm of May representing the maximum global solar radiation of 834,5 W/m^2, see Figure 4.19
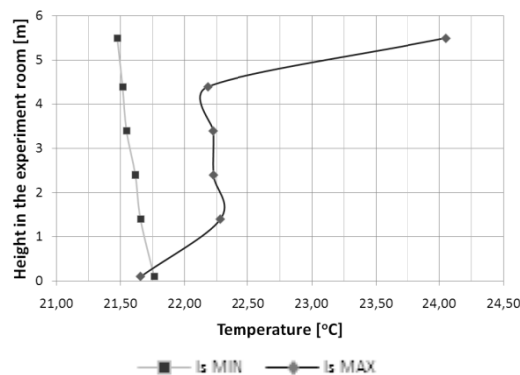
Figure 4.19 *Hourly averages of the vertical temperature gradient in the experiment room for both the minimum and maximum value of global solar irradiation during the DSF_SH measurements.*

It is clear that in the periods with no or low solar gains in the experiment room, there is no temperature gradient. In the case with high global solar radiation hitting the DSF the air in the experiment room between heights 1,4m and 4,4m is almost constant. The air

supplied at the floor level has lower temperature in order to maintain a stable temperature in the room. The temperature of the air supplied into the room from the DSF cavity influences the readings from the measurement point at 5,5m. It is so called 'Coanda' effect, when the stream of fluid 'sticks' to the nearest surface. In this case the fresh air flows along the ceiling and increases the temperatures. This could cause a potential drawback to occupants' comfort, when applying DSFs to a real office building. In general in DSF_SH, as in DSF_1_1 and DSF_1_2, it is assumed that there is no temperature gradient in the experiment room.
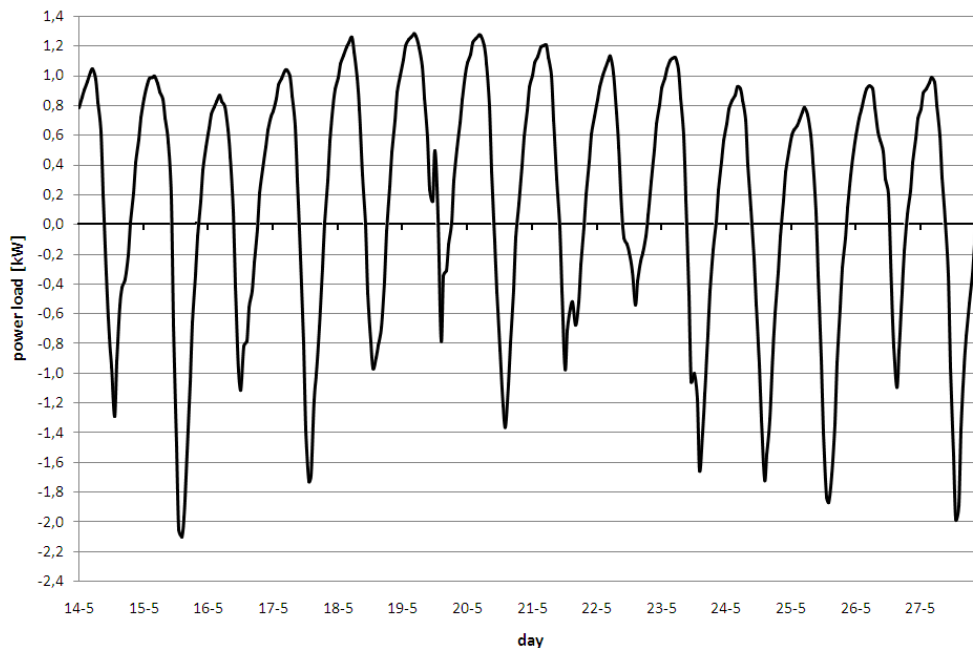
Figure 4.20 *Hourly averages of measured energy consumption, based on results from DSF_SH.*

Figure 4.20 shows the measured energy consumption. In DSF_SH there was no significant domination of either heating or cooling load during the measurement period. The energy need for heating during the entire period summed up to 149,25kW, which corresponds to 60% of total energy consumption both for cooling and heating. The cooling loads appeared of course on sunny days with high solar radiation giving the average of 0,76 kW and total energy usage of 96,43 kW. When considering the absolute values, the total energy needed for both heating and cooling during the whole experiment period was the lowest of all models 245, 68 kWh (17,55 kW/day).

More detailed investigation of energy consumption in DSF_SH model has confirmed the theory mentioned in chapter 4.2.2, that it depends more on solar radiation than on the outdoor temperature. The shading device used in DSF_SH has reduced the values of hourly peaks and the period of the cooling loads, thereby total usage of the energy.

The solar shading device has also an influence on the temperature gradient in the double skin façade. The average global solar irradiation from the entire measurement period is 343,1 W/m^2, when taking into consideration only values above 0. As in

DSF_1_1 and DSF_1_2, three ranges of solar irradiation were defined: 0 to ≤ 200 W/m^2 representing values below average, 200 to ≤ 450 W/m^2 for average values and above 450 W/m^2 for high solar irradiation. The position of the shading device in the DSF cavity divides the air-gap into two 'zones': in front of (closer to the external skin) and behind the shading. Therefore, in DSF_SH model two dimensionless temperature gradients are made for each position of thermocouples, see Figure 4.21.
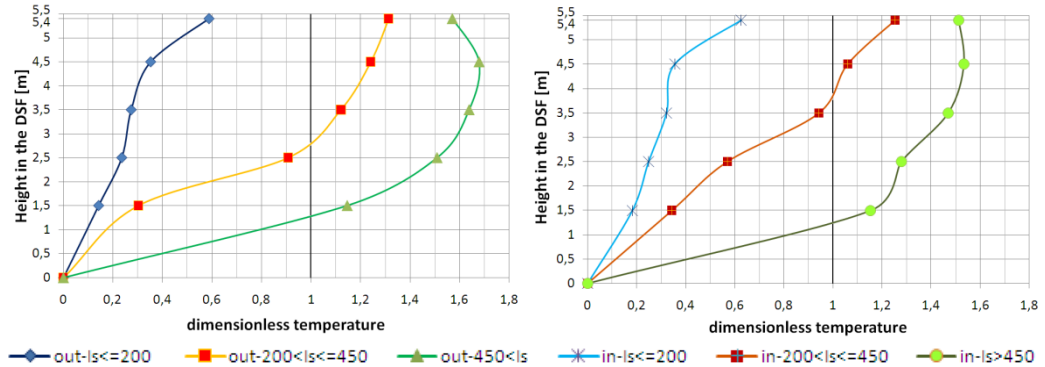
Figure 4.21 *Vertical temperature gradient inside the DSF in front of the shading device (left), behind the shading device(right), based on hourly averages of values measured for DSF_SH.*
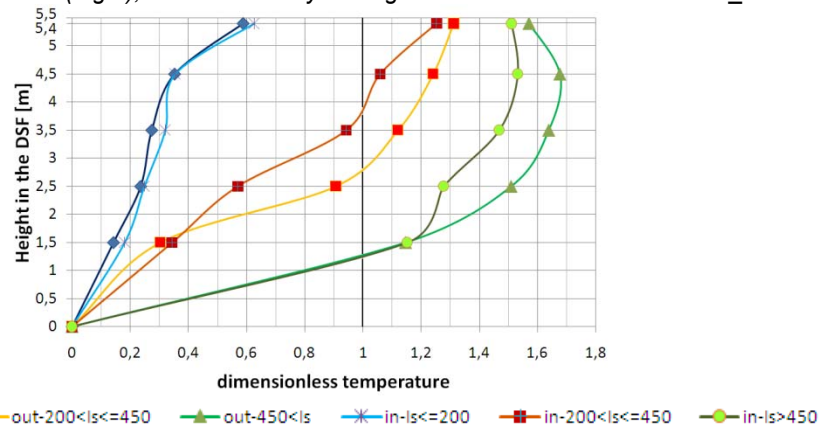
Figure 4.22 *Vertical temperature gradient inside the DSF in front of and behind the shading device, based on hourly averages of values measured for DSF_SH.*

In the first range, when solar radiation is below 200 W/m^2, the shape of the vertical gradient is almost the same in front and behind the shading and differs from the others ranges of solar radiation. In this case influence of the shading device on the temperature gradient behind it is unnoticeable. For both thermocouples stes the air in the cavity is heat up by 8,5^{o}C, which results in savings in the energy need for heating the air in the experiment room. The heating potential of the DSF with solar radiation lower than 200 W/m^2 is around 60%.

From Figure 4.22 it is clear, that with solar radiation between 200 and 450 W/m^2 the shading device fulfils its role and protect test room from too high solar radiation and excessive heat gains. The best example is the measurement point at the height of 3,5m,

where behind the shading the temperature in the cavity is slightly lower than in the experiment room and with the outlet point at this height the incoming air would be preheated and in consequence decrease the energy need for heating. As in the same height, but on the other side of the shading the incoming air would overheat the room and increase the cooling need. In reality with the outlet point at 5,4m the air temperature in front of and behind the shading is higher by 31% and 25%, respectively, than the air in the room. In fact the air from both sides of the shading device flows into the experiment room as one so the fresh incoming air from the DSF cavity has a heating potential too high by 28%. This results an increase in the energy need for cooling and finally in the total energy consumption.

For the solar radiation over 450 W/m^2 the air temperature at 1,5m for both thermocouple poles is higher than in the experiment room. The temperature of the outlet air increases the energy need for cooling for about 60% - for the thermocouples in front and 50% for the ones behind the shading, which together results in 55%.

The volume average temperatures were calculated for every global solar radiation range. It is a mean value from volume averages in front of and behind the shading device for every solar radiation interval. For the first range the volume average temperature is 11,72 $^{\circ}$C. So although in this range the air temperature in the outlet is beneficial for the energy consumption of the cube, small ventilation heat losses, the volume average temperature in the cavity indicates heat losses through heat transfer from the room. For two other ranges, 200 – 450 w/m^2 and over 450 W/m^2, the volume average temperatures were 9,94 $^{\circ}$C 28,90 $^{\circ}$C, respectively.
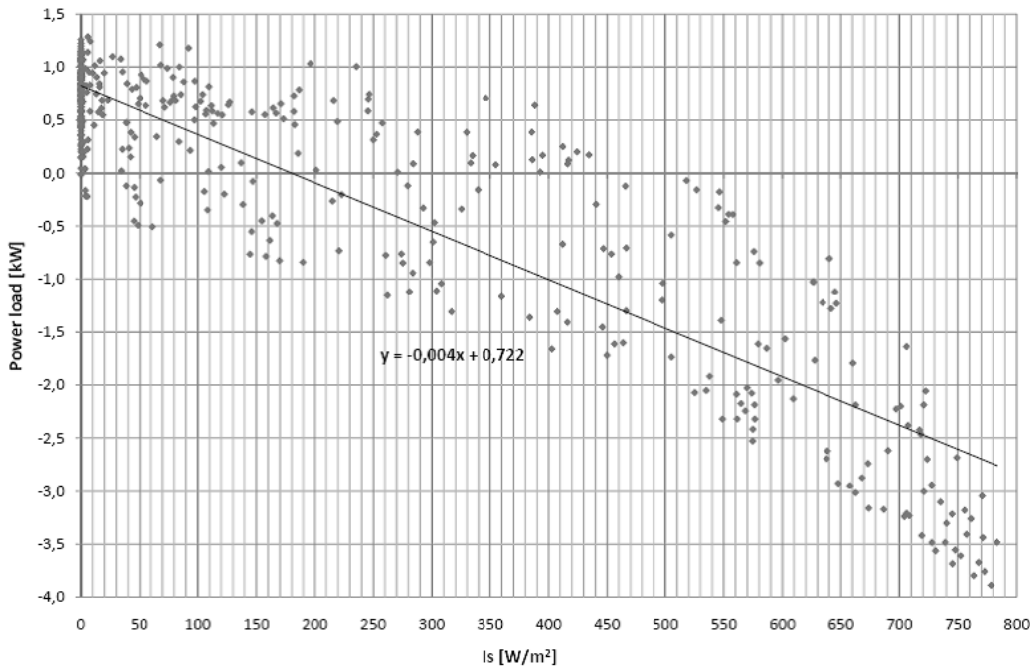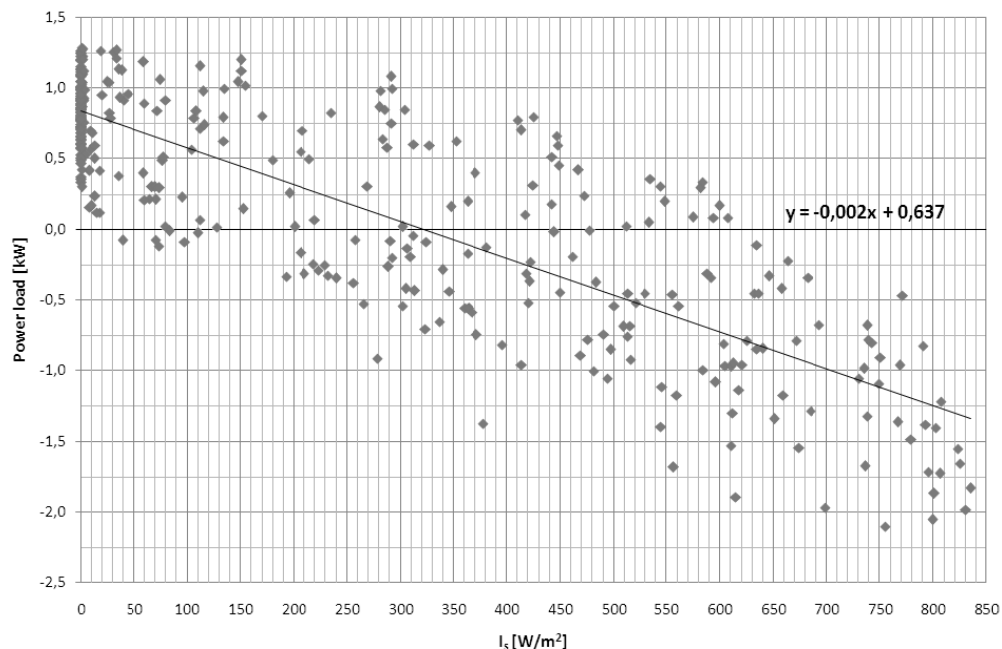

Figure 4.23 *Hourly values of measured power load depending on the global solar irradiation at that time, based on DSF_SH measurements.*

Figure 4.23 shows the correlation between the energy consumption and the global solar irradiation. The trend line resembles the lines for DSF_1_1 and DSF_1_2, but is more tilted. During the DSF_SH measurements the outdoor conditions were very similar to the ones in DSF_1_2. However, the values for the cooling loads in DSF_SH are only half of the values in DSF_1_2. This is one more proof that the shading device fulfilled its role and decreased the energy need for cooling.
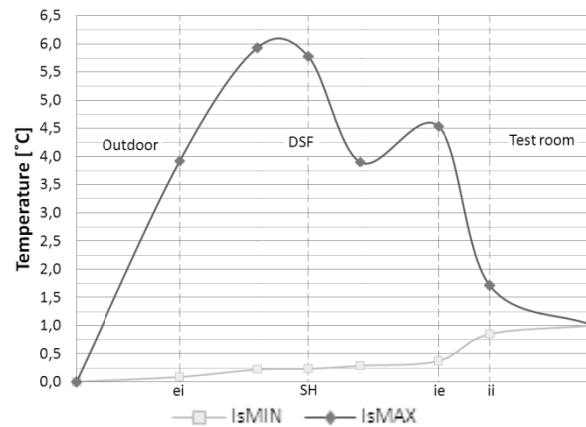
Figure 4.24 *Horizontal temperature gradient through the DSF, based on hourly averages of DSF_SH measurements. The dashed lines stand for: ei – external window's internal surface, ie – internal window's external surface, ii – internal window's internal surface.*

Figure 4.24 illustrates the dimensionless temperature gradient on a horizontal plane through the DSF cavity at the height of 2,5 m in the case of the lowest global solar irradiation of 0 W/m^2 and the highest – 834,5 W/m^2. In the first case, with I_s = 0 W/m^2, the shape of the horizontal gradient is almost the same as in the DSF_1_1 and DSF_1_2. For high solar radiation the horizontal gradient is similar to the one from DSF_1_2. However, this time the temperature difference – 9,24^{o}C between measurements closer to the outside and closer to the internal skin results not only due to the 'back flow', which occurs near the external skin, but also due to the shading's reflectance and absorptance. Also in DSF_SH the argon layer inside the internal window form a significant protection against heat losses / gains due to heat transfer through the DSF.

4.2.4. Shading coefficient

The shading coefficient given by Faber for the shading device used in the DSF cavity is 0,55. The shading coefficient can also be assessed from the measurement results as a ratio of the energy consumption with and without shading device, at times of similar solar radiation. For SC calculations were used equations describing the correlation between power load and global solar irradiation obtained for the Figure 4.25 were used. The elevations above zero in both equations are almost the same and for SC calculations are neglected. The result is a shading coefficient of 0,5, which is a value slightly differing from the theoretical one. The reason for this might be the influence of the placement of the shading device, which is different than assumed by Faber, and the

airflow in the cavity. It should be noted that there were inevitable differences between the conditions in the DSF_1_2ans DSF_SH model and therefore, the obtained values should be confirmed by laboratory experiments.
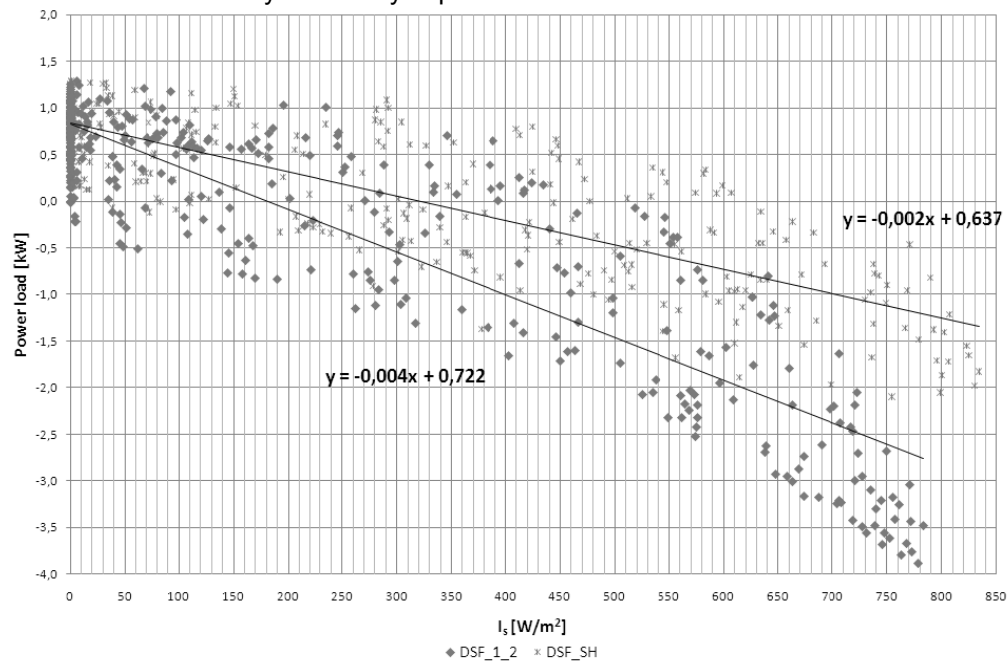
Figure 4.25 *Hourly values of measured power load depending on the global solar irradiation at that time for DSF_1_2 and DSF_SH.*

4.3.   Summation

Comparison of gathered data indicates that the overall energy consumption of 'the cube' as well as the proportion of it dedicated to the heating and cooling loads, depend on the season of the year and the outdoor conditions. It is interesting to see, that the heating load for the DSF_1_2 mode is higher by 22,9 kW than for DSF_SH, , see Figure 4.26. This is so, although in the latter case the outdoor temperature was lower and there were less solar gains entering the experiment due to the protection provided by the shading device. In order to further investigate this result, the mean volume temperature and outlet temperature at the time of heating loads for each model have been calculated, see Figure 4.27**Błąd! Nie można odnaleźć źródła odwołania.**.
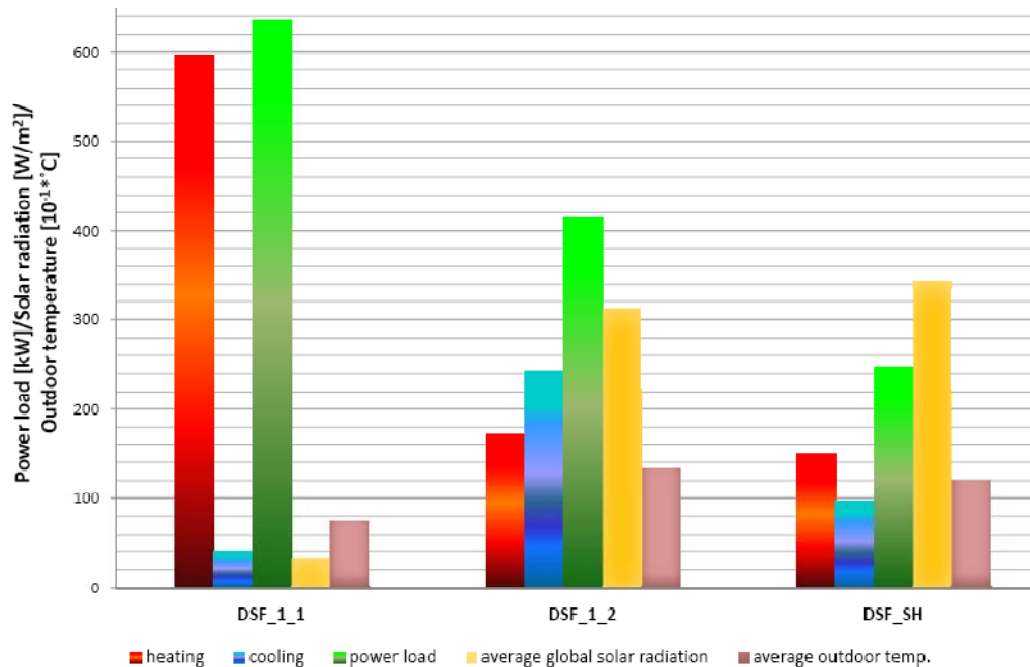
Figure 4.26 *Comparison of measured heating load, cooling load, total power load, average global solar radiation and average outdoor temperature, obtained from measurements for different models.*
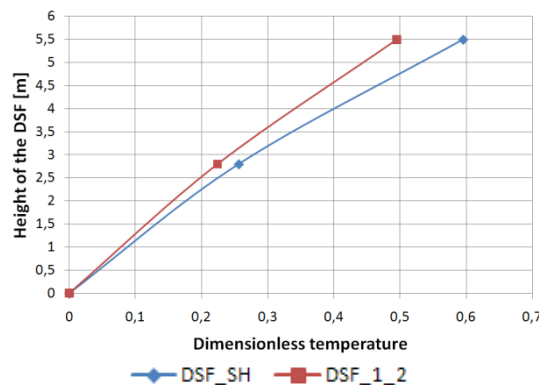
Figure 4.27 *Comparison of average dimensionless temperature gradient in the DSF at times of heating load for DSF_1_2 and DSF_SH measurements.*

The difference in the heating potential of the outlet points (10 %) is higher than in the volume averages (3,3 %). This indicates that the overall heating demand is lower in DSF_SH mode, mainly because less energy is needed for heating the incoming air. The temperature profile in the cavity with shading is more tilted. This shows an additional effect of the shading device. It not only protects the experiment room, but also absorbs part of the solar radiation entering the DSF and reflects part of it back to the external skin, both of which create additional heat gains in the incoming air.

In general out of all weather parameters, the most influential one seems to be solar radiation. It is responsible for cooling loads, which occurred even at times of low outdoor

temperatures, as was the case for DSF_1_1, see Figure 4.26. This shows the importance of solar shading. When comparing results from DSF_1_2 and DSF_SH, obtained at times of similar outdoor conditions, it is clear that solar shading of double skin façades can significantly decrease the energy consumption of a building. The difference in the cooling load in both models is 145,51 kW (60,14% of the energy need for cooling in DSF_1_2). Whereas, the average global solar radiation was higher by 31,2 W/m^2 in the case of DSF_SH. Of course, the protection from excessive solar heat gains provided by the shading device is more important during the summer time. Additional energy gains can be beneficial during the heating season, but still need to be controlled. It is thought, that if solar shading were applied in the DSF_1_1 model during times of high solar radiation, the cooling load could have been significantly reduced and perhaps even eliminated. This is especially important because in the late fall and winter the sun's altitude is lower and the angle of direct solar radiation on a Southern façade is closer to a perpendicular one. Thus, the amount of solar radiation hitting a vertical plane is quite high.

In order to optimize the energy performance of double skin façades it is necessary to define an all-year operation strategy involving both concepts of air-supply through the DSF as well as application of shading devices. For example, preheating fresh air in a DSF should be used during the heating season together with a shading device lowered at noon time. However, during the cooling season shading is needed almost through the entire day and the DSF should operate accordingly to the outdoor air curtain principle, see chapter 1.1. As mentioned before, this project deals only with a theoretical investigation of a double skin façade preheating the incoming air. Detailed measurements during a whole year or in different climate conditions are suggested for further research, as their comparison with this investigation would provide important insight into the energy performance of double skin façades.

Perhaps, the benefits of a double skin façade could also be increased if the building had a heavier construction or contained thermal mass. This would allow the solar gains to be accumulated and increase the time constant of the building.

5. Simple calculation method

Currently the assessment of the thermal behaviour and the energy efficiency of double skin façade can be calculated with complex simulation tools, which required extensive information, data and are often very time consuming. Those are the main reasons why it is impossible to obtained reliable predictions of energy consumption and indoor climate in early designing phases and reduce the uncertainties for designers and investors. Therefore the Bestfaçade Project Group in a work package 4 developed the simple calculation method, which aims on the one hand to be easily integrated in the calculation methods of the EPBD (Energy Performance Building Directive) and on the other hand to offer sufficient accuracy for the early planning stage of the thermal behaviour and the energy performance of the buildings with double skin façade [4].

The main aim is to validate the simple calculation method through comparison with measurement results.

5.1. Theoretical background

The theoretical background for simple method calculation is based on 'Bestfaçade Project Group in a work package 4' [4], where more detailed information can be found.

The whole calculation algorithm used as a simple method in this project and all equations with symbols description can be found in the Appendix.

In the Bestfaçade method the holistic calculation of the energy demand for heating and cooling for building with double skin façade uses the monthly based balancing method according to EN/ISO 13790. The energy demand for lighting uses the method described in EN-15193-1. In this project lighting energy is not investigated. The calculation of the net heating and cooling demand is described by an energy balance of a conditioned

zone, using the elements transmission and ventilation losses and solar and internal gains.

- The energy need for heating is calculated according to Equation 5.1.

$$Q_{H,nd} = Q_{H,ls} - \eta_{H,gn} \cdot Q_{H,gn}$$

Equation 5.1 *Energy need for heating.*

- The energy need for cooling is calculated according to Equation 5.2.

$$Q_{C,nd} = Q_{C,gn} - \eta_{C,ls} \cdot Q_{C,ls}$$

Equation 5.2 *Energy need for cooling.*

- The total heat transfer for a building zone for calculation period is calculated according to Equation 5.3.

$$Q_{ls} = Q_{tr} + Q_{ve}$$

Equation 5.3 *Total heat transfer.*

- The total heat gains for a building zone for calculation period are calculated according to Equation 5.4.

$$Q_{gn} = Q_{int} + Q_{sol}$$

Equation 5.4 *Total heat gains.*

In this project the internal heat gains Q_{int} are equal zero.

The influence of the double skin façade on the energy consumption is calculated according to the DIN V 18599, in which the DSF constructions are a subsystem of unheated glazed annexes.
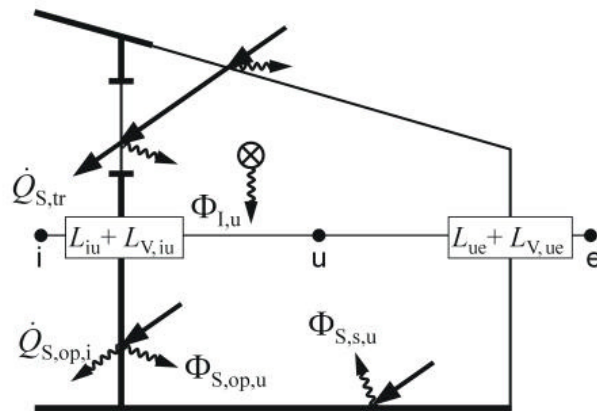
Figure 5.1 *Diagram representing the thermal quantities to be taken into consideration for glazed annexes [4]*

The glazing of an annex must be taken into consideration when calculating the heating - $Q_{H,gn}$ and cooling - $Q_{C,gn}$ gains due to solar radiation. The direct solar heat gains via transparent building components are thus calculated using Equation 5.5.

$$Q_{s,tr} = F_{F,iu} \cdot A_{iu} \cdot g_{eff,iu} \cdot F_{F,ue} \cdot \tau_{e,ue} \cdot I_S \cdot t$$

Equation 5.5 *Direct solar heat gains due to transparent components.*

Direct solar heat gains due to opaque components of the dividing wall should be ignored. These are evaluated indirectly by including them in the temperature increase within the glazed annex. The mean temperature in the glazed annex is calculated as described in EN ISO 13789 using Equation 5.6. The temperature in a the cavity of DSF is taken into consideration when calculating the heating - $Q_{H,ls}$ and cooling - $Q_{C,ls}$ losses due to transmission and ventilation. It takes into consideration the buffer effect between the room and the external environment.

$$\vartheta_u = \frac{\phi_u + \vartheta_i (H_{T,iu} + H_{V,iu}) + \vartheta_e (H_{T,ue} + H_{V,ue})}{H_{T,iu} + H_{V,iu} + H_{T,ue} + H_{V,ue}}$$

Equation 5.6 *Temperature in the unheated building zone – DSF.*

The outlet temperature in the outlet of DSF can be approximated as the double of the temperature difference between mean in the cavity and inlet, see Equation 5.7. This equation is also used to calculate the vertical temperature gradient in the DSF cavity.

$$\vartheta_{out} = 2 \cdot (\vartheta_u - \vartheta_{in})$$

Equation 5.7 *Outlet temperature from unheated building zone - DSF cavity.*

When calculating the heat flow - Φ_u, see Equation 5.8, which is needed in order to determine the temperature, the sum of total solar radiation entering through the external glazing of the annex – $\Phi_{S,u}$ must be taken into account, as well as any internal heat sources – $\Phi_{I,u}$. The radiant heat $Q_{S,tr}$ which is transferred directly via transparent building components into the building zone being evaluated must be subtracted from this.

$$\phi_u = \sum \phi_{S,u} - \frac{\sum Q_{S,tr}}{t} + \sum \phi_{I,u}$$

Equation 5.8 *Heat gains affecting the unheated annex – DSF.*

The shading and solar protection devices of the transparent components of the dividing wall must be accounted for when calculating the direct heat gains $Q_{S,tr}$ in the building zones. The solar protection devices must be taken into consideration when calculating the total energy transmittance g_{tot} of the internal glazing. It has to be also taken into consideration as a internal heat sources - $\Phi_{I,u}$, when calculating the heat gains affecting the unheated annex - Φ_u.

5.2. Results

In all cases, the data for the calculations has been acquired from measurements in the full-scale model, with mechanically driven fresh air supplying through the DSF. The temperature inside the experiment room and the volume airflow through the DSF have been assumed to be stable, which corresponds to the results of measurements. The details of 'the cube's' construction served as basis for calculating the building's time constant, U-values and g-value as well as the transmission and ventilation heat transfer coefficients. These values can be found in the spread sheet "constants" in all simple calculation method Excel files on the attached CD.

The outdoor temperature, ground temperature under the foundations, temperature in the equipment room and engine room as well as the total solar irradiation on the surface of the external DSF skin had been changing in time. The hourly average values of these parameters are in the spread sheet "variables" in all simple calculation method Excel files on the attached CD.

Four measured values have been considered for comparison with the calculation results:
- The temperature in the DSF cavity - calculated for the middle of the air-gap and in some cases measured in section 2 at the height of 2,5 m and in others measured volume average temperature in section 2
- The outlet temperature - the air entering the experiment room from the DSF, measured at the top openings.
- The energy consumption for heating – measured by a wattmeter connected to the heating device inside the air-conditioning unit in the experiment room.
- The energy consumption for cooling – measured as the water flow and temperature difference of the cooling water supplied to the air-conditioning unit.

These values can be found in the spread sheet "reference results" in all simple calculation method Excel files on the attached CD.

Although the Bestfaçade Project Group recommends the simple calculation method for assessing a monthly or even seasonal performance of a double skin façade, the calculations for this project have been performed on hourly basis. It has been decided that a detailed approach could provide more insight in the accuracy of the calculation method. It should be noted that during a period of even one day there may occur heating as well as cooling loads in a building. A daily or monthly average would not show such fluctuations and might be a too farfetched simplification. This has been confirmed by the comparison of results calculated for variable values for 1-hour averages, 24-hour and the entire measurement period, for each of the three models. In addition to this, BSim simulations are also conducted for hourly intervals, and thus comparison between the different ways of assessing the DSF performance is easier.

5.2.1. DSF_1_1

The first set of calculations was based on measurements in the full scale model DSF_1_1 conducted by Olena Kalyanova in November 2006 for a period of 22 days

[11]. At that time the airflow rate was set to 143,11 m³/h and there was no shading device in the DSF.

Figure 5.2 compares the results of the simple method calculations of the power load based on hourly, 24-hour and 22-day averages of the variable data, such as the outdoor air temperature. The average power load for the entire measurement period is 0,54 kW. It should be noted that average calculations for a longer period correspond better to the purpose of the simple calculations method, as it is meant for assessing the energy performance of double skin façades during an entire season. However, this average results in a total energy use during the measurement period of 285,36 kWh, which is lower than the sum of the measured angry consumption by 349,87 kWh. Also calculations based on 24-averages significantly differ from the measured values, especially when considering the heating demand. The sum of the calculated energy use for heating is 322,56 kWh, whereas the heating load based on hourly averages of measurements resulted in 595,55 kWh. This is a very disappointing result and therefore the rest of this chapter deals with values based on hourly averages. A comparison of all calculated and measured values has been shown in Table 5.1, Table 5.**2** and Table 5.**3**.
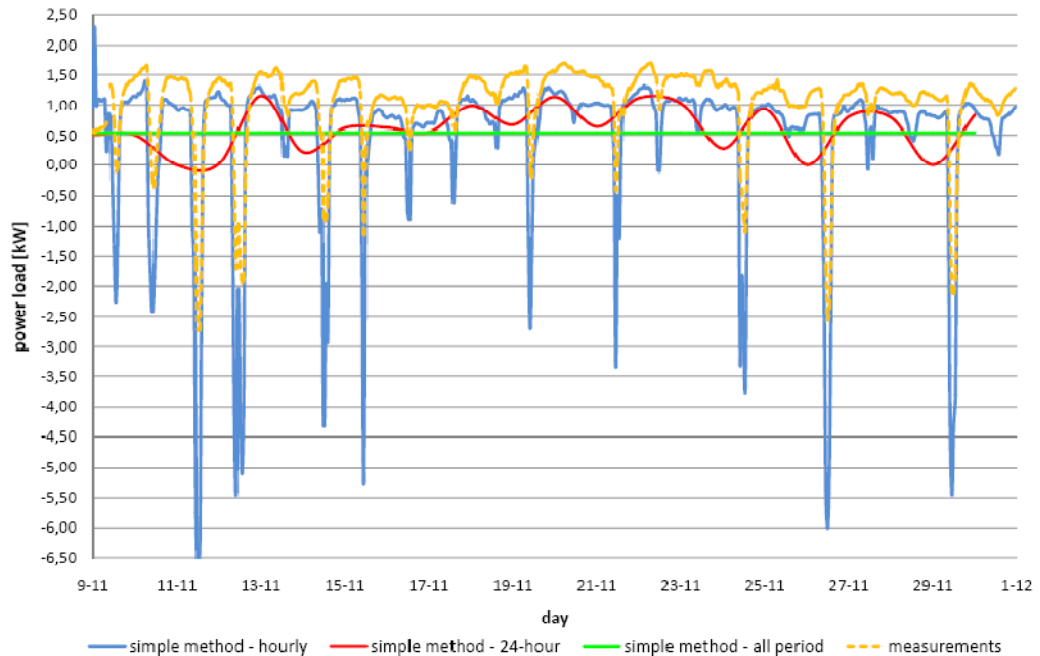
Figure 5.2 *Comparison of hourly averages of measure power load, simple method calculation results for hourly averages, 24-hour averages and the average for the entire period, based on DSF_1_1 measurements.*

	Toal energy consumption* [kWh]
DSF_1_1 measurements	635,23
Simple calculation method	349,87
Difference	285,36
Precentage	-45 %

* This is the sum of the absolute values both for heating and cooling energy consumption.

Table 5.1 *Comparison of the sum for the whole measurement period of the measured energy consumption based on hourly averages and the calculated energy consumption based on the average for the entire period, for DSF_1_1 measurements.*

	Energy need for heating [kW]	Energy need for cooling [kW]	Toal energy consumption* [kWh]
DSF_1_1 measurements	595,55	39,68	635,23
Simple calculation method	322,56	35,52	358,08
Difference	272,99	4,16	277,15
Precentage	-46 %	-10,5 %	-43,6 %

* This is the sum of the absolute values both for heating and cooling energy consumption.

Table 5.2 *Comparison of the sum for the whole measurement period of the measured energy consumption based on hourly averages and the calculated energy consumption based on 24-hour averages, for DSF_1_1 measurements.*

	Energy need for heating [kW]	Energy need for cooling [kW]	Toal energy consumption* [kWh]
DSF_1_1 measuremnets	595,55	39,68	635,23
Simple calculation method	428,00	146,94	574,94
Difference	167,55	107,26	60,29
Precentage	-28,1%	+270,3%	-9,5%

* This is the sum of the absolute values both for heating and cooling energy consumption.

Table 5.3 *Comparison of the sum for the whole measurement period of the measured energy consumption based on hourly averages and the calculated energy consumption based on hourly averages, for DSF_1_1 measurements.*

Figure 5.3 compares the hourly averages of the calculated and measured energy consumption, which formed the basis for Table 5.3. It should be noted that negative values represent the cooling load, but for the comparison of energy consumption absolute values are considered. It is clear that the calculated values of the heating load are lower than the measured ones, the average difference between the hourly results is 0,35 kW. It is an unsatisfying result, because the simple calculation method was

expected to give higher results than the measurements, in order to be "on the safe side". This is especially important since it is meant to be used for preliminary assessment of DSF performance in the early design stage. During the measuring period there were mainly heating loads in 'the cube' and therefore this result has a significant influence on the overall energy consumption.
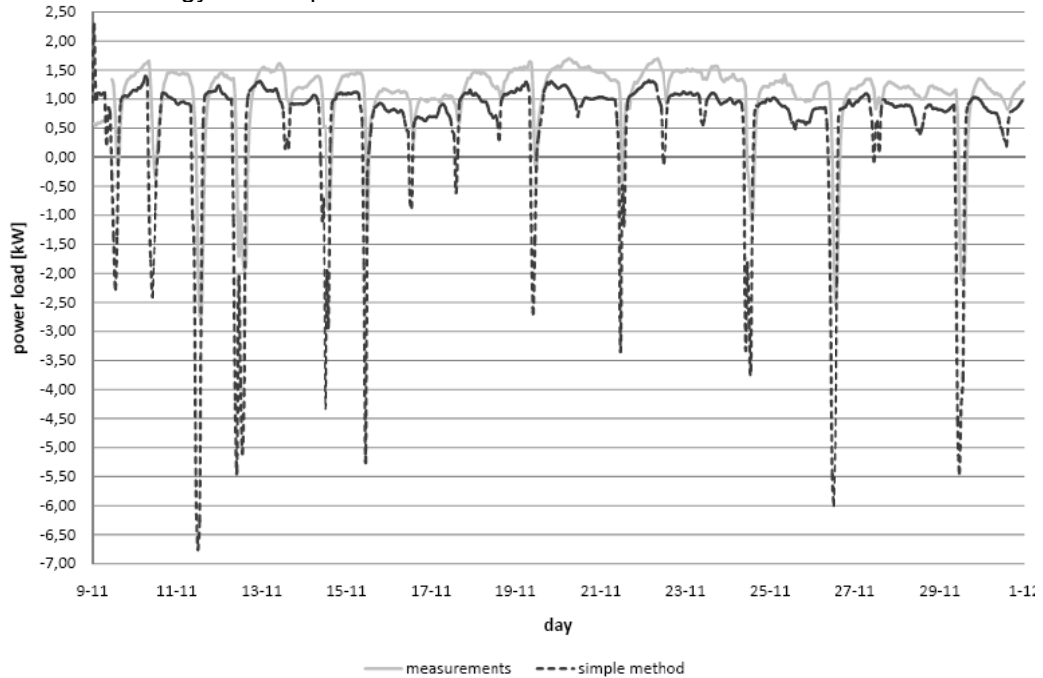
Figure 5.3 *Measured and calculated hourly average values of power load, based on DSF_1_1 measurements.*

Comparison of the measured and calculated energy use for cooling gives oposite results – the calculated values are much lower than in the case of the measurements, which corresponds to a higher energy consumption. The average difference between hourly results is 1,89 kW, see Figure 5.3. However, the cooling loads seem to be less important, since in this case the DSF was operating in such a way as too preheat the incomming fresh air during the heating season.

	Maximum difference	Minimum difference	Average difference
Energy need for heating [kW]	1,75	0	0,35
Energy need for cooling [kW]	6,76	0,007	1,89

Table 5.4 *Differences between the measured and the calculated hourly values of the heating and cooling load, based on Figure 5.3.*

For the entire considered period the total energy consumption measured in 'the cube' was heigehr from the calculated one by 60,29 kW, see Table 5.3. This might be a very significant difference when applying the simple calculaion method to assesing the

energy performance of a whole office building with a double skin façade. Figure 5.4 shows the correlation between the calculation results and the global solar irradiation. According to the trend line, values of solar radiaiton as low as 42 W/m^2 cause cooling loads. A similar graph has been done for the measurement results of DSF_1_1 model, but the obtained trend line indicated that cooling loads appear above 105 W/m^2 of solar irradiation, so values higher by 60 %. Such differences obviously create errors in the calculation results.
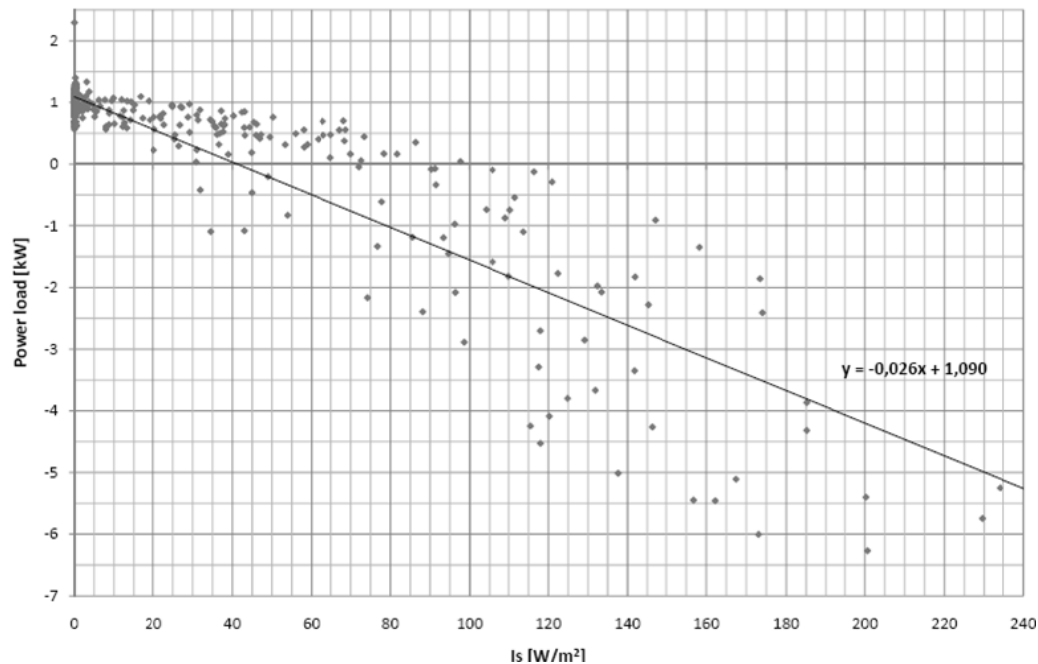
Figure 5.4 *Hourly values of calculated power load depending on the global solar irradiation at that time, based on DSF_1_1 measurements.*

The reason for the differences in measurement and sipmle method calculation results may be explained by comparing the calculated and measured airtemperature in the middle of the DSF cavity and in the outlet, see Figure 5.5. In general, the simple calculation method gives higher temperature values in the middle of the DSF, the average difference is 2,06 ˚C. It's important to remember, that the reference temperature in the air-gap was measured at the height of 2,5m, which is not the exact middle of the DSF. Of course, the temperature increases with height, so it is possible that the real value was closer to the calculated one. If a higher temperature inside the DSF is taken into consideration in the simple calculation method, the heat losses through the internal skin would be much smaller. This could be the reason why the calculated energy need for heating is smaller than in reality.

In the case of the outlet temperature, the simple calculation method gives on average 0,7 ˚C lower results than the measurements. However, during the peaks the calculated values are much higher than the measured ones. This corresponds to the time when cooling loads occurred and would explain why the calculated energy consumption for

cooling is higher than the measured one. It should be noted that the measured temperature values for the outlet were not available from the beginning of the measurement period.
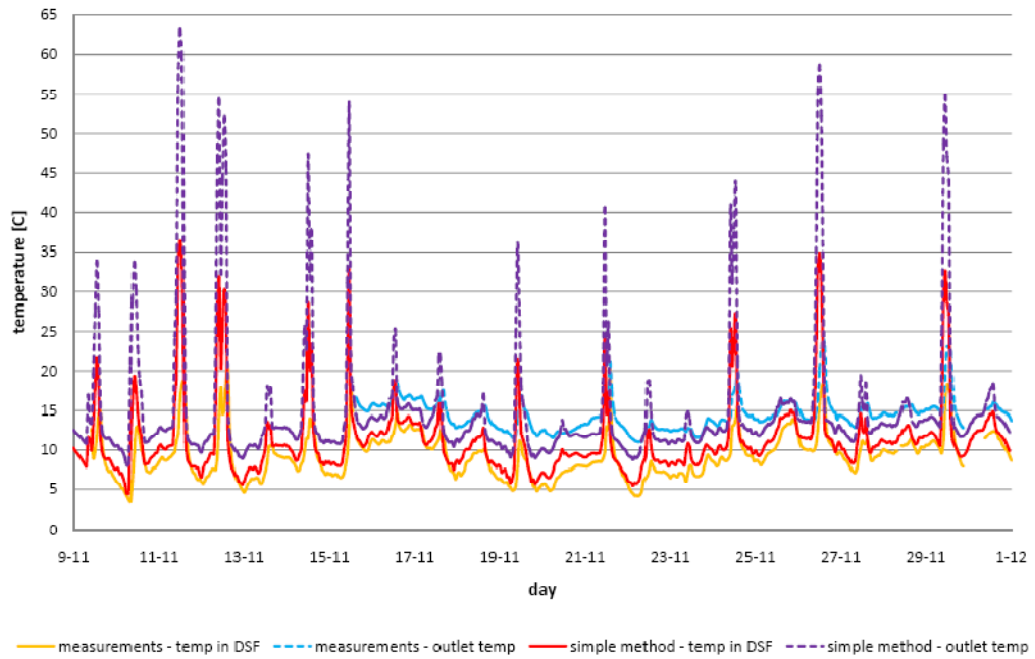
Figure 5.5 *Measured and calculated hourly averages of air temperature in the middle of the DSF and in the outlet, based on DSF_1_1 measurements .*

In general, the differences between the simple calculation method and the measurement results seem to be due to a wrongly assumed temperature gradient in the DSF cavity. In the calculations it is considered to be linear, whereas in reality it is not. Figure 5.6 compares the temperature gradient plots obtained from the measurements with the ones based on the calculated values of the temperature in the outlet and middle of the DSF. Hourly averages for cases have been taken into consideration – 8:00 on November 23rd and 12:00 on November 26th 2006. The first case corresponds to low temperatures in the outlet as well as the middle of the DSF and a peak in the energy need for heating. During this time the average solar irradiation on the external skin of the DSF was 10,82 W/m^{2}. The second case represents the opposite situation – a major rise of temperature values as well as the energy need for cooling and an average solar irradiation of 617,67 W/m^{2}. Clearly, the calculated temperature gradient is closer to the measured one in the first case, which would explain why the calculated heating loads are on average closer to reality than the cooling loads. The volume average temperature in the air cavity measured in the first case is 6,3 ˚C, whereas the calculated value in the middle of the DSF is 8,1 ˚C. In the second case the difference between the two values is much bigger – measured volume average temperature is 17,6 ˚C and the calculated value is 34,9 ˚C. Clearly the difference increases with the amount of solar radiation hitting the DSF surface.
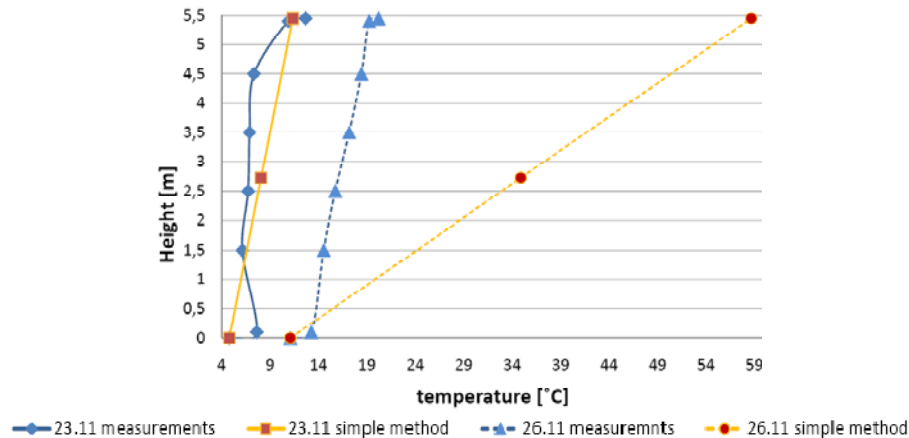
Figure 5.6 *Measured and calculated temperature gradients inside the DSF cavity, based on measurements from 23.11.2006 at 8:00 and 26.11.2006 at 12:00.*

It should be noted that the simple calculation method takes into consideration only the total area of the DSF's skins, in order to calculate the heat transfer through them. Other construction parameters, like the height or depth of the air-gap or the airflow path are neglected. These are key factors in determining how long does the air stay in the DSF cavity and therefore, how much solar energy it can accumulate. This also explains why the error of simple method calculations is bigger for periods of high solar irradiation. All of these parameters create doubts about the reliability of the simple calculation method.

5.2.2. Measured temperature in the simple calculation method

Another analysis has been done in order to further investigate the influence of the assumed temperature gradient in the DSF cavity on the calculation results. A set of two additional simple method calculations has been done for the data gather during the DSF_1_1 measurements. In the first one, the measured volume average temperature instead of the calculated air temperature in the middle of the DSF cavity was taken into further calculations of the power load. In the second one, apart from the temperature in the air gap, the calculated outlet temperature was replaced with the measured values. As mentioned in chapter 5.2.1, the values of the outlet air temperature were only gathered later in the measurement period. Therefore, for comparing the results of this last set of simple method calculations, only measured values from the relevant period have been used. Very small gaps in the measured values appear in both calculation sets during periods of low solar radiation. These have been filled by the calculated values, because as shown before, when the influence of solar irradiation is not significant, the temperatures calculated by the simple method are quite accurate. The results of hourly values of the power load have been shown in Figure 5.7.
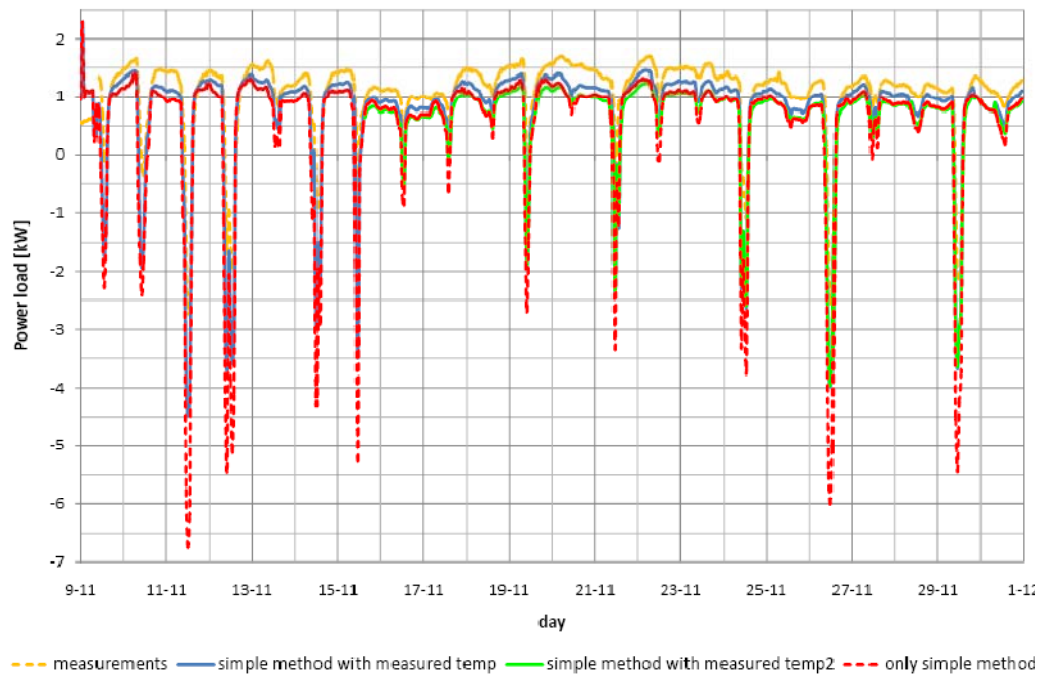
Figure 5.7 *Comparison of hourly values of power load based on results from measurements, simple method calculations, calculations with the measured volume average temperature and calculations with the measured volume average and outlet air temperature, based on data gather for DSF_1_1.*

It seems that the simple calculation using the measured volume average temperature in the DSF gives results closest to the measurements. However, it is surprising to see that the set of calculations using both the volume average temperature and the measured outlet air temperature has worst results than the first calculation.

Detailed values have been shown in Table 5.5. The overall error for the total energy consumption of the calculations done using the measured temperature in the DSF cavity is almost 3 % lower than in the case of only the simple calculation method. This is due to a smaller error in the calculated heating demand and even more importantly the cooling demand. The reason for the error was the particularly big difference between the measured and calculated temperature inside the cavity during cooling peaks, see Figure 5.5. Therefore, accurate temperature values in the DSF influence the calculated amount of energy gains / losses due to heat transfer through the internal skin and give more realistic results.

On the other hand, the simple method calculations performed using both the measured temperature in the DSF cavity and outlet give very unsatisfying results. The error for the results of the total energy consumption is higher than for only the simple calculation method by 15,3 %. The main source of error in this case is the energy need for cooling, which has been overestimated by 137,1 %. Still, in this case the difference between the measured and calculated cooling load is smaller than in the other cases. The reason for the error before was the fact that, when heating loads occurred the originally calculated

outlet air temperature was lower than the measure one, but in the case of cooling peaks the correlation between the two values was the opposite, see Figure 5.5. This increased the error both in the case of heating and cooling loads.

	DSF_1_1 measurements	Only simple calculation method	Simple calculation method with measured volume average temp.	Simple calculation method with measured volume average and outlet air temp.
Energy need for heating [kW]	595,55 (431,07)**	428,00	494,44	294,5
Difference from measurements	-	167,55	101,11	136,57
Percentage	-	-28,1 %	-17 %	-31,7 %
Energy need for cooling [kW]	39,68 (18,37)**	146,94	98,19	43,55
Difference from measurements	-	107,26	58,51	25,18
Percentage	-	+270,3 %	+147,5 %	+137,1 %
Total energy consumption* [kWh]	635,23 (449,44)**	574,94	592,63	338,05
Difference from measurements	-	60,29	42,6	111,39
Percentage	-	-9,5 %	-6,7 %	-24,8 %

* This is the sum of the absolute values both for heating and cooling energy consumption.
** Values only for the relevant measurement period, when all the necessary data was collected. Used for comparison with the results of simple calculation method with measured volume average and outlet air temperatures.

Table 5.5 *Comparison of energy consumption results for measured values and three different sets of calculations, based on data gathered for DSF_1_1.*

It seems that optimal calculation results could be achieved if using the measured volume average temperature in the DSF for calculating the energy demand for heating. On the other hand, when calculating the cooling load, the measured temperature inside the cavity as well as in the outlet, should be inputted. This indicates that the wrongly assumed temperature gradient in the double skin façade is a major but the only drawback of the simple calculation method. Another source of error may be that the simple calculation method does not consider the heat transfer due to convection from construction surfaces to the air.

5.2.3. DSF_1_2

The next simple method analysis was based on measurements in the full-scale model DSF_1_2 conducted for 17 days on the turn of April and May 2008. The same as in the DSF_1_1 the air flow was set to around 136,5 m^3/h and there was no shading device in the DSF.

In DSF_1_2, the same as in DSF_1_1, there has been made a comparison of the energy results obtained from simple calculation method based on hourly, 24-hour and 17-day averages of the variables data, see Figure 5.8.
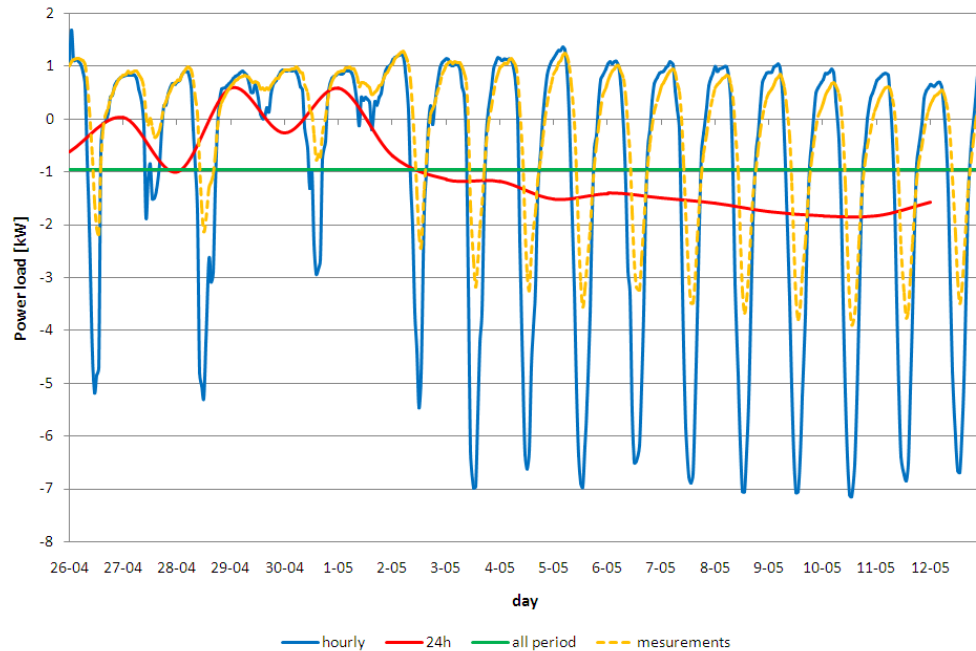
Figure 5.8 *Comparison between measurements and simple method calculation results for hourly averages, 24-hour averages and the average for the entire period, based on DSF_1_2 measurements.*

In DSF_1_2 case, where cooling loads are slightly dominating over the heating loads and form 58% of total usage, the simple calculation method gives the best results of total energy consumption for the 24-hour averages. Then the sum of total energy consumption is higher than measurements by 10,7%. However, when comparing separately the energy need for heating and cooling the 24-hour averages differ significantly from the measurements, see Table 5.7. As the differences in heating and cooling loads are very similar, but with opposite sign, in the final result of the total energy consumption they compensate for each other and give satisfying result. The smallest difference between measurements and simple calculation method appears when comparing measurements and average for the whole period -6,3%, see Table 5.6. However, this result is unsatisfying, because in early design stage the calculations should give higher values than reality in order to be on 'safety side'. The hourly averages results for total energy consumption are from one point of view satisfying, because simple calculation method gives higher values than the measurement +79,6%. From the other point, this difference is too big for preliminary energy investigation. Hourly calculations results most accurately follow the tendency of the measurements, see Figure 5.8. As mentioned in chapter 5.2 the hourly averages are the best to investigate the detailed energy performance of DSF and to compare with measurements and outputs from BSim simulations. Therefore the rest of this chapter deals with values based on hourly averages.

	Toal energy consumption* [kWh]
DSF_1_2 measurements	414,09
Simple calculation method	388,11
Difference	25,98
Percentage	-6,3%

* This is the sum of the absolute values both for heating and cooling energy consumption
Table 5.6 *Comparison of the sum for the whole measurement period of the measured energy consumption based on hourly averages and the calculated energy consumption based on the average for the entire period, for DSF_1_2 measurements.*

	Energy need for heating [kW]	Energy need for cooling [kW]	Toal energy consumption* [kWh]
DSF_1_2 measurements	172,15	241,94	414,09
Simple calculation method	29,24	429,14	458,38
Difference	142,91	187,20	44,29
Percentage	-83,0%	+77,4%	+10,7%

* This is the sum of the absolute values both for heating and cooling energy consumption
Table 5.7 *Comparison of the sum for the whole measurement period of the measured energy consumption based on hourly averages and the calculated energy consumption based on 24-hour averages, for DSF_1_2 measurements.*

	Energy need for heating [kW]	Energy need for cooling [kW]	Toal energy consumption* [kWh]
DSF_1_2 measurements	172,15	241,94	414,09
Simple calculation method	178,49	565,15	743,64
Difference	6,34	323,21	329,65
Percentage	+3,7%	+133,5%	+79,6%

* This is the sum of the absolute values both for heating and cooling energy consumption
Table 5.8 *Comparison of the sum for the whole measurement period of the measured energy consumption based on hourly averages and the calculated energy consumption based on hourly averages, for DSF_1_2 measurements.*

The main aim of the simple method calculations is to assess the energy consumption Figure 5.9 shows the hourly average values of the measured and calculated energy consumption for the whole measuring period. As mentioned in chapter 5.2.1 the negative values represent the cooling load, but for comparison the absolute values are

used. From the graph it can be noticed, that calculated values of heating loads are very close to the measured ones. From 26.04 till 4.05 they are almost the same and for the remaining 8 days the calculated values are a little higher. In general the calculated energy need for heating is higher than measured one. The average difference between hourly results is 0,16 kW.
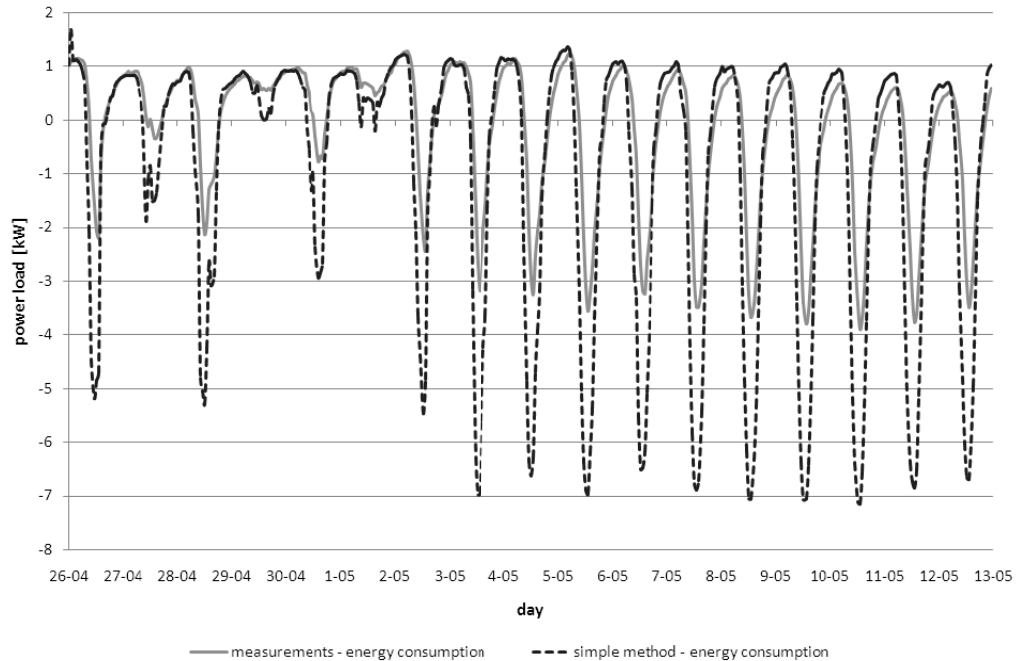
Figure 5.9 *Measured and calculated energy consumption, based on DSF_1_2 measurements.*

Comparison between measured and calculated cooling loads gives similar result. The calculated values are higher than the measured ones. The average difference between hourly results is 0,84 kWh.

	Maximum difference	Minimum difference	Average difference
Energy need for heating [kW]	0,91	0	0,16
Energy need for cooling [kW]	4,67	0	0,84

Table 5.9 *Differences between the measured and the calculated hourly values of the heating and cooling load, based on Figure 5.9.*

Both heating and the cooling simple method hourly results are satisfying, because as mentioned in chapter 5.2.1 the simple method results are expected to give higher values than the measurements.

The simple calculation method is recommended for assessing a monthly or even seasonal performance of a double skin façade, see chapter 5.2. Therefore more important than the hour values is the comparison of the sum of the energy need for heating and cooling and total energy consumption for the entire measuring period (17

days), see Table 5.8. The comparison of the results for the heating load is satisfying. The calculated value is bigger than measured one for 6,34 kW (3,7 %). For cooling load the total energy consumption the difference is too big +133,5%. The simple method should give higher values than the measurement, as it is meant to be used for preliminary assessment of DSF performance. On the other hand, in the early design stage the calculation results for total energy consumption cannot be overestimated by 79,6%.
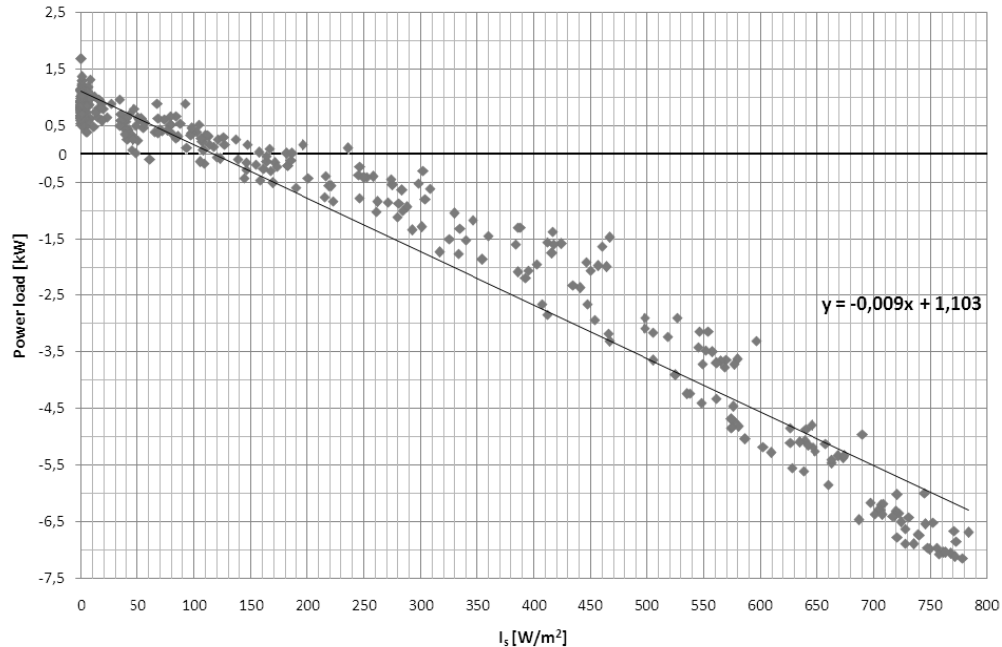
Figure 5.10 *Hourly values of calculated power load depending on the global solar irradiation at that time, based on DSF_1_2 measurements.*

Figure 5.10 shows the power load in function of the global solar irradiation. It is clear that in simple calculation method the correlation between those two is even stronger than in the measurements and the calculated power load values are concentrated around the trend line, see Figure 4.17. The trend line is more tilted than in reality and the cooling loads already appear with solar radiation of 120W/m^2. Moreover, for the same value of solar radiation the calculated values of the cooling loads are higher than measured ones.

The explanation for energy results can be a comparison of calculated and measured air temperature in the middle of DSF cavity and outlet temperature from DSF, see Figure 5.11. In this case, DSF_1_2, the measured air temperature in the middle of DSF cavity is the mean value calculated from thermocouples placed closer to the internal skin and those near the external window.
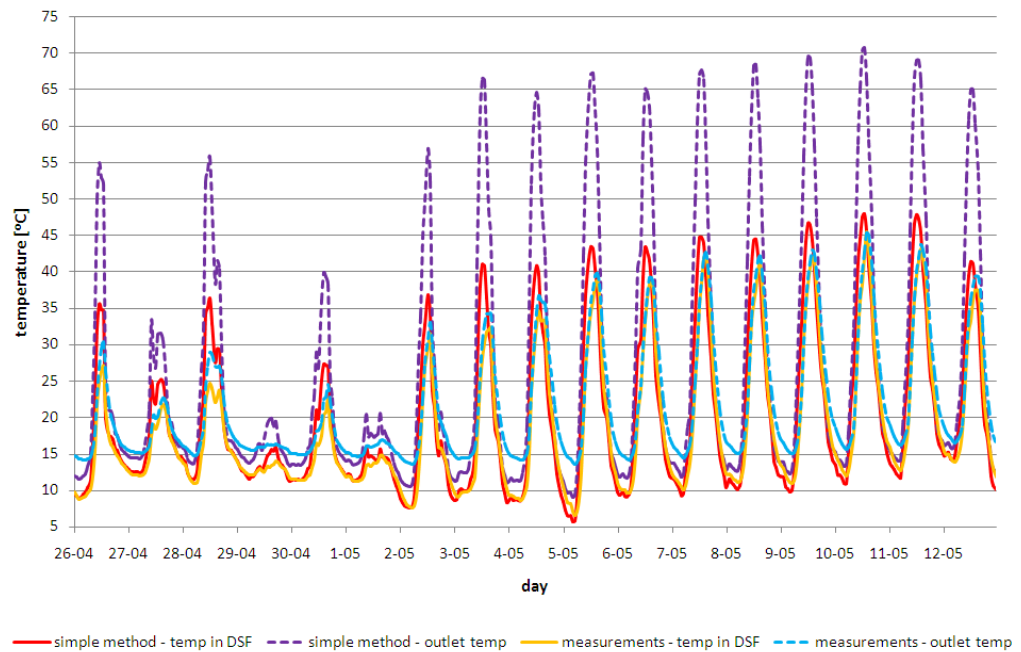
Figure 5.11 *Measured and calculated air temperature in the middle of the DSF and in the outlet, based on hourly values for DSF_1_2.*

The result regarding the air temperature in the middle of DSF cavity is similar to the one obtained in DSF_1_1 for the daytime. The simple calculation method gives higher values then the measurements. In the nights, when mostly heating is needed, the calculated air temperatures are lower than measured ones. This could be the reason why the calculated energy need for heating is bigger than in reality.

As mentioned in chapter 4.2.2 the outlet temperature is the air temperature measured at height 5,4m, because the readings for the outlet point at 5,5m are not reliable.

The comparison of the outlet temperature gives surprising results. During the night-time and the days when the heating loads are predominating over the cooling loads (29th of April and 1st of May) the measured outlet temperature is mostly higher than the calculated one. Whereas in sunny days with clear sky, from 2nd till 12th May, when the cooling loads occurred more often during the daytime, the measured values are significantly lower from the calculated outlet temperatures. The maximum difference is 36,2°C. So big difference in the calculated and measured outlet temperature is the explanation, why the calculated energy need for cooling is higher than the measured one.

In general in the DSF_1_2, like in the DSF_1_1, the difference between simple calculation method and measurements is the result of assuming the vertical temperature gradient in DSF cavity to be linear. Figure 5.12 shows the calculated and the measured mean air temperature in the middle of the DSF for both thermocouples stets together and separately. From Figure 5.12 indicates that in the simple calculation method also

the horizontal temperature gradient is not used and the depth of the DSF is not considered in the calculations. This is another proof that in simple calculation method no DSF dimensions is taken into account.
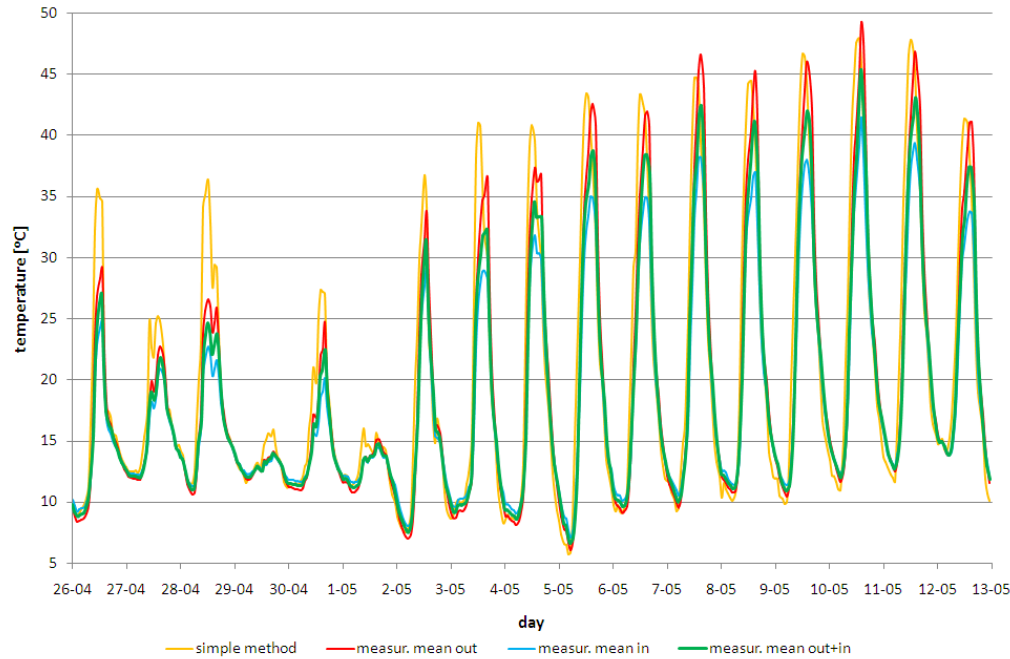
Figure 5.12 *Measured and calculated air temperature in the middle of the DSF, based on measurements from April – May 2008. The legend description: measur. mean – measurement mean value: out – thermocouples near to the external window, in – thermocouples closer to the interior skin, out+in – mean value from both reading*

5.2.4. DSF_SH

The last set of simple method calculations was based on measurements in the full-scale model from May 14th till 27th 2008. At this time the shading device was mounted inside the double skin façade air gap and the operation concept was the same as in the case of previous models. In order to implement the effect of shading, certain changes had to be done to the equations used in the simple calculation method. The shading coefficient of SC = 0,55 had to be considered when determining the direct solar heat gains via transparent building components, see Equation 5.9.

$$Q_{s,tr} = F_{F,iu} \cdot A_{iu} \cdot g_{eff,iu} \cdot F_{F,ue} \cdot \tau_{e,ue} \cdot I_S \cdot t \cdot SC$$

Equation 5.9 *Direct solar heat gains due to transparent components with shading.*

Another change was done when calculating the heat gains effecting the double skin façade cavity. In this case, the solar heat gains reflected by the shading devices and then stopped by the external skin had to be added, see Equation 5.10.

$$\phi_u = \sum \phi_{S,u} - \frac{\sum Q_{S,tr}}{t} + \sum \phi_{I,u} + \sum \phi_{S,u} \cdot R \cdot \left(1 - g_{eff,ue}\right)$$

Equation 5.10 *Heat gains effecting the unheated annex – DSF with shading.*

Again, calculation results for hourly, 24-hour and all-period average values of variable parameters have been compared, see Figure 5.13. Values below 0 represent the cooling load. It seems that neither the average for the entire period nor the 24-hour average values correspond to the measurement results. On the other hand, the hourly calculation results give quite accurate values of the heating demand but overestimate the cooling load. Details of this comparison can be found in Table 5.10, Table 5.**11** and Table 5.**12**.
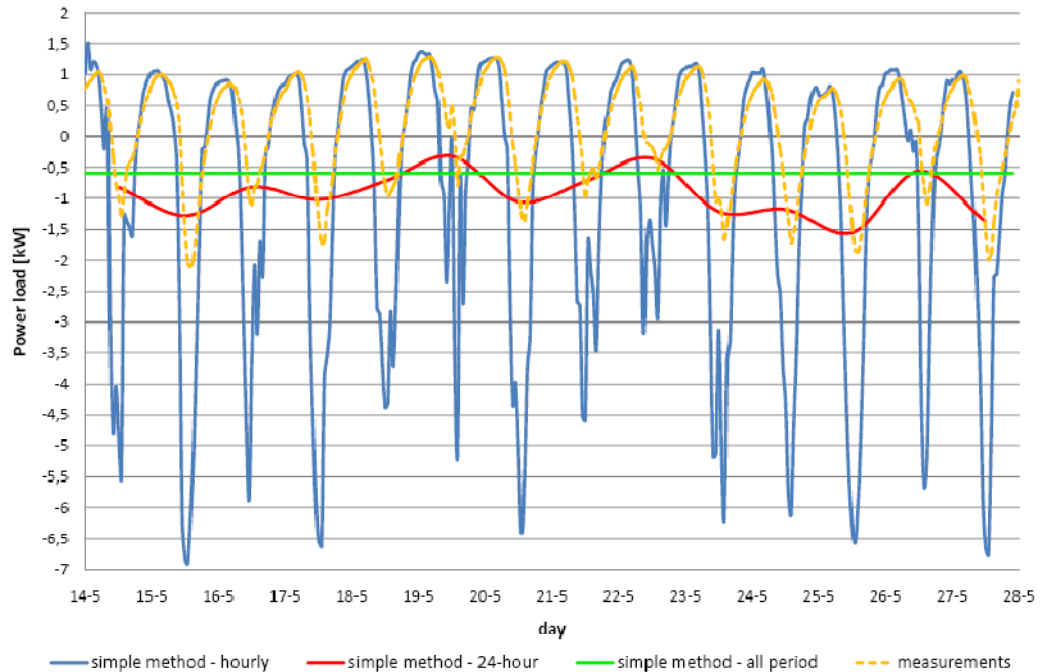
Figure 5.13 *Comparison of hourly averages of measure power load, simple method calculation results for hourly averages, 24-hour averages and the average for the entire period, based on DSF_SH measurements.*

	Toal energy consumption* [kWh]
DSF_SH measurements	245,68
Simple calculation method	200,44
Difference	45,12
Precentage	-18,4 %

* This is the sum of the absolute values both for heating and cooling energy consumption.

Table 5.10 *Comparison of the sum for the whole measurement period of the measured energy consumption based on hourly averages and the calculated energy consumption based on the average for the entire period, for DSF_SH measurements.*

	Energy need for heating [kW]	Energy need for cooling [kW]	Toal energy consumption* [kWh]
DSF_SH measurements	149,25	96,43	245,68
Simple calculation method	0	326,0	326,0
Difference	149,25	229,57	80,32
Precentage	-100 %	+238,1 %	+32,7 %

* This is the sum of the absolute values both for heating and cooling energy consumption.

Table 5.11 *Comparison of the sum for the whole measurement period of the measured energy consumption based on hourly averages and the calculated energy consumption based on 24-hour averages, for DSF_SH measurements.*

	Energy need for heating [kW]	Energy need for cooling [kW]	Toal energy consumption* [kWh]
DSF_SH measuremnets	149,25	96,43	245,68
Simple calculation method	143,07	454,47	597,53
Difference	6,18	358,04	351,85
Precentage	-4,1 %	+371,3 %	+143,2 %

* This is the sum of the absolute values both for heating and cooling energy consumption.

Table 5.12 *Comparison of the sum for the whole measurement period of the measured energy consumption based on hourly averages and the calculated energy consumption based on hourly averages, for DSF_SH measurements.*

It seems that the calculation error for the total energy consumption is smallest in the case of the average power load for the entire considered period. However, this simplification makes it impossible to distinguish between heating and cooling loads. These values are essential not only for the analysis performed in this project but also when applying the calculation method for a preliminary assessment of a double skin façade construction and design of a heating / cooling system cooperating with it.

The results are similar in the case of calculations based on 24-hour average values of the variable parameters. The error of the total energy consumption is 32,7 %, but the cooling load is overestimated by 238,1 % and the heating demand is completely neglected. The difference between the sum of the measured and calculated energy consumption is thought to be relatively small, because the errors for the cooling and heating load compensate each other. This situation was also described in chapter 5.2.3.

The only calculations that result in both a heating and cooling load are the ones based on hourly average input values. Therefore these values have been considered in the following investigation. The error for the heating demand is only 4,1 %. However, the cooling load is unacceptably overestimated by 371,3 %. This can also be seen in Figure 5.14, showing the measured and calculated hourly values of the power load, and Table 5.13, comparing the average differences in the heating and cooling demand.
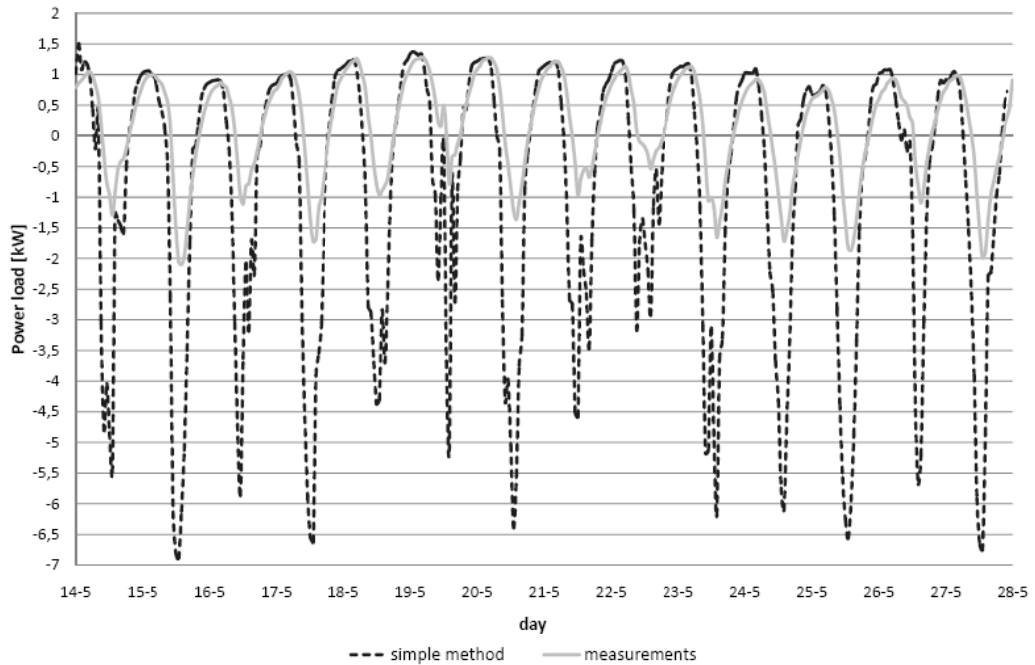
Figure 5.14 *Measured and calculated hourly average values of power load, based on DSF_SH measurements.*

	Maximum difference	Minimum difference	Average difference
Energy need for heating [kW]	0,25	0	0,16
Energy need for cooling [kW]	3,17	0	0,84

Table 5.13 *Differences between the measured and the calculated hourly values of the heating and cooling load, based on Figure 5.14.*

As mentioned before, solar radiation has a big influence on the energy consumption. Therefore, in order to find the reason for the error of the simple calculation method, the correlation between the power load and global solar irradiation at that time has been investigated, see Figure 5.15. A similar graph has been made for the DSF_SH measurement results in Figure 4.23. There is a significant difference between the trend lines in both figures – the measurements indicate that cooling loads are caused by solar irradiation above 319 W/m^2, but the calculation results give cooling demands already at values of solar irradiation above 151 W/m^2. This means that the protection provided by the shading device is underestimated in the simple calculation method, and thus the cooling load is overestimated.
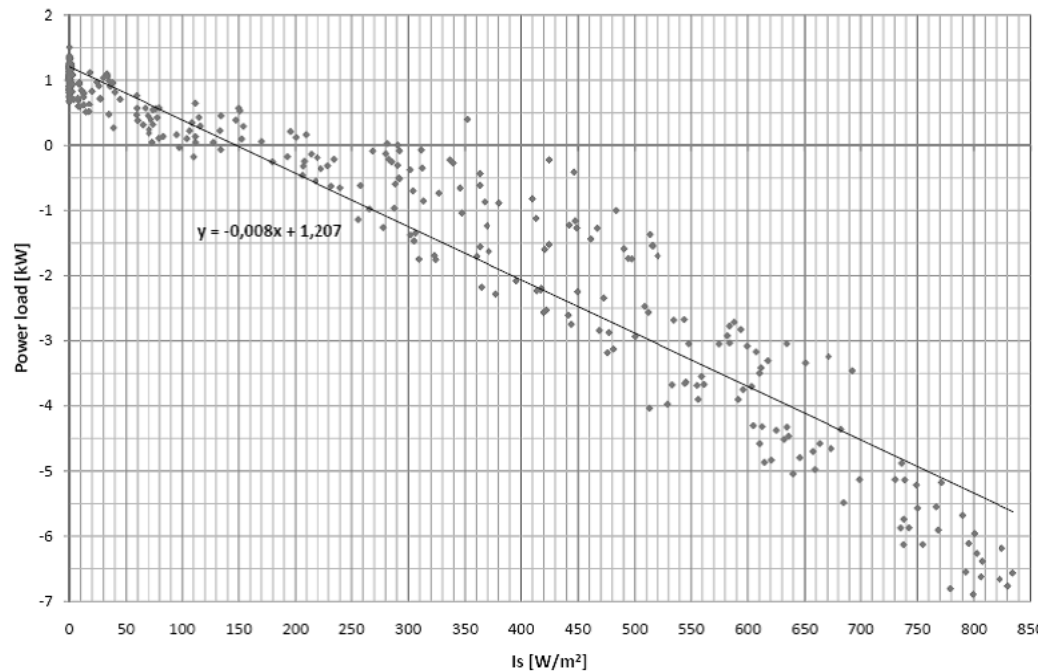
Figure 5.15 *Hourly values of calculated power load depending on the global solar irradiation at that time, based on DSF_SH measurements.*

The errors of the simple calculation method may also be explained by analyzing the temperatures in the DSF. Figure 5.16 compares the measured temperature at the height of 2,5m and the calculated temperature in the middle of the cavity as well as the measured and calculated outlet air temperature. As explained in chapter 4.2.1, in this case the readings from the measurement point at the height of 5,4 m are considered as the outlet temperature.

At times of lower temperatures in the DSF, which correspond to the heating demand, the temperatures inside the cavity are almost identical. However, the measured outlet air temperatures are higher than the calculated ones. This indicates, that the energy gain / losses due to heat transfer through the internal skin, which is influenced by the mean temperature in the air gap, has a bigger impact on the calculated energy consumption than the heating demand due to ventilation.

On the other hand, at times of high temperatures in the DSF, the calculation results are much higher than the measured values. This is especially the case for the outlet air temperature, for which the biggest difference between the measured and calculated value is 55 °C. The reason for this is probably the wrongly assumed temperature gradient inside the DSF, which has been described in chapter 5.2.1. The calculated temperatures inside the DSF are also higher because the solar gains effecting the cavity have been increased to take into consideration the reflection from the shading device, see Equation 5.10. It seems that peaks of calculated air temperatures correspond to unusually high errors in the energy consumption for cooling.
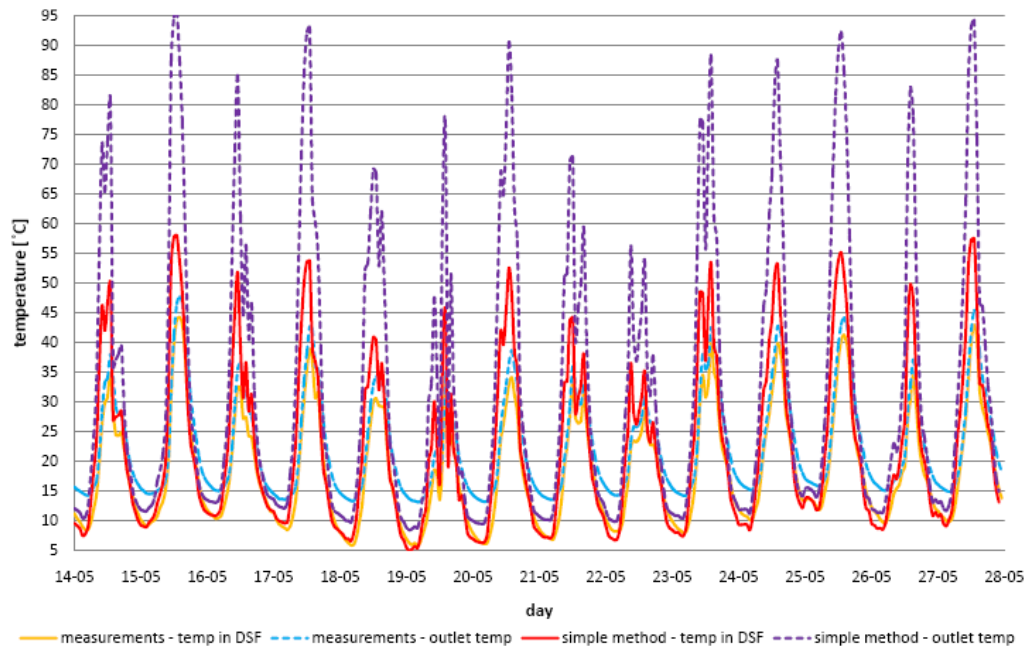
Figure 5.16 *Measured and calculated air temperature in the middle of the DSF and in the outlet, based on hourly values for DSF_SH.*

The simple calculation method gives unsatisfactory results mainly because of the difference in temperature values inside the DSF. However, another source of error seems to be the proportion between the parts of the power load covering the energy losses / gains due to heat transfer, ventilation and solar heat gains.

5.3. Summation

In general, the simple calculation method overestimates the cooling load, in each of the investigated models, see Figure 5.17. Unlike the measurement results, the simple calculation method indicates that the DSF_1_2 gave the highest energy consumption. Both of the mentioned errors are thought to be a result of overrating the influence of solar radiation on the performance of the double skin façade. In the simple calculation method the energy losses / gains are considered to be due to direct solar gains, heat transmission through construction elements and energy need for ventilation. The two latter are mainly influenced by air temperatures in the DSF – the temperature in the middle of the cavity is responsible for heat transfer through the internal skin, whereas the outlet temperature is taken into consideration in the energy consumption due to ventilation. However, this investigation showed that the temperature profile inside the DSF is assumed to be a linear function with a wrong slope coefficient. This gives too big temperature values in the DSF, especially at times of high solar radiation. The reason for this error is the fact that the simple calculation method does not take into consideration the dimensions of the double skin façade. Therefore, the length and path of the airflow as well as the time period during which the fresh air stays in the DSF are unknown. This makes it impossible to correctly calculate the amount of solar radiation absorbed by the air. The investigation described in chapter 5.2.2 confirms that the lack

of DSF geometry is an important, but not the only, drawback of the simple calculation method. Another source of error may be neglecting heat transfer due to convection.
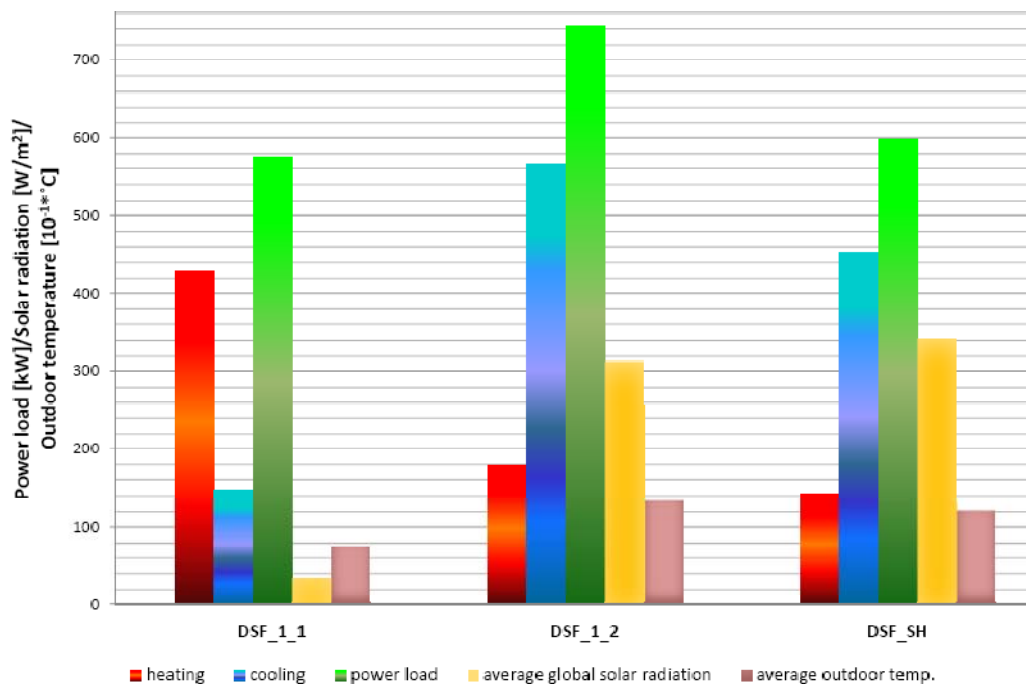
Figure 5.17 *Comparison of calculated heating load, cooling load, total power load, average global solar radiation and average outdoor temperature, obtained from measurements for different models.*

Errors are also noticeable when comparing different simple calculation results, without considering the measured data as a reference point. For example, the difference in the energy need for cooling between DSF_SH and DSF_1_2 is 110,68 kW, which constitutes 19,58% of the calculated DSF_1_2 cooling load. In reality this difference is 145,51 kW (60,14% of the measured DSF_1_2 cooling demand). This indicates that the simple calculation method gives unrealistic analysis of the sensitivity of different parameters. The reason for this could be that the theoretical value of the shading coefficient might differ from the actual performance of the shading device in the full-scale model.

6. BSim simulations

BSim is a user-friendly, flexible computer program for calculating and analyzing indoor climate conditions, power demand and energy consumption in buildings. By developing a detailed mathematical model for the building, it is possible to simulate even highly complex buildings with advanced heating and ventilation systems and operating strategies that vary over the course of the day and year. The software calculates power outputs and energy flows within the building and between the building and its surroundings. For all the spaces or zones being simulated, the software will therefore calculate heat loss through transmission, infiltration and ventilation, heat input in the form of solar heat, heat and moisture given off by people and equipment, electricity consumption for lighting, and power demand and energy consumption for every component of the heating, cooling and ventilation systems. Indoor climate is calculated using hourly values for indoor air temperatures, surface temperatures, relative atmospheric humidity and air exchange for each zone [12].

As mentioned in chapter 1.2 the results from the measurements are compared with results obtained from the building simulation software BSim. The main purpose of this comparison is to test BSim's ability to model double skin façade as air supply for mechanical ventilation system.

For every measurement model: DSF_1_1, DSF_1_2 and DSF_SH separate simulation have been made. The simulations and their results can be found as – Excel files on the attached CD.

6.1. Structure of 'the cube' model in BSim

The model of 'the cube' in BSim is build with all the thermal and structural properties of the full-scale model. Structural properties are U-values, thermal resistance and thickness of the walls as well as the U-values of the windows. Thermal properties are the temperatures in each room – zone.

The full-scale model consists of the experiment room, the double skin façade and the two rooms (instrument and engine), which are only used as a technical backup. In the

BSim simulation only the experiment room (in BSim named 'test room') and the DSF (both marked red in the Figure 6.1) are modelled, the two other rooms are used to include into calculation different heat transmission through the North wall of the experiment room [6].
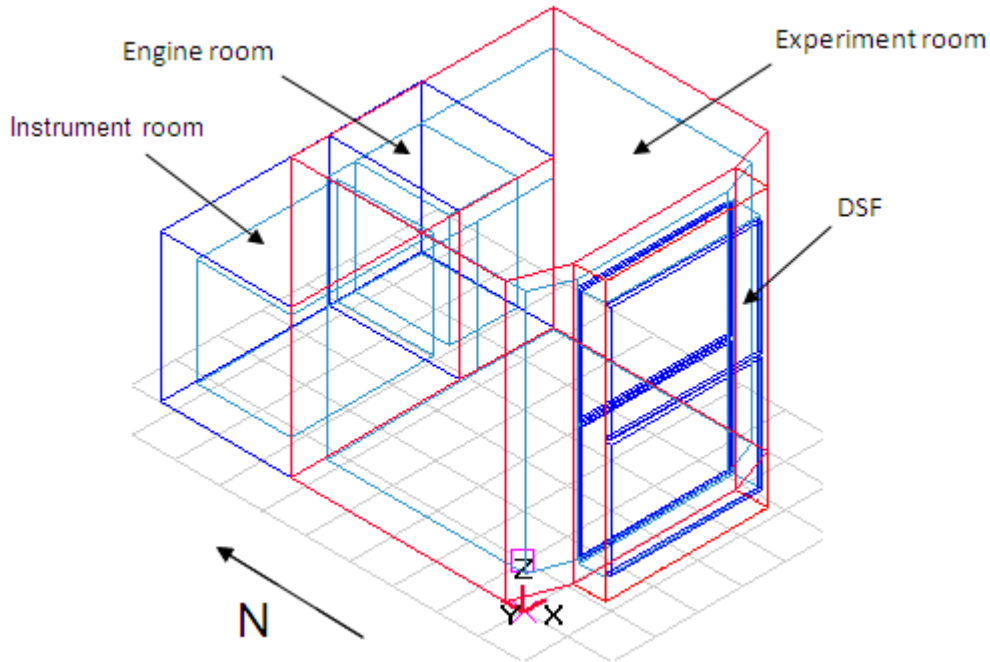
Figure 6.1 *BSim model*

In the BSim experiment room is a single zone, which represents the indoor environment behind the DSF. To investigate the DSF performance in BSim, it is necessary to define it as a single zone [6]. The instrument room and the engine room (in BSim named 'cold room') are two separate zones. The geometry and zone division of the BSim model is shown in the Figure 6.1.

In order to simulate in BSim the performance of double skin façade with the shading device in the model DSF_SH, a shading system was added to the internal DSF window, with the shading coefficient of 0,55, as defined in chapter 2.5.

6.2. Inputs for the simulations

In the simulation the indoor as well as outdoor environment has to be defined as close to reality as possible. The Excel file with weather data is based on the measurements results and meteorological data from the Danish Meteorological Institute. For every measurement model: DSF_1_1, DSF_1_2 and DFS_SH the Excel file is created separately. The indoor conditions are different for each zone and they are defined by special systems. In the working schedule for all systems every day is equal. There is also no difference between times of the day. In all simulations the maximum thickness of

sub-division of material layers is 0,005m in order to obtain more accurate simulation result.

Instrument and cold room
In those two zones cooling and heating system are defined in order to keep a constant air temperature. The air temperature is the average value for the whole period of the measurements. The energy consumption of those systems is no taken into consideration when calculating the total energy consumption of 'the cube'.

Test room
In this zone the heating and cooling systems fulfil the function of the air conditioning system described in chapter 2.1. The mechanical ventilation system defined in the zone is responsible for the constant air flow from the DSF into the test room. The air flow is set up to 136,5 m^3/h, which corresponds to about 1 h^{-1} air change rate of the volume of the test room. The ventilation system is equipped only with an input and output fan, there is no heating or cooling unit. The input fan provides the air from the DSF to the test room. The output fan is just defined for the simulation needs, because BSim required both fans in the mechanical ventilation. The pressure losses are the same at the inlet and exhaust part of the system and their value is 1200 Pa.

Double Skin Façade – DSF
System in this zone consists only of the mechanical ventilation, whose main function is to keep the constant air flow, around 136,5 m^3/s, from the outside to the DSF. The system is equipped with the input fan, which provides the air from outside to the DSF, and output fan, which has the same function as in the test room.

6.3.   Kappa model

In BSim the energy and comfort conditions in mechanically ventilated zones are calculated with the assumption, that the air in the zone is completely mixed, κ=1. In zones ventilated according to the displacement principle, this assumption should not be used, as this form of ventilation in particular will generate gradients (in a vertical direction). In this cases kappa should be below 1 and the value depends on the zone geometry and internal heat sources [12].

In this report in BSim model of 'the cube' the double skin façade should be modelled as a zone with displacement ventilation to simulate best the full-scale model. On the other hand, when kappa coefficient is defined for the zone it remains constant for the whole simulation time, days and nights. In the real model the air temperature gradient is different for days and nights, it is even changing during the day. To investigate the influence of the κ≠1 on the DSF performance, two simulations in BSim were made. One with κ=1 and second with κ=0,35 (the value suggested by the BSim help file).

The results show, that κ=0,35 creates the vertical gradient in the DSF cavity, but it is only accurate for the lower part of the DSF cavity. For temperatures at the top of the air-gap the difference between the measured and simulated values is significant, see Figure 6.2.
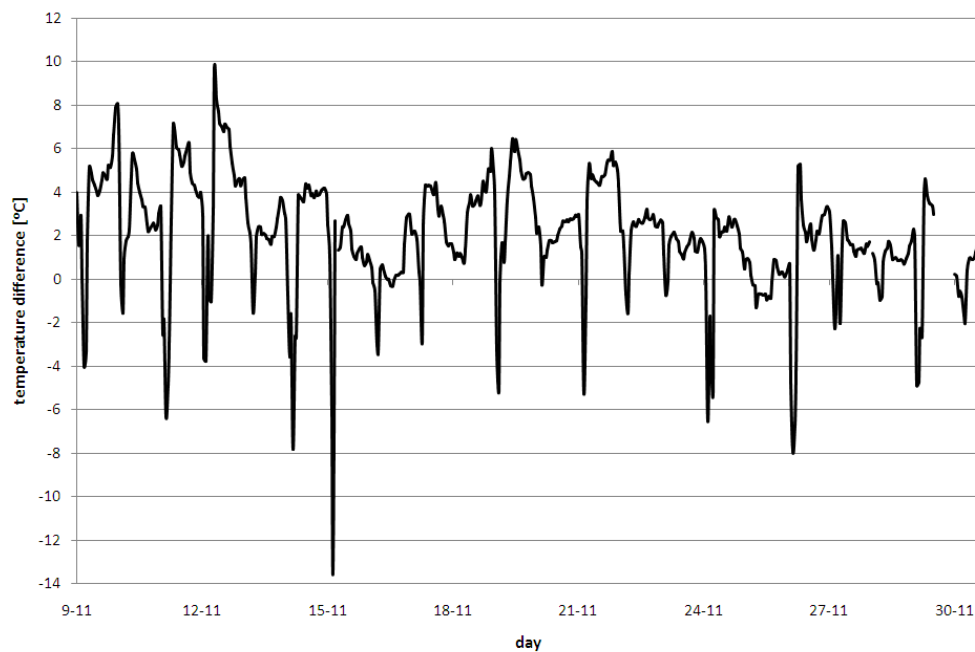
Figure 6.2 *Difference between measured and simulated with κ = 0,35 air temperature in DSF cavity at height 5,5m, based on hourly average values.*

Comparison between measurements and two BSim models of the mean outlet temperature form DSF to the test room for whole period shows that kappa value has very small influence on this parameter, see Table 6.1.

	Measurements	κ=1	κ=0,35
Outlet temperature [C]	14,5	11,04	10,87

Table 6.1 *Mean outlet temperatures for measurements, κ=1, κ=0,35*

Similar result as for the outlet temperature appears for the total energy consumption, but in this case the model with κ=0,35 gives result closer to the measurements, see Table 6.2.

	Measurements	κ=1	κ=0,35
Total energy consumption [kWh]	635,23	589,25	594,21

Table 6.2 *Total energy consumption for measurements, κ=1, κ=0,35.*

In general the comparison of those two BSim simulations with different κ shows, that the vertical gradient in double skin facade cavity has mostly influence on the heat losses due to heat transfer between DSF and test room. It has almost no effect on the outlet temperature from DSF, because in BSim in mechanically ventilated it is impossible to define the geometry of inlet and outlet points.

After analyzing all the results, it was decided, that in this report in BSim simulations 'kappa model' will not be used– κ=1. Firstly, because in previous researches on double skin façade – 'the cube' in BSim models was defined with κ=1 and to be able to compare previous simulation results with present ones the same simulation settings have to be used. Secondly, the main aim of this report is to investigate the energy performance of double skin façade and the difference in total energy consumption between BSim simulations is only 4,96 kW.

6.4. Simulations results

As mentioned in chapter 5.2 BSim calculations are conducted for hourly values and comparison between the simulations results and measurements is very easy. Four measured values, the same as used in the simple calculation method (see chapter 5.2), have been considered for comparison with the calculation results: the energy consumption for cooling and heating, the outlet air temperature from DSF and the air temperature in DSF cavity. The only difference is that, the temperature in the DSF cavity is the volume average calculated from all the measuring points on different heights in section 2. The mean air temperature for whole air-gap is calculated, because as mentioned in chapter 6.3 in BSim model's with κ=1 the air in the mechanically ventilated zones is fully mixed and only mean air temperature is calculated.

6.4.1. DSF_1_1

The first simulation was based on measurements in the full scale model DSF_1_1 conducted by Olena Kalyanova from 09.11.2006 till 30.11.2006 [11]. In this simulation there was no shading device in the DSF. The first compared value is the energy consumption. In Figure 6.3 the measured and simulated energy need are presented. As mentioned in chapter 5.2.1, the negative values represent the cooling load, but for comparison the absolute values are used.
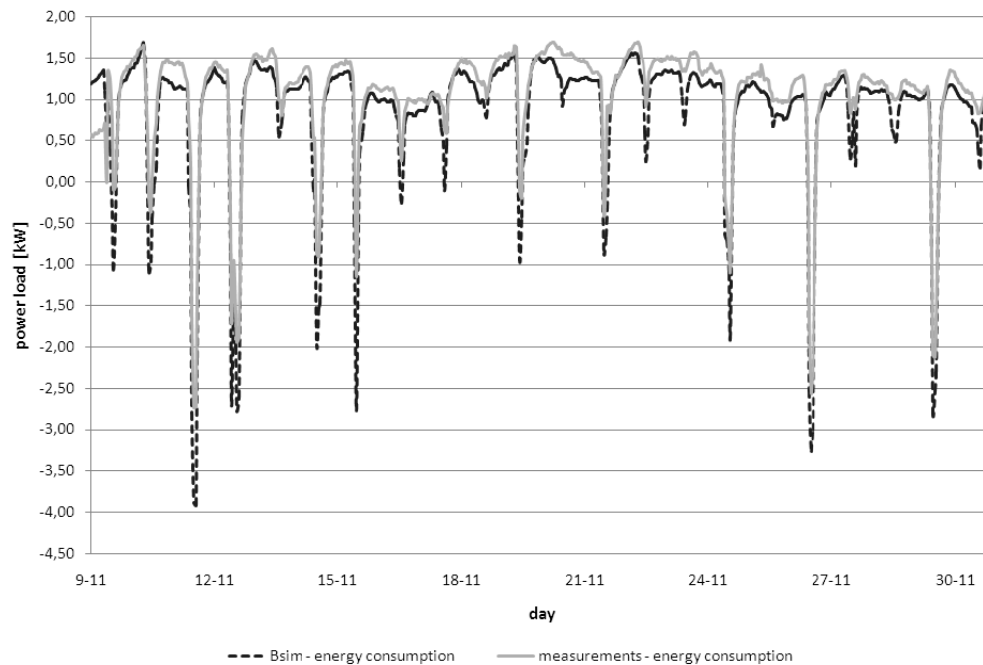
Figure 6.3 *Comparison of hourly average measured and simulated power load, based on data gathered for DSF_1_1.*

From the graph it can be noticed, that the simulated heating load is lower that the measured one. The average difference between hourly values is 0,171 kW. Comparison of the simulated and measured cooling load in 'the cube' gives the opposite results. The simulated values are bigger than the measured ones. The average difference between hourly values is 0,516 kW.

	Maximum difference	Minimum difference	Average difference
Energy need for heating [kW]	0,915	0,001	0,171
Energy need for cooling [kW]	1,625	0,005	0,516

Table 6.3 *Differences between the measured and the calculated hourly values of the heating and cooling load, based on Figure 6.3*

During the simulation period the heating load constitute around 90 % of the total energy consumption. It is due to the fact, that the data was gathered in the heating season of the year. The cooling load is stronlgy connected with the solar radiation. It apears only during sunny days with strong solar radiation. So high predominance of heating over cooling load has a significant influence on the overall energy consumption of 'the cube'. For the entire considered period the total energy consumption simulated in BSim was lower from the measured in the "cube" by 45,98 kW (-7,2%), see Table 6.4.

	Energy need for heating [kW]	Energy need for cooling [kW]	Toal energy consumption* [kWh]
DSF_1_1 measurements	595,55	39,68	635,23
BSim simulation	521,77	67,48	589,25
Difference	73,78	27,80	45,98
Precentage	-12,4%	+70,1%	-7,2%

* This is the sum of the absolute values both for heating and cooling energy consumption.

Table 6.4 *Comparison of measured and simulated sum of energy consumption for the whole considered period.*
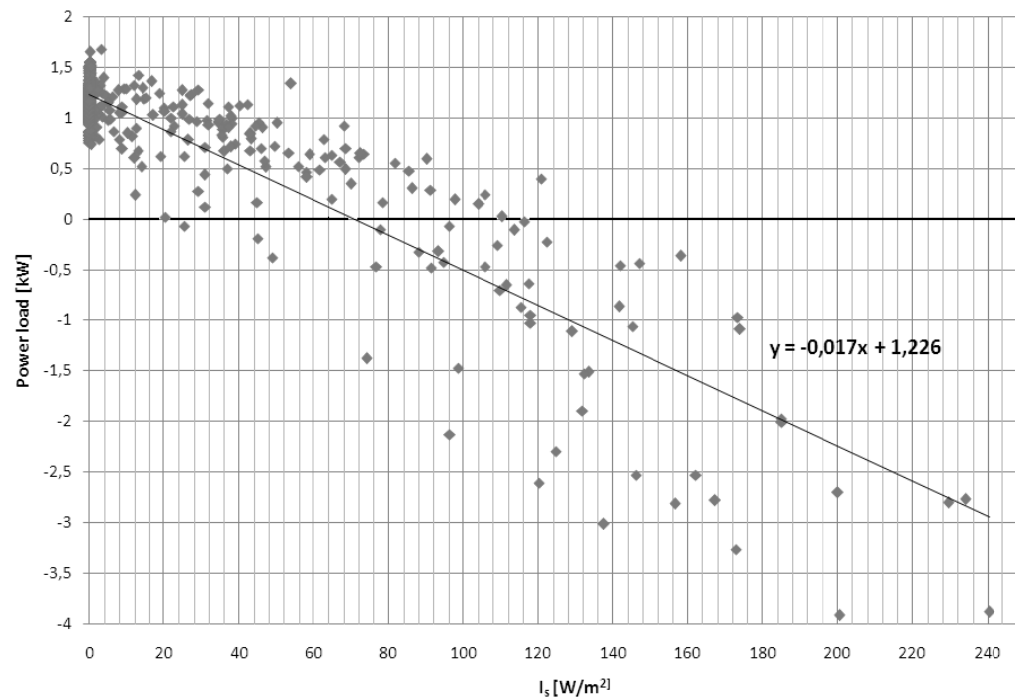
Figure 6.4 *Hourly values of simulated power load depending on the global solar irradiation at that time, based on DSF_1_1 measurements.*

The first explanation, why the simulated cooling loads are so overestimated and heating loads are lower than the measurement's results, can be the correlation between the power load and the global solar radiation shown in the Figure 6.4. The trend line obtained from BSim simulation is more tilted than the one from measurements. Thereby in the simulation results the cooling loads appear with solar radiation above 70 W/m^2, which is 35 W/m^2 lower than in reality, and values of cooling demand are higher.
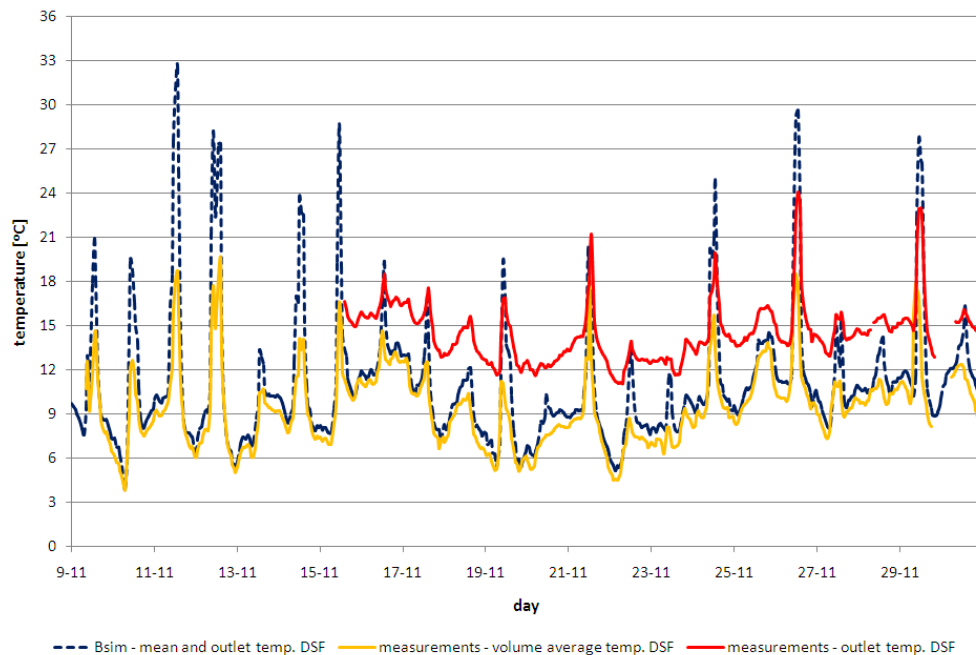
Figure 6.5 *Comparison of hourly average measured outlet temperature, mean volume average temperature and simulated mean - outlet air temperature in DSF, based on data gathered for DSF_1_1.*

The second reason for the differences in results may be explained by comparing the mean and outlet air temperature in DSF measured and simulated in Bsim, see Figure 6.5. In general the mean air temperatures in DSF simulated in BSim are very close to the volume average measured values. The mean values for the whole period are: BSim - 10,99 $^{\circ}$C, measurements – 9,40 $^{\circ}$C . It's important to remember, that BSim assumes complete air mixing in the mechanically ventilated zone and the temperatures are the same in every point of the zone. In realty in the DSF cavity the temperature increases with height and the mean air temperature is the mean value calculated from the readings on different heights. If a higher temperature inside the DSF is taken into consideration in BSim simulation, the heat losses due to heat transmission through the internal skin would be much smaller. This could be one of the reasons why the calculated energy need for heating is smaller than in reality. The peaks in the simulated temperature are firstly strongly connected with the solar radiation. Secondly in BSim outdoor conditions such as wind speed and direction have no influence on DSF performance, because in zones with mechanical ventilation those parameters are no taken into account. In reality they influence the bottom parts of the DSF, as proven by the tracer gas experiments.

In the case of the outlet temperatures, BSim gives much lower results than measurements, the average different is 3,89°C. Peaks correspond to the time when cooling loads occurred and the simulated values were higher than the measure ones. This would explain why the calculated energy consumption for cooling is higher than the measured one. BSim shows the same tendency as the simple calculation method for

mode DSF_1_1. The main reason for this outcome is that, reference outlet temperature was measured at height 5,4m and in the BSim's models with mechanical ventilated zones the outlet point is undefined and the outlet temperature is taken as a mean air temperature for the whole zone.

In general the differences between BSim simulations and measurement results seem to be firstly due the complete mixing of air in the DSF cavity in BSim and secondly due to the undefined position of the outlet point of the incoming air from DSF to the test room but also from the outsider to the DSF.

6.4.2. Double skin façade contra single glass façade.

A new BSim simulation of 'the cube' with one glass surface was made to investigate the energy performance of the double skin façade in comparison with a traditional single glass façade. The new model of 'the cube' is almost the same as DSF_1_1 the only difference is that there is no internal window and the external surface has the properties of the internal one.

The energy result of the comparison is shown in the Figure 6.6. It is clear, that both energy need for heating and cooling in the case with single façade gives higher values, than the model with double skin façade. The difference in heating loads is mainly caused by the higher air temperature in DSF cavity in comparison to the outdoor temperature. The temperature difference has an influence, firstly on heat losses due to heat transmittance and secondly on the inlet temperature to the experiment room.
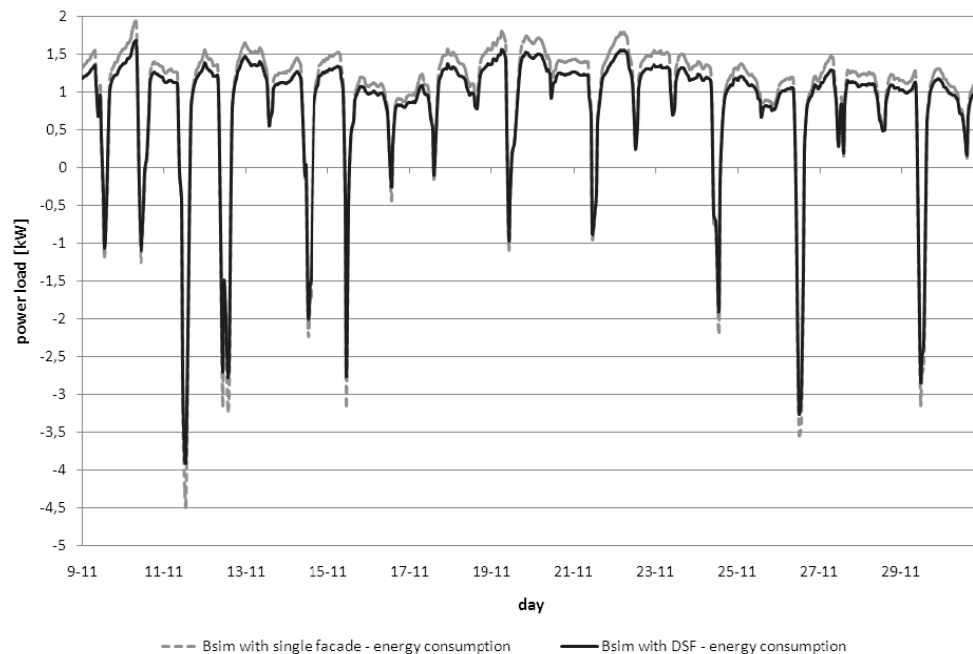
Figure 6.6 *Total energy performance based on hourly average values simulated in BSim with and without DSF.*

The main reason for the differences in cooling results can be explained by the lower solar gains in the experiment room in the case with double skin facade. That heat sources due to solar radiation in the experiment room are decreased of amount of heat accumulated in the DSF cavity. Figure 6.7 shows the solar gains in the experiment room for both cases with DSF and with single glass façade.
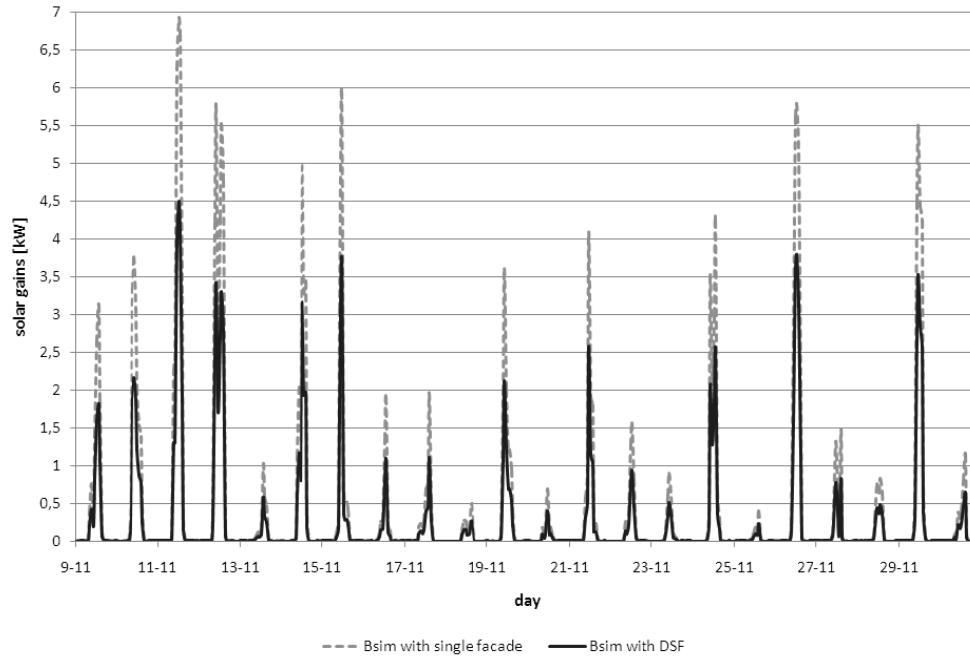
Figure 6.7 *Solar gains, based on hourly average values, for both BSim simulations: with and without DSF.*

In general the total energy consumption in the case with single facade is higher than with double skin façade for about 12%, see Table 6.5.

	Toal energy consumption [kWh]
Single facade	660,70
DSF	589,25
Difference	71,45
Presentage	+12,12%

Table 6.5 *Comparison of sum of energy consumption for both cases with and without DSF.*

6.4.1. DSF_1_2

The BSim model used for simulating the DSF_1_2 case was identical as for DSF_1_1, except for the weather conditions. This had a significant influence on the character of the simulated energy consumption, which in 58,3 % was caused by the cooling load. Comparison of the measured and simulated power load have been shown in Figure 6.8. Values below 0 represent the cooling demand. The cooling peaks according to results

from BSim are almost the same as the measured ones, but the heating load is significantly lower. The average difference for the hourly cooling demand is 0,08 kW and for the heating 0,29 kW.
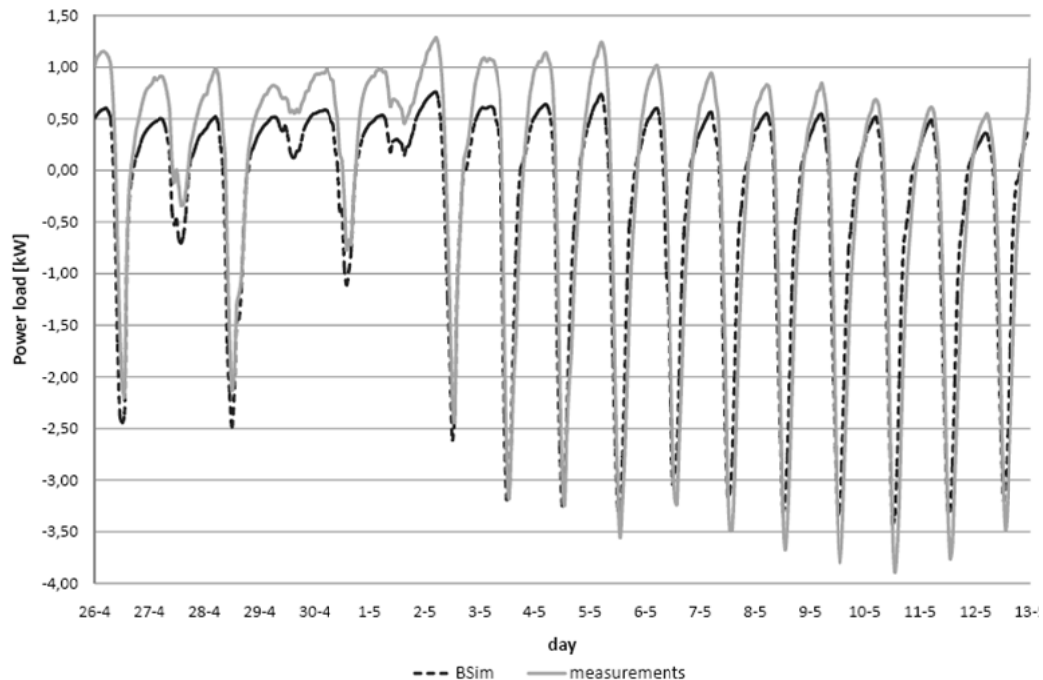
Figure 6.8 *Comparison of hourly average measured and simulated power load, based on data gathered for DSF_1_2.*

A more detailed comparison of those values can be found in Table 6.6. In general the error of simulation results is much higher than in the case of DSF_1_1 and unlike before, it is mainly caused by the heating and not cooling of the cube. The big difference in the energy need for heating appeared mainly in the first half of the simulated period, when the heating loads dominated over the cooling ones.

	Energy need for heating [kW]	Energy need for cooling [kW]	Toal energy consumption* [kWh]
DSF_1_2 measurements	173,23	241,94	415,17
BSim simulation	94,57	227,91	322,48
Difference	78,66	14,03	92,69
Precentage	-45,4%	-5,8%	-22,3%

* This is the sum of the absolute values both for heating and cooling energy consumption.

Table 6.6 *Comparison of the sum for the whole measurement period of the measured energy consumption based on hourly averages and the simulated energy consumption based on hourly averages, for DSF_1_2 measurements.*

As mentioned in chapter 4.2.1, solar radiation is thought to have a decisive impact on the energy performance of double skin façades. Figure 6.9 shows the correlation

between the power load obtained from BSim simulation results and the global solar radiation. It should be noted that global solar radiation is one of the input values in the BSim weather file and therefore is identical as in the case of the measurements. According to the trend line, values of solar irradiation above 138 W/m² contribute to the cooling demand. The angle of the trend line is the same as for the one obtained from the measurement results. However, in reality cooling loads are caused by values of solar radiation higher by almost 50 W/m². An explanation for the differences between the real and simulated energy consumption can be found when analyzing the temperatures in the DSF zone.
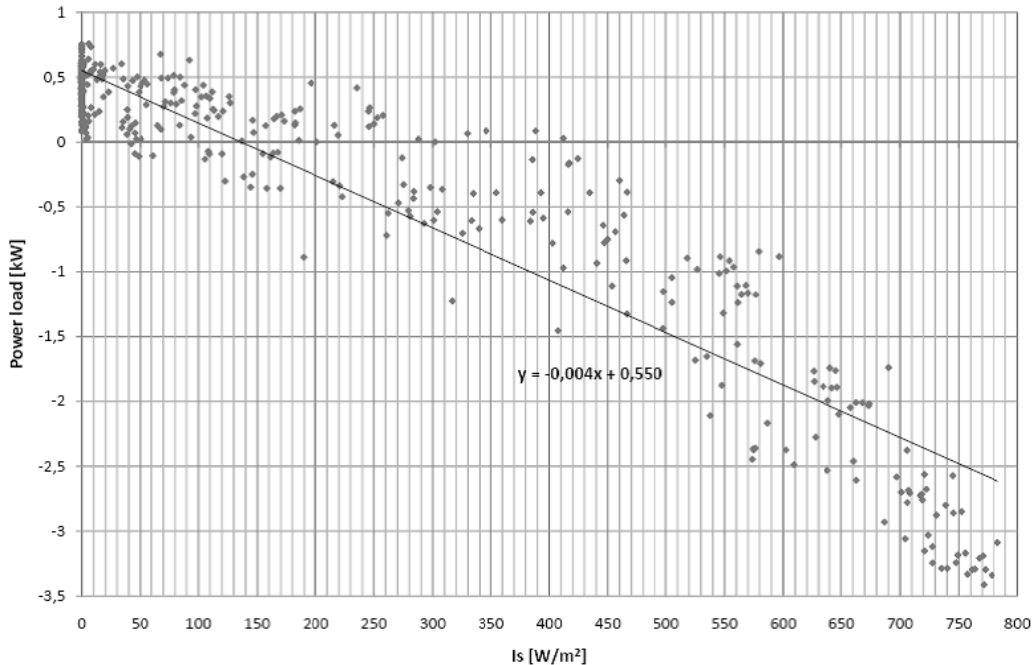
Figure 6.9 *Hourly values of simulated power load depending on the global solar irradiation at that time, based on data gathered for DSF_1_2.*

It should be noted, that as mentioned in chapter 6.4, in BSim it is impossible to define the geometry of the mechanical ventilation outlet and the air inside the DSF is considered to be fully mixed. Therefore, both the measured volume average temperature in the cavity and the air temperature in the outlet have to be compared to the same value from the BSim simulation – the mean operation temperature in the DSF zone, see Figure 6.10. As explained in chapter 4.2.1, in order to minimize the influence of the indoor air temperature, readings from the measurement point at the top of the DSF (and not exactly in the outlet) are considered as the outlet temperature.

During peaks of high temperatures in the DSF, BSim on average overestimates the outlet temperature by 6 ˚C. BSim results are also on average higher by 2,24 ˚C from the volume average temperature. The reason for higher temperatures indicated by BSim might be the fact, that the simulation programme does not take into consideration the position of the inlet into the DSF and the outlet from the zone. Therefore, there is no indication of the airflow path and time, so the calculation of the solar heat gains

accumulated in the air is imprecise. This would indicate, that although the simulation results for the energy need for cooling are quite accurate, their cause is different than in reality. It seems that in BSim the main reason for this were the high temperatures of the incoming air. Whereas for the measurements the main cause of cooling loads was different, possibly excessive solar heat gains entering the experiment room. This is also confirmed by the volume average temperatures in the DSF corresponding to the heating demand, which are almost identical with BSim results. Still, the error of simulated energy need for heating is very significant. Unfortunately, it is impossible to compare the measured and simulated amount of solar radiation entering the cavity and the experiment room because the pyranometers in the cube were shaded and did not give an accurate reading.
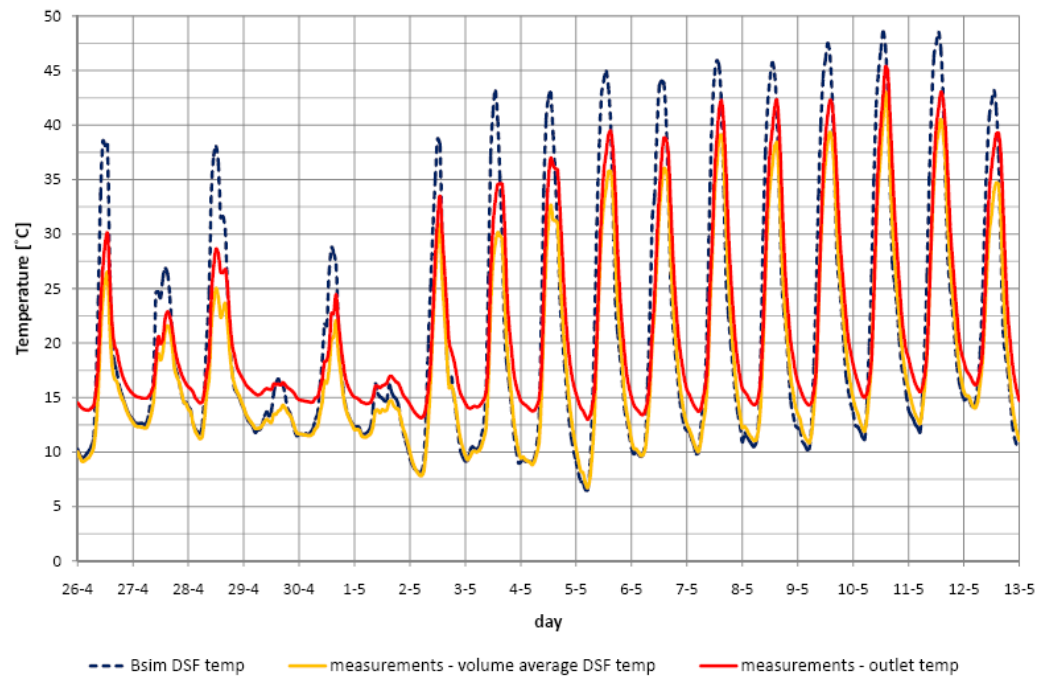
Figure 6.10 *Comparison of hourly average simulated temperature in the DSF, measured volume average temperature in the DSF and outlet air temperature, based on data gathered for DSF_1_2.*
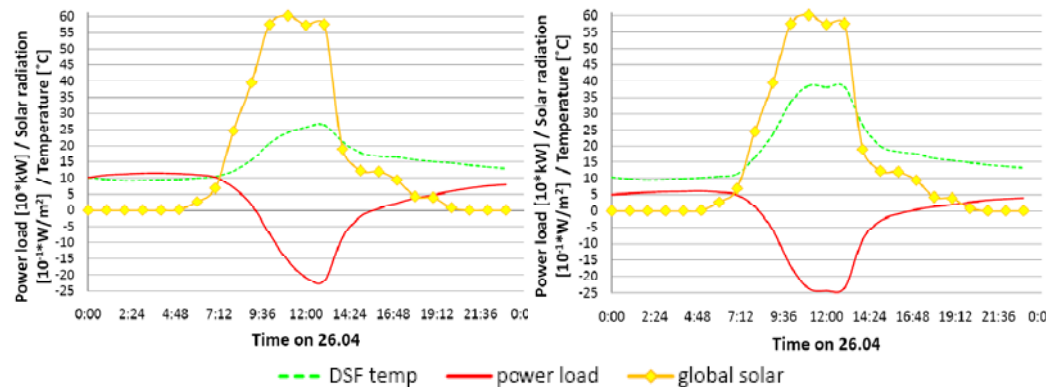
Figure 6.11 *Hourly averages of measured power load, volume average air temperature in the DSF cavity and global solar irradiation on 26.04.2008 (left). Hourly values of simulated power load, air temperature in the DSF cavity and global solar irradiation, on 26.04.2008, based on data gathered for DSF_1_2 (right).*

The biggest differences in measured and simulated DSF temperatures occurred on April 26th at 11:00 am – 11,60 °C in terms of the outlet air temperature and 14,54 ° for volume average temperature. The measured and simulated situation on that day has been compared in more detail in Figure 6.11. It seems that both the values of measured and simulated power load are comparable. However, in the case of the BSim simulation, the cooling load is mainly due to the high air temperature in the cavity, which is later taken into the experiment room. Another difference between reality and BSim, is that in the case of mechanical ventilation the simulation programme does not take into consideration wind, which might influence the airflow and temperature in the bottom parts of the cavity.

Clearly there is a significant error in BSim results. The reason for this is probably the fact that in BSim, when applying mechanical ventilation, it is impossible to define the DSF inlet / outlet geometry as well as an accurate temperature gradient in the zone. It could also be the case that differences occur in the simulated heating load due to convection and the programme has problems when dealing with solar radiation.

6.4.2. DSF_SH

In BSim the model of DSF_SH is similar to the two earlier models DSF_1_1 and DSF_1_2. In this case the shading device was assigned to the internal window as protection of the experiment room – zone and weather conditions were changed. Out of all three BSim models the DSF_SH was most inconsistent with reality in terms of 'the cube's' constructions. The difference is that in reality the roller blades are physically placed in the DSF cavity and in BSim only one shading property is defined in the model – the shading coefficient. The rest like transmittance, absorbance and reflection are undefined.
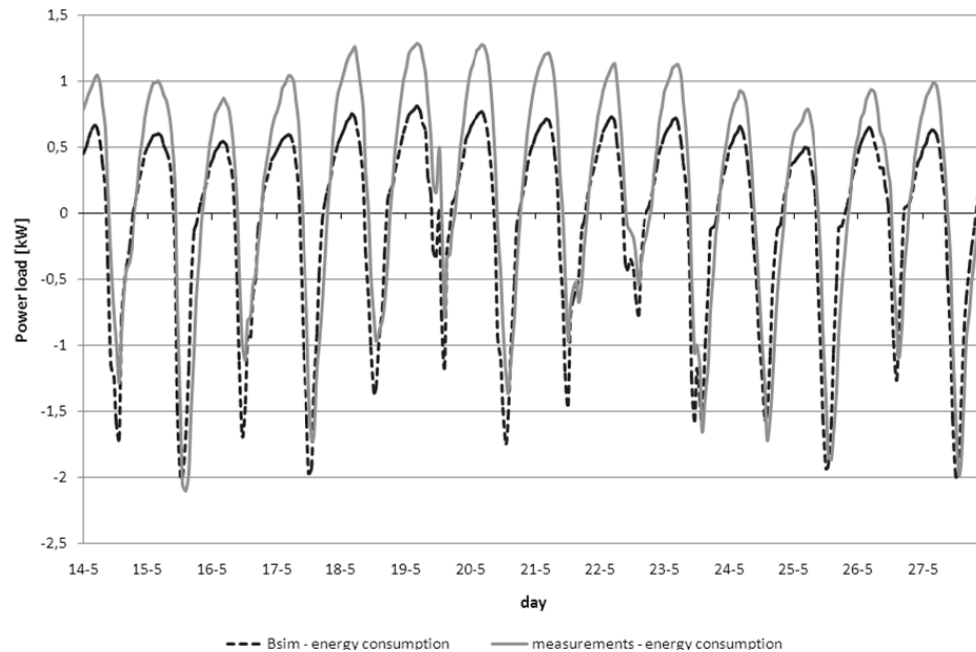
Figure 6.12 *Comparison of hourly average measured and simulated power load, based on data gathered for DSF_SH.*

The shading device has a significant influence in the energy consumption. Comparison between measured and simulated energy consumption is shown in the Figure 6.12. Values below 0 stand for the cooling loads. In the simulated total energy consumption for the DSF_SH the ratio of the cooling and heating loads is very similar, 54% and 46%, respectively, while in the measurements the heating demand in slightly dominating. From Figure 6.12 it can be notice that the simulated cooling loads are mostly very close to the measured values, except for a few peaks. The average difference cooling demand is 0,36 kW. For the heating loads the situation is different, for whole measurement's period the simulated heating demand in lower than the measured values. The average difference for the hourly values is 0,28 kW. However, more important is the comparison between the total energy need for heating, cooling and total energy consumption, see Table 6.7.

	Energy need for heating [kW]	Energy need for cooling [kW]	Toal energy consumption* [kWh]
DSF_SH measurements	149,25	96,43	245,68
BSim simulation	88,78	104,82	193,57
Difference	60,38	14,03	52,11
Precentage	-40,5%	+8,7%	-21,2%

* This is the sum of the absolute values both for heating and cooling energy consumption

Table 6.7 *Comparison of the sum for the whole measurement period of the measured energy consumption based on hourly averages and the simulated energy consumption based on hourly averages, for DSF_SH measurements.*

In general the error of simulation results is very similar to the case of DSF_1_2, around -20%, and also in DSF_SH it is mainly caused by the heating loads, which is underestimated for about 40% in proportion to the measurements. However, in DSF_SH the simulated cooling loads are slightly higher than the measurement's results (+8,7%).
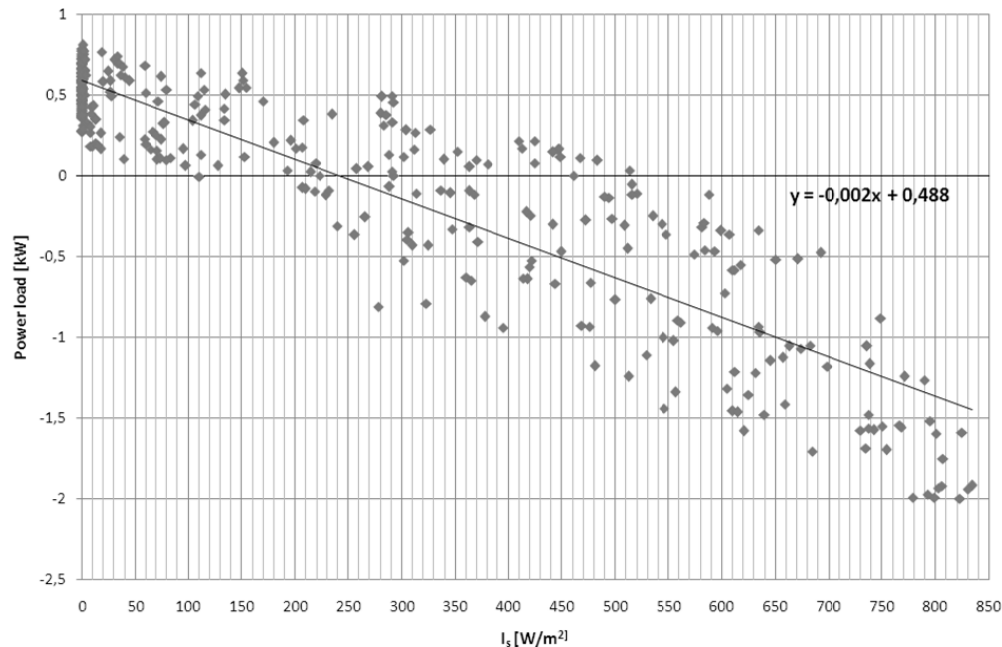
Figure 6.13 *Hourly values of simulated power load depending on the global solar irradiation at that time, based on data gathered for DSF_SH.*

In previous investigations it was noticed that solar radiation has significant influence on the energy performance of double skin façades. Also in BSim model with the shading device the correlation between those two values is analysed, see Figure 6.13. In DSF_SH BSim model as well as in DSF_1_1 and DSF_1_2 BSim models the global solar radiation is identical as in the measurements. Comparing the simulation results with the measurements, the trend line has the same slope coefficient (-0,002), but the elevation above zero is slightly lower, which means that in BSim the cooling loads accrue with lower solar radiation. The difference between BSim outputs and measurements can have two reasons.

Firstly, because of the placement of the shading device in BSim simulation. It is different than in reality, instead of being in the DSF cavity the shading device is defined as protection against the solar radiation, which enters the experiment room. It results in a BSim limitation that the shading device is always assign to a window and the position cannot be changed. With this limitation of the software the shading device in the simulation could be also assign to a external window. However, in this case the solar radiation would be decreased not only for the experiment room but also for the whole DSF cavity and in this situation the BSim model would differ from reality even more.

Secondly, because of the temperature difference in DSF cavity between BSim and measurements, see Figure 6.14.
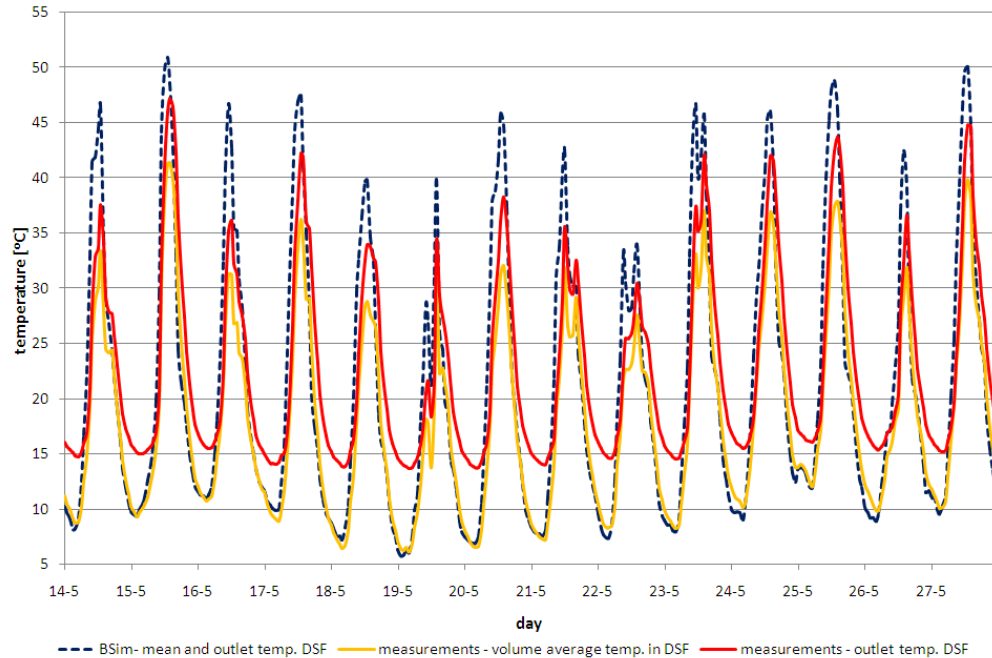
Figure 6.14 *Comparison of hourly average measured outlet temperature, mean volume average temperature and simulated mean - outlet air temperature in DSF, based on data gathered for DSF_SH.*

During night-time the simulated mean temperature in DSF cavity is almost the same as the mean from the volume average temperatures in front of and behind the shading device in reality. However, in the daytime, with solar radiation, the BSim results are higher than the measured ones. It results in slightly higher peaks in simulated cooling loads than in the measurements. This temperature difference is also caused indirectly by the different position of the shading device in the simulation and in the reality.

The difference in the outlet temperature between BSim and reality is best noticeable during night-time, when measured outlet temperatures are higher than the simulated ones, the average difference for night-time is around $6,5^{o}$C. It is surprising, because at that time also the measured heating loads are higher than the BSim results while the mean temperatures are similar. It can be concluded that both in measurements and BSim simulation the heat losses/ gains due to transmission are similar, but the energy needed for preheat the ventilation air for the double skin façade is underestimated in BSim results.

6.5. Summation

When comparing all BSim simulation results a general tendency can be noticed, that the programme always underestimates the heating load and, when there is no shading device defined, it overrates the cooling demand. The biggest errors in the energy need

for heating occurred with high global solar radiation – in the case of DSF_1_2 the mistake was -45,4 % and -40,5 % for DSF_SH. When comparing the simulation results among themselves, the difference in the cooling load between DSF_1_2 and DSF_SH is 123,09 kW, which makes up 54,01 % of the simulated DSF_1_2 cooling demand. Therefore, BSim gives values closer to reality and a better assessment of the sensitivity of different parameters than the simple calculation method. The reason for such underestimation of the effect of the solar shading might be the placement of the shading device in BSim. The programme defines it only as protection of the test room, whereas in reality the roller blinds were also shading the internal skin and part of the DSF cavity.
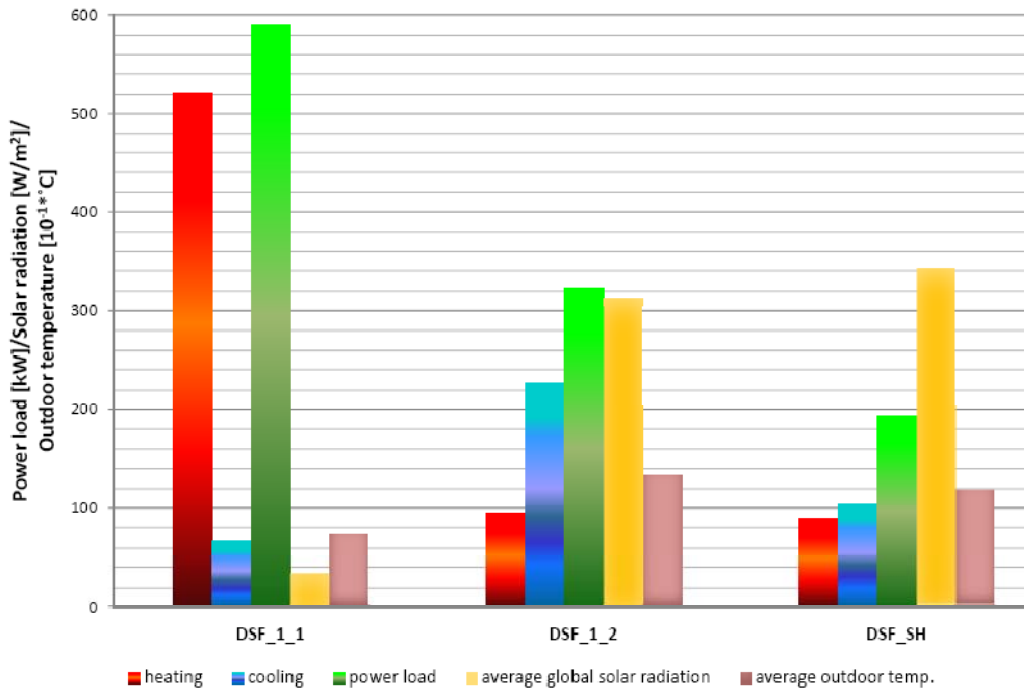
Figure 6.15 *Comparison of simulated heating load, cooling load, total power load, average global solar radiation and average outdoor temperature, obtained from measurements for different models.*

Another major drawback of BSim is that, when applying a mechanical ventilation system to a zone, it is impossible to define the geometry of the inlet and outlet and the air is considered to be fully mixed, which excludes a temperature gradient. Therefore, the difference between the temperature in the DSF zone indicated by BSim and both the measured outlet air and volume average temperature are quite big. Even when applying the Kappa model, the simulation results do not correspond well to the measurements.

The BSim model could be improved by dividing the DSF into three or more adjacent zones. This would allow the air to be taken from the bottom of the cavity upward and be realised into the experiment room at the top. Such a solution would compensate the lack of temperature gradients in the individual zones.

7. Final conclusion

The results presented above strongly emphasize of the impact of solar radiation on the performance of double skin façades and the need for solar shading. Protection against excessive heat gains is necessary even during the heating season. This has been proved by the results of DSF_1_1 measurements conducted at the end of November. Double skin façades are thought to have great potential in reducing the energy consumption of a building. It should be noted that this project focussed on a theoretical case study concerned with only one operation strategy. When used in a proper way, DSFs can significantly preheat the fresh air when needed and provide natural lighting. This last aspect is particularly important, when considering that an average European office, school or industrial building dedicates 40 % of its overall energy consumption to electric lighting. Artificial lighting in those building types is usually used during the working hours, when daylight is available [13]. However, this issue has not been investigated in this project, although both the simple calculation method and BSim are capable of taking it into consideration. Therefore, it is a suggestion for further investigation.

These arguments make double skin façades a very important type of building construction. Therefore, the ability of proper assessment of their energy performance at an early design stage is crucial to a project. This is why, the results obtained both from the simple calculation method and BSim simulations are disappointing., as they are not on the 'safe side'. However, it should be noted that BSim is thought to be a much more advanced tool than the calculation method, because it is possible to perform in it a more detailed and dynamic analysis. Still the simple calculation method seems to follow the tendency of the measured values nearly as well as BSim. This was especially the case in the DSF_1_1 mode. It seems that at times of high solar radiation (DSF_1_2 and DSF_SH) the results obtained from both tools significantly vary from measurements and overestimate the cooling demand. The cooling load is strongly connected to solar heat gains and therefore, shading has an important role in calculating it. It should be noted, that the shading coefficient given by the producer of the roller blades used has been defined for a shading device mounted inside a room, behind the window. Its actual value may be influenced by the placement of the shading device and the ventilation mode

used. This has been proven by comparing the theoretical shading coefficient with the measurement results, see chapter 4.2.4. Therefore the theoretical shading coefficient of 0,55, which was the input both in the simple calculation method and BSim, may not be accurate. Another dynamic parameter is the g-value of the DSF skins, which is the resultant coefficient of transmittance, convection and heat transfer. Therefore, it is influenced among other factors by the temperature and angle of solar radiation. This is taken into consideration in BSim, where it is possible to define a curve corresponding to the g-value. However, the calculation method is too simple to include variations of this parameter, which could be an additional source of error. Finally, BSim has a more realistic approach, because in a dynamic simulation the time line is taken into consideration and the simulated conditions from the previous time step influence the present ones. In the simple calculation method, on the other hand, there is no correlation between the results obtained for the present moment and its predecessor. BSim seems to have potential to give better results. However, both tools call for significant improvements when calculating the performance of double skin façades. One of these might be specifying the geometry of the DSF and the outlet / inlet points, in order to consider in more detail the airflow path.

The data gathered in this project deals with only three short periods of the year. It is recommended to perform measurements as well as calculations and simulations for a longer period of an entire year. This would be an opportunity for the investigation of different operation concepts of the DSF and the shading device, which could result in long-term strategy. The obtained results would provide a better overview of the impact of a double skin façade construction on the energy consumption of a building.

Bibliography

1 - Ana Maria Leon Crespo, M.Des.S. Candidate, Graduate School of Design Harvard University *History of the Double Skin Facade*

2 - Harris Poirazis *Double Skin Façdes. A Literature Reviews.* A report for IEA SHC Task 34 ECBCS Annex 43, 2006

3 - Belgian Building Research Institute, Department of Building Physics, Indoor Climate and Building Services *Ministry of Economic Affairs Project. Active façades. Source book for a better understanding of conceptual and operational aspects of active façades.* Version no 1, June 2002

4 - Erhorn H. (et all) Bestfaçade *Best Practice for Double Skin Façades. EIE/04/135/S07.38652 WP4 Report "Simple calculation method"*, 30.06.2007

5 - Kalyanova, O and Heiselberg, P. *Experimental Set-up and Full-scale measurements in the 'Cube': 1st Draft. Aalborg: Aalborg University : Department of Civil Engineering.* ISSN 1901-726X DCE Technical Report No.034, 2008

6 - Kalyanova, O and Heiselberg, P. *Empirical Test Case Specification: Test Case DSF400_e: Aalborg: Aalborg University : Department of Civil Engineering.* ISSN 1901-726X DCE Technical Report No.027, 2008

7 - Elisabeth Gratia, André de Herde, Université Catholique de Louvain, Architecture et Climat *The most efficient position of shading devices in a double-skin facade.* 1st September 2006

8 - *Solar shading solutions* Faber catalogue from www.faber.com

9 - Hitchen E.R. Wilson C. B. *A review of experimental techniques for the investigation of natural ventilation in buildings.* March 1967

10 - http://www.wunderground.com/history

11 - gathered data can be found In an Excel file *DSF_1_1 – data from Olena Kalyanova* on the attached CD

12 - Bsim User's Guide 'Foreword'

13   - Rasmus Lund Jensen, lectures on Integrated Design of Buildings and Building Systems *Day lighting: Utilizing daylight, daylight factor.* Aalborg University : Department of Civil Engineering March 2007

Appendix

Table of contents

1. Calibration of CO₂ measuring devices

In order to measure the CO_2 concentration two devices are used:
- URAS measures the CO_2 outdoors
- BINOS measures the CO_2 concentration in the room (CO_2 will be used in the experiment to ensure constant air flow through the DSF)

For the calibration of both the devices as a reference points were used a pure gas of 1000ppm CO_2 and a neutral gas N_2 (0ppm CO_2). The gases in the bottles are dry in this reason they were humidified before the measuring devices. The readings of CO_2 concentration from URAS and BINOS were transformed from ppm to volts in an external device, which was not used in the actual experiments. The data logger used in 'the Cube' takes the reading of CO_2 concentration in volts. The calibration post is shown on Figure 1.1

Figure 1.1 *Calibration post.*

1.1. BINOS calibration

The main result from the calibration is the equation, achieved from the graph *Figure* 1.*2*. It will be used to transform readings of CO_2 concentration in the room in V from the data logger to the real value in ppm.
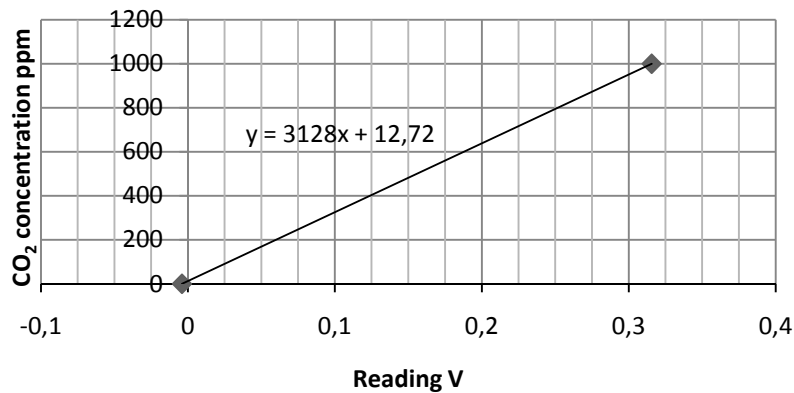
Figure 1.2 *Result of BINOS calibration.*

1.2. URAS calibration

The main result from the calibration is the equation, achieved from the graph Figure 1. It will be used to transform readings of outdoors CO_2 concentration in V from the data logger to the real value in ppm.
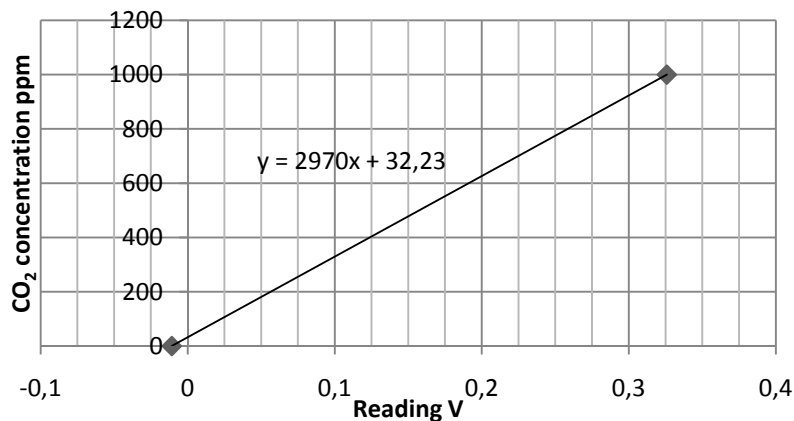
Figure 1 *Result of URAS calibration.*

1.3. Calibration of CO_2 flow meter

In order to measure the CO_2 flow provided into the DSF from the CO_2 container during the experiment with tracer gas the flow meter no. 362 was calibrated. The flow meter is shown on Figure 1.3.
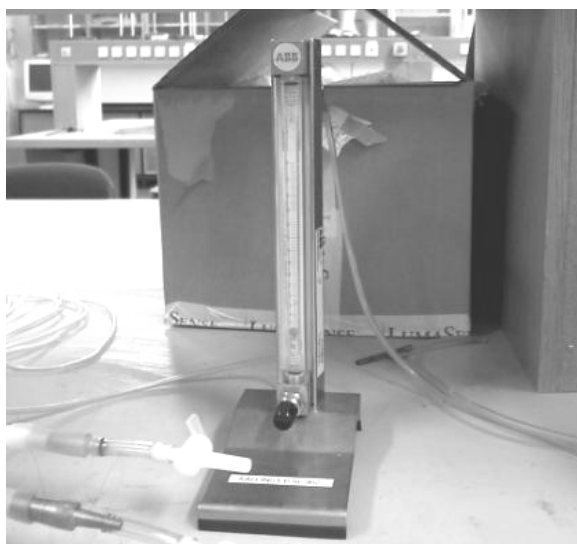
Figure 1.3 *Flow meter*

The flow meter was connected to the CO_2 container and the calibration device, from which the true flow values were readied. The results of calibration is shown on Figure 1.**4**

$$y = 0,042x^2 + 0,682x + 0,110$$
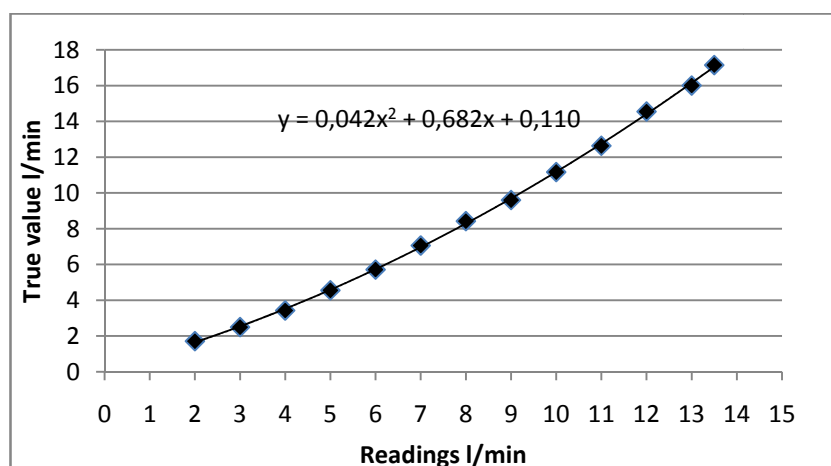
Figure 1.4 *Result of flow meter calibration*

2.   Calibration of thermocouples

For measurements of the air temperature under direct solar irradiation the thermocouples type K (Chromel/Alumel) with silver coating need to be used [1]. All of them have been connected to the HELIOS 272 data logger. During the measurements conducted by Olena Kalyanova in 2006, 77 thermocouples have been used and calibrated. For the new measurement setup from April 2008, 30 of the old tc have been replaced with new ones measuring the temperature inside the DSF. According to unpublished researched conducted by Nicolai Artmann, PhD student at Aalborg University, it is not the thermocouple itself but its place in the data logger, which influences the tc calibration. Therefore, there was no need for calibrating the 30 new thermocouples, because the equations created for their old equivalents can be used. This has been validated by calibrating three of the new tcs and comparing the calibration graphs with the old ones.

The previous and the new thermocouples were calibrated in four points: 0, 15, 25 and 35°C. The results were collected by the Helios 272 data logger a frequency of 60 Hz. For each calibration point measurements were collected for 6 minutes and then the average was taken into consideration. An example of comparison of old and new calibration result is shown in Figure 2.1. It is clear that there is no significant difference between them and so the old calibration can be used.
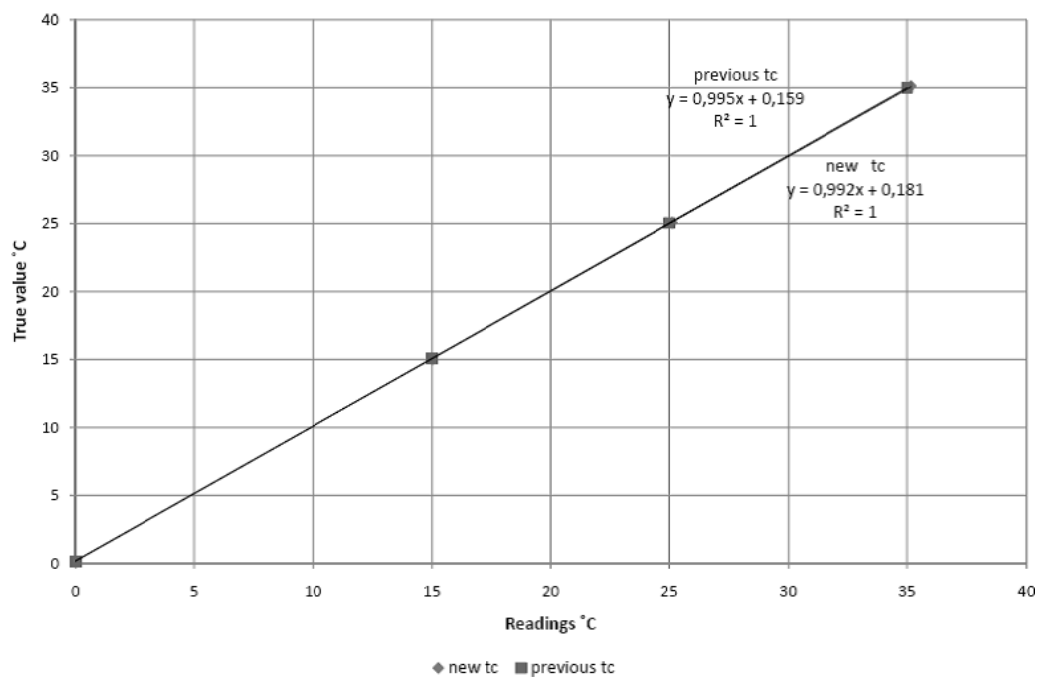
Figure 2.1 Result of thermocouple71 calibration.

3. Mechanical air exhaust installation

The purpose of the air exhaust installation is to take the same volume of air out of the experiment room, regardless of the outdoor conditions, by means of a mechanically powered fan. It is build out of Spiro ducts of various diameters and a short segment of a flexible duct. All the equipment necessary for setting and measuring the volume airflow has been connected as shown in Figure 3.**1**. The two dampers have been set to ensure the pressure loss of 600 Pa. The setup has been validated in laboratory condition prior to mounting the installation in the 'cube'. For this purpose, in addition to measuring the pressure loss over the orifice, which indicates the volume airflow; the dynamic pressure difference between the inlet and outlet of the fan has been measured. This value gives the total pressure loss in the installation.
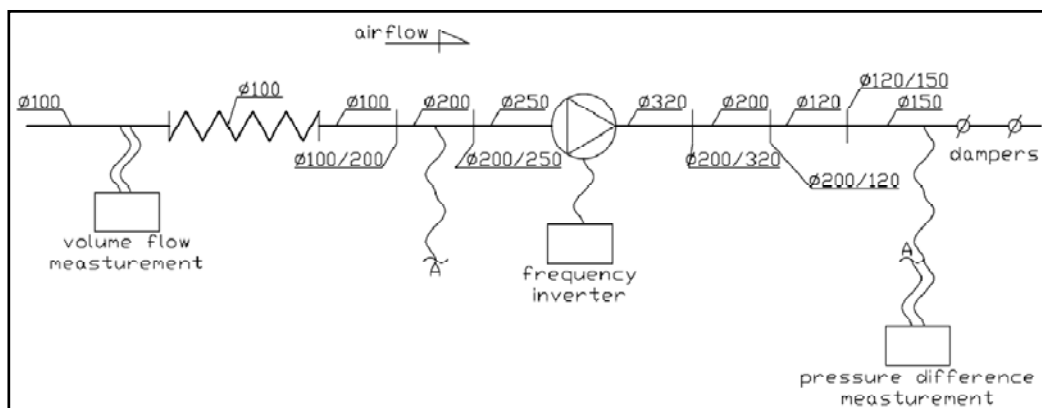
Figure 3.1 *Scheme of the mechanical exhaust installation*

4. Equations used in simple method calculation

For simple method calculation the following equations ware used.

1. **Energy need for heating – EN ISO 13790 [2]**

$$Q_{H,nd} = Q_{H,ls} - \eta_{H,gn} \cdot Q_{H,gn}$$

where

$Q_{H,nd}$ - is the building energy need for heating [kWh]
$Q_{H,ls}$ - is the total heat transfer for the heating mode [kWh]
$Q_{H,gn}$ - are the total heat gains for the heating mode [kWh]
$\eta_{H,gn}$ - is the dimensionless gain utilisation factor for heating.

2. **Energy need for cooling – EN ISO 13790 [2]**

$$Q_{C,nd} = Q_{C,gn} - \eta_{C,ls} \cdot Q_{C,ls}$$

where

$Q_{C,nd}$ - is the building energy need for cooling [kWh]
$Q_{C,ls}$ - is the total heat losses for the cooling mode [kWh]
$Q_{C,gn}$ - are the total heat gains for the cooling mode [kWh]
$\eta_{C,gn}$ - is the dimensionless gain utilisation factor for cooling.

3. **Total heat transfer – EN ISO 13790 [2]**

$$Q_{ls} = Q_{tr} + Q_{ve}$$

where

Q_{ls} - is the total heat transfer [kWh]
Q_{tr} - is the total heat transfer by transmission [kWh]
Q_{ve} - is the total heat transfer by ventilation [kWh]

4. **Total heat gains – EN ISO 13790 [2]**

$$Q_{gn} = Q_{int} + Q_{sol}$$

where

Q_{gn} - are the total heat gains [kWh]

Q_{int} - is the sum of the internal heat gains over a given period [kWh]

Q_{sol} - is the sum of the solar heat gains over a given period [kWh]

5. Solar radiation entering the DSF – DIN V 18599 [3]

$$\phi_{S,u} = F_{F,ue} \cdot A_{ue} \cdot g_{eff,ue} \cdot I_S$$

where

$F_{F,ue}$ - is the correction factor to account for the proportion of the frames of the external glazing

A_{ue} - is the area of each external surface of the annex with a specific orientation [m]

$g_{eff,ue}$ - is the effective total energy transmittance of the transparent section of the external glazing, taking the following factors into consideration:

— shading,

— the effective total energy transmittance of the external glazing taking into account solar protection devices and their activation,

— deviation of the radiation incidence from the perpendicular,

— dirt on the glazing (pollution);

I_S - is the global solar radiation intensity for the orientation of the respective dividing surface [W/m^2]

6. Direct solar heat gains due to transparent components – DIN V 18599 [3]

$$Q_{s,tr} = F_{F,iu} \cdot A_{iu} \cdot g_{eff,iu} \cdot F_{F,ue} \cdot \tau_{e,ue} \cdot I_S \cdot t$$

where

$F_{F,iu}$ - is the correction factor accounting for the proportion of the frames of the internal glazing

A_{iu} - is the area of the component of the surface separating the evaluated building zone from the unheated glazed annex - DSF [m]

$g_{eff,iu}$ - is the effective energy transmittance of the transparent section of the component, taking the following into consideration:

— the total energy transmittance $g$tot of the internal glazing including solar protection devices,

— the activation of solar protection devices,

— shading by surroundings and parts of the building,

— deviation of the radiation incidence from the perpendicular,

— dirt on the glazing (pollution);

$F_{F,ue}$ - is the correction factor accounting for the proportion of the frames of the external glazing

$\tau_{eu,e}$ - is the transmittance of the external glazing

I_S - is the global solar radiation intensity for the orientation of the respective dividing surface [W/m^2]

For the case with the shading device DSF_SH in the equation for the direct solar heat gains shading coefficient – SC is considered:

$$Q_{s,tr} = F_{F,iu} \cdot A_{iu} \cdot g_{eff,iu} \cdot F_{F,ue} \cdot \tau_{e,ue} \cdot I_S \cdot t \cdot SC$$

7. Heat gains affecting the DSF – DIN V 18599 [3]

$$\phi_u = \sum \phi_{S,u} - \frac{\sum Q_{S,tr}}{t} + \sum \phi_{I,u}$$

where

$\sum \Phi_{S,u}$ - is the sum total of solar incident radiation in the unheated glazed annex – DSF or for all transparent external components of the respective part of the building [kWh]

$\sum Q_{S,tr}$ - is the sum total of solar radiation passing through the glazed annex – DSF into the adjacent building zone, calculated for all transparent components of the surface separating the building zone under evaluation and the unheated glazed annex or conservatory [kWh]

$\sum \Phi_{Iu}$ - is the sum of the heat flows due to internal heat sources in the glazed annex – DSF [kWh]

For the case with the shading device DSF_SH in the equation for the heat gains affecting the DSF solar gains reflected by the shading device and stopped by the external skin is considered:

$$\phi_u = \sum \phi_{S,u} - \frac{\sum Q_{S,tr}}{t} + \sum \phi_{I,u} + \sum \phi_{S,u} \cdot R \cdot (1 - g_{eff,ue})$$

8. The mean temperature in the unheated building zone – DSF - EN ISO 13789 [4]

$$\vartheta_u = \frac{\phi_u + \vartheta_i (H_{T,iu} + H_{V,iu}) + \vartheta_e (H_{T,ue} + H_{V,ue})}{H_{T,iu} + H_{V,iu} + H_{T,ue} + H_{V,ue}}$$

where

Φ_u - is the heat flow (from heat sources) into the unheated building zone (e. g. due to solar heating or internal heat sources) [kWh]

v_i - is the internal temperature [K]

$H_{T,iu}$ - is the heat transfer coefficient of transmission of the components between the zone being evaluated and the adjacent unheated building zone [W/K]

$H_{T,ue}$ - is the heat transfer coefficient of transmission of the building components between the unheated building zone and the exterior [W/K]

$H_{V,iu}$ - is the heat transfer coefficient of ventilation between the building zone being evaluated and the adjacent unheated building zone (normally, $H_{V,iu} = 0$ can be assumed) [W/K]

$H_{V,ue}$ - is the heat transfer coefficient of ventilation between the adjacent unheated building zone and the outside atmosphere [W/K]

9. The outlet temperature in the unheated building zone – DSF

$$\vartheta_{out} = 2 \cdot (\vartheta_u - \vartheta_{in})$$

where

v_u - is the mean temperature in the unheated building zone-DSF [K]

v_{in} - is the inlet temperature to the unheated building zone-DSF [K]

10. Gain utilization factor for heating – pr EN ISO 13790-2005 [5]

$$\eta_{H,gn} = \frac{1 - \gamma_H^{a_H}}{1 - \gamma_H^{a_H+1}} \qquad \text{if } \gamma_H \neq 1$$

$$\eta_{H,gn} = \frac{a_H}{a_H + 1} \qquad \text{if } \gamma_H = 1$$

with: $\gamma_H = \dfrac{Q_{H,gn}}{Q_{H,ls}}$

where

$\eta_{H,gn}$ - is the dimensionless gain utilisation factor for heating

γ_H - is the dimensionless gain/loss ratio for the heating mode

$Q_{H,ls}$ - is the total heat transfer for the heating mode [kWh]

$Q_{H,gn}$ - are the total heat gains for the heating mode [kWh]

a_H - is the dimensionless numerical parameter depending on the time constant τ_H

$$a_H = a_{0,H} + \frac{\tau_H}{\tau_{0,H}}$$

where

$a_{0,H}$ - is the dimensionless reference numerical parameter in this project equal 1,0.

τ_H - is the time constant of a building or building zone [h]

$\tau_{0,H}$ - is the reference time constant in this project equal 15h

11. Gain utilization factor for cooling – pr EN ISO 13790-2005 [5]

$$\eta_{C,ls} = \frac{1 - \lambda_C^{a_C}}{1 - \lambda_C^{a_C+1}} \qquad \text{if } \lambda_C \neq 1 \ \text{ and } \ \lambda_C > 0$$

$$\eta_{C,ls} = \frac{a_C}{a_C + 1} \qquad \text{if } \lambda_C = 1$$

$$\eta_{C,ls} = 1 \qquad \text{if } \lambda_C < 0$$

with: $\lambda_C = \dfrac{Q_{C,gn}}{Q_{C,ls}}$

where

$\eta_{C,ls}$ - is the dimensionless gain utilisation factor for cooling
λ_C - is the dimensionless gain/loss ratio for the cooling mode
$Q_{C,ls}$ - is the total heat losses for the cooling mode [kWh]
$Q_{H,gn}$ - are the total heat gains for the cooling mode [kWh]
a_C - is the dimensionless numerical parameter depending on the time constant τ_C

$$a_C = a_{0,C} + \frac{\tau_C}{\tau_{0,C}}$$

where

$a_{0,C}$ - is the dimensionless reference numerical parameter in this project equal 1,0.
τ_C - is the time constant of a building or building zone [h]
$\tau_{0,C}$ - is the reference time constant in this project equal 15h

12. Time constant for a building or building zone - pr EN ISO 13790-2005 [5]

$$\tau = \frac{C_m / 3,6}{H_L}$$

where

τ - is the time constant of a building or building zone [h]
C_m - is the internal heat capacity of a building [kJ/K]
H_L - is the heat losses coefficient of a building [W/K]

$$C_m = \sum_j \sum_i \rho_{ij} c_{ij} d_{ij} A_j$$

where

C_m - is the internal heat capacity of a building [kJ/K]
ρ_{ij} - is the density of the material of a layer i in element j [kg/m^3]
c_{ij} - is the specific heat capacity of the material of a layer i in element j [kJ/kgK]
d_{ij} - is the thickness of a layer i in element j [m] for the utilisation factor calculation d = 0,10m

13. Ventilation heat transfer coefficient - pr EN ISO 13789-2005 [6]

$$H_V = \rho_a \cdot c_a \cdot \dot{V}$$

where

V - is the airflow rate through the heated or cooled space
$\rho_a c_a$ - is the heat capacity of air per volume.

If the air flow rate V is in [m³ /s], $\rho_a c_a$ = 1200 [J/(m³ ·K)]. If V is given in [m³/h], $\rho_a c_a$ = 0,33 [Wh/(m³ ·K)].

14. Transmission heat transfer coefficient - pr EN ISO 13789-2005 [6]

$$H_D = \sum_i A_i \cdot U_i$$

where

A_i - is the area of element i of the building envelope [m²]
U_i - is the thermal transmittance of element i of the building envelope [W/(m²·K)]

5. Bibliography

1 - Kalyanova, O and Heiselberg, P. 2008 Experimental Set-up and Full-scale measurements in the 'Cube': 1st Draft. Aalborg: Aalborg University: Department of Civil Engineering. ISSN 1901-726X DCE Technical Report No.034

2 - EN ISO 13790 Thermal performance of a buildings – Calculation of energy use for space heating (ISO 13790:2006)

3 - DIN V 18599, Energy efficiency of buildings – Calculation of the net, final and primary energy demand for heating, cooling, ventilation, domestic hot water and lighting. Available at www.beuth.de

4 - EN ISO 13789, Thermal performance of buildings – transmission heat loss coefficient calculation method (ISO 13789:1999)

5 - DRAFT prEN ISO 13790 Thermal performance of a buildings – Calculation of energy use for space heating and cooling (ISO/DIS 13790:2005)

6 - DRAFT prEN ISO 13789, Thermal performance of buildings – Transmission and ventilation heat transfer coefficient - Calculation method (ISO/DIS 13789:2005)

This project focuses on the energy performance of a Double Skin Façade operating accordingly to the concept of preheating fresh air incoming into the building in cooperation with a mechanical ventilation system. The first part of this report deals with three sets of results from measurements performed in a full scale model during: November 2006, the turn of April and May 2008 and May 2008. In the last case a shading device was added in the Double Skin Façade air cavity. The experimental set-up has been validated through tracer gas experiments determining the airflow. Different weather conditions have been analyzed, with special focus on solar radiation and the effect of solar shading. This provided important insight on how such building constructions can have a beneficial or negative influence on a building's power load. Conclusions have been drawn considering application of solar shading in Double Skin Façades and their operation strategies.

Later on the gathered data formed the basis for conducting three sets of theoretical energy calculations, according to a simple method developed by the Bestfaçade Project Group, as well as three dynamic computer simulations in BSim. The aim of these tools is to provide a preliminary assessment of the impact of a Double Skin Façade on a building's energy consumption, which might be used in the conceptual phase of a project. The obtained results have been compared with the measurements and both theoretical methods have been evaluated. Unfortunately, in most cases results from the theoretical tools gave values very different from reality. Finally, conclusions have been drawn including suggestions for improvement of Double Skin Façade and solar shading modelling methods.